

BLEJSKE DELAVNICE IZ FIZIKE

BLED WORKSHOPS IN PHYSICS

LETNIK 8, ŠT. 1

VOL. 8, NO. 1

---

ISSN 1580-4992

Proceedings of the Mini-Workshop

# Hadron Structure and Lattice QCD

Bled, Slovenia, July 9–16, 2007

Edited by

Bojan Golli

Mitja Rosina

Simon Širca

*University of Ljubljana and Jožef Stefan Institute*

---

DMFA – ZALOŽNIŠTVO

LJUBLJANA, NOVEMBER 2007

# The Mini-Workshop *Hadron Structure and Lattice QCD*

was organized by

*Jožef Stefan Institute, Ljubljana  
Department of Physics, Faculty of Mathematics and Physics, University of Ljubljana*

and sponsored by

*Slovenian Research Agency  
Department of Physics, Faculty of Mathematics and Physics, University of Ljubljana  
Society of Mathematicians, Physicists and Astronomers of Slovenia*

## Organizing Committee

*Mitja Rosina, Bojan Golli, Simon Širca*

## List of participants

*Mike Birse, Manchester, mike.birse@manchester.ac.uk  
Wojciech Broniowski, Cracow, b4bronio@cyf-kr.edu.pl  
Thomas Cohen, Maryland, cohen@physics.umd.edu  
Veljko Dmitrašinović, Belgrade, dmitrasin@yahoo.com  
Svjetlana Fajfer, Ljubljana, svjetlana.fajfer@ijs.si  
Harald Fritzscht, München, fritzscht@mppmu.mpg.de  
Luca Girlanda, Pisa, luca.girlanda@pi.infn.it  
Leonid Glozman, Graz, leonid.glozman@uni-graz.at  
Bojan Golli, Ljubljana, bojan.golli@ijs.si  
Jernej Kamenik, Ljubljana, jernej.kamenik@ijs.si  
William Klink, Iowa, william-klink@uiowa.edu  
Nejc Košnik, Ljubljana, nejc.kosnik@ijs.si  
Christian Lang, Graz, christian.lang@uni-graz.at  
Martin Lavelle, Plymouth, m.lavelle@plymouth.ac.uk  
Keh-Fei Liu, Kentucky, liu@pa.uky.edu  
Harald Markum, Wien, markum@tuwien.ac.at  
Judith McGovern, Manchester, judith.mcgovern@manchester.ac.uk  
Willibald Plessas, Graz, plessas@bkfug.kfunigraz.ac.at  
Milan Potokar, Ljubljana, Milan.Potokar@ijs.si  
Saša Prelovšek, Ljubljana, Sasa.Prelovsek@ijs.si  
Mitja Rosina, Ljubljana, mitja.rosina@ijs.si  
Simon Širca, Ljubljana, simon.sirca@fmf.uni-lj.si  
Michele Viviani, Pisa, michele.viviani@pi.infn.it*

Electronic edition

<http://www-fl.ijs.si/BledPub/>

# Contents

<b>Preface</b> .....	V
<b>Renormalisation in quantum mechanics</b>	
<i>Michael C. Birse</i> .....	1
<b>Large-<math>N_c</math> Regge models and the <math>\langle A^2 \rangle</math> condensate</b>	
<i>Wojciech Broniowski and Enrique Ruiz Arriola</i> .....	10
<b>In order to form a more perfect fluid ... Is there a fundamental bound on <math>\eta/s</math> for fluids?</b>	
<i>Thomas D. Cohen</i> .....	16
<b>Does nucleon parity doubling imply <math>U_A(1)</math> symmetry restoration?</b>	
<i>V. Dmitrašinović</i> .....	17
<b>Constituent quarks as quasiparticles of QCD</b>	
<i>Harald Fritzsch</i> .....	24
<b>Covariant description of the few-nucleon systems from chiral dynamics</b>	
<i>L. Girlanda, M. Viviani and W.H. Klink</i> .....	25
<b>Excited baryons and QCD symmetries</b>	
<i>L. Ya. Glozman</i> .....	30
<b>Modeling the QCD Vacuum</b>	
<i>W. H. Klink</i> .....	31
<b>Dynamical CI fermions: Some results for Hadron Masses</b>	
<i>C.B. Lang</i> .....	35
<b>Charges in QED and QCD</b>	
<i>Martin Lavelle</i> .....	37
<b>Pattern of scalar mesons</b>	
<i>Keh-Fei Liu</i> .....	42

<b>Topology of non-commutative U(1) gauge theory on the lattice</b> <i>R. Achleitner, W. Frisch, H. Grosse, H. Markum, F. Teitschinger</i> . . . . .	43
<b>Chiral extrapolation of the nucleon mass</b> <i>Judith A. McGovern, Michael C. Birse</i> . . . . .	52
<b>New Baryon Results from Relativistic Constituent Quark Models</b> <i>W. Plessas</i> . . . . .	55
<b>Parity violating electron scattering on <math>^4\text{He}</math></b> <i>M. Viviani</i> . . . . .	57
<b>Dynamics of P11 and P33 resonances in quark models with chiral mesons</b> <i>B. Golli and S. Širca</i> . . . . .	61
<b>Sigma meson in a two-level Nambu – Jona-Lasinio model</b> <i>Mitja Rosina and Borut Tone Oblak</i> . . . . .	66
<b>Exclusive processes on the nucleon at MAMI and Jefferson Lab</b> <i>S. Širca</i> . . . . .	70

# Preface

We are continuing our popular Mini-Workshops on hadronic physics. The traditional meeting issues such as production and decays of baryon and meson resonances have been augmented this year by an interdisciplinary topic: the interplay between Lattice QCD and few-body techniques used for hadronic spectroscopy, aimed at what knowledge the quark modelists can adopt from Lattice QCD experts and, conversely, what Lattice QCD practitioners can learn from quark-model wave-functions.

First, lattice derivations of hadronic properties, also for excited hadrons, were introduced. There have been proposals on how bare quarks evolve into dressed quarks as quasi-particles of QCD. Chiral extrapolations in Lattice QCD can improve the calculation of nucleon mass but the convergence turned out to be questionable. Can suitable propagators lead to gluon condensate? Important issues of quantum field theory, QCD vacuum, string picture, as well as the choice of appropriate correlators and interpolating fields in Lattice QCD were discussed.

New rounds of experiments at Mainz and JLab have advanced the understanding of the electromagnetic and spin structure of the nucleon. The important role of the pion cloud was re-confirmed in the Roper and other P11 and P33 resonances. Incorporation of chiral dynamics and relativistic recoil corrections are important to reproduce the experimental nucleon-nucleon scattering phase shifts. Isospin breaking was analysed in the parity-violating asymmetry of electron scattering on  $^4\text{He}$ , and the strange-quark contribution to the proton charge and magnetism was precisely determined.

The baryonic decay widths computed in various quark models remain too narrow in spite of improved treatment of relativity and current conservation. The approximate degeneracy of highly excited mesons and baryons calls for a more fundamental understanding of chiral symmetry restoration and ordering of chiral multiplets. The classification of scalar mesons is still controversial: it is unclear whether they can be understood as quasi-bound states of two mesons and what is their role in nuclear forces.

In cases where authors preferred not to duplicate the material published elsewhere, only the title and/or abstract is included.

We have witnessed unusually fruitful discussions which we hope will initiate further cross-fertilization of the fields. It was our pleasure to be the host at Bled and to edit the Proceedings as a testimony to these exciting developments.

Ljubljana, November 2007

*M. Rosina  
B. Golli  
S. Širca*

## Workshops organized at Bled

- ▷ *What Comes beyond the Standard Model* (June 29–July 9, 1998)  
Bled Workshops in Physics **0** (1999) No. 1
- ▷ *Hadrons as Solitons* (July 6–17, 1999)
- ▷ *What Comes beyond the Standard Model* (July 22–31, 1999)
- ▷ *Few-Quark Problems* (July 8–15, 2000)  
Bled Workshops in Physics **1** (2000) No. 1
- ▷ *What Comes beyond the Standard Model* (July 17–31, 2000)
- ▷ *Statistical Mechanics of Complex Systems* (August 27–September 2, 2000)
- ▷ *Selected Few-Body Problems in Hadronic and Atomic Physics* (July 7–14, 2001)  
Bled Workshops in Physics **2** (2001) No. 1
- ▷ *What Comes beyond the Standard Model* (July 17–27, 2001)  
Bled Workshops in Physics **2** (2001) No. 2
- ▷ *Studies of Elementary Steps of Radical Reactions in Atmospheric Chemistry*
- ▷ *Quarks and Hadrons* (July 6–13, 2002)  
Bled Workshops in Physics **3** (2002) No. 3
- ▷ *What Comes beyond the Standard Model* (July 15–25, 2002)  
Bled Workshops in Physics **3** (2002) No. 4
- ▷ *Effective Quark-Quark Interaction* (July 7–14, 2003)  
Bled Workshops in Physics **4** (2003) No. 1
- ▷ *What Comes beyond the Standard Model* (July 17–27, 2003)  
Bled Workshops in Physics **4** (2003) No. 2-3
- ▷ *Quark Dynamics* (July 12–19, 2004)  
Bled Workshops in Physics **5** (2004) No. 1
- ▷ *What Comes beyond the Standard Model* (July 19–29, 2004)
- ▷ *Exciting Hadrons* (July 11–18, 2005)  
Bled Workshops in Physics **6** (2005) No. 1
- ▷ *What Comes beyond the Standard Model* (July 18–28, 2005)
- ▷ *Progress in Quark Models* (July 10–17, 2006)  
Bled Workshops in Physics **7** (2006) No. 1
- ▷ *What Comes beyond the Standard Model* (September 16–29, 2006)
- ▷ *Hadron Structure and Lattice QCD* (July 9–16, 2007)  
Bled Workshops in Physics **8** (2007) No. 1
- ▷ *What Comes beyond the Standard Model* (July 18–28, 2007)

## Also published in this series

- ▷ Book of Abstracts, *XVIII European Conference on Few-Body Problems in Physics*, Bled, Slovenia, September 8–14, 2002, Edited by Rajmund Krivec, Bojan Golli, Mitja Rosina, and Simon Širca  
Bled Workshops in Physics **3** (2002) No. 1–2







# Renormalisation in quantum mechanics

Michael C. Birse

Theoretical Physics Group, School of Physics and Astronomy  
The University of Manchester, Manchester, M13 9PL, U.K.

**Abstract.** This lecture provides an introduction to the renormalisation group as applied to scattering of two nonrelativistic particles. As well as forming a framework for constructing effective theories of few-nucleon systems, these ideas also provide a simple example which illustrates general features of the renormalisation group.

## 1 Effective theories

As particle and nuclear physicists, we are familiar with renormalisation in quantum field theory. We meet it first as a trick to get rid of mathematically unpleasant divergences. Later we learn to see it as part of a larger structure based on scale-dependence: the renormalisation group (RG). This is also how it appears in condensed-matter physics, in the context of critical phenomena [1].

The same ideas can also be used to study scale dependence in much simpler systems: just two or three nonrelativistic particles. They are of particular interest in nuclear physics, where we are trying to construct systematic effective field theories of nuclear forces (see [2] for recent reviews). They can also be applied to systems of cold atoms in traps, where magnetic fields can be used to tune the interactions between the atoms. In addition, these applications provide tractable examples of RG flows. Without the complications of a full field theory, the equations can often be solved exactly while still illustrating all of the general features of these flows [3].

Effective field theories describe only the low-energy degrees of freedom of some system and so they are not “fundamental”. In general they are not renormalisable and so they contain an infinite number of terms. This is potentially a disaster for their predictive power, but not if we can find a systematic way to organise these terms. Then, at any order in some expansion, only a finite number of terms will contribute. Having determined the coefficients of these by fitting them to data (or to simulations of the underlying physics), we can use them to predict other observables.

This works provided there is a good separation of scales, as illustrated in Fig. 1. Here  $Q$  generically denotes the experimentally relevant low-energy scales and  $\Lambda_0$  the scales of the underlying physics. In the case of nuclear physics, the low scales include particles’ momenta and the pion mass, while the high scales include the scale of chiral symmetry breaking,  $4\pi f_\pi$ , and the masses of hadrons

like the  $\rho$  meson and nucleon. If these are well separated, we can expand observables in powers of the small parameter  $Q/\Lambda_0$ . The terms in the effective theory can then be organised according to a “power counting” in the low scales  $Q$ .

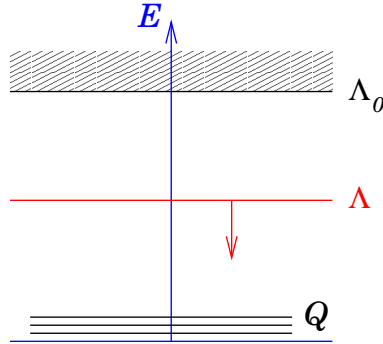


Fig. 1. Scales and the running cut-off.

The effective theory describes physics at low momenta. Short-range physics is not resolved by it and so is just represented by contact interactions ( $\delta$ -functions and their derivatives). However scattering by these is ill-defined since they couple to virtual states with arbitrarily high momenta. The basic nonrelativistic loop diagram (which is relevant for the rest of this talk) is shown in Fig. 2.

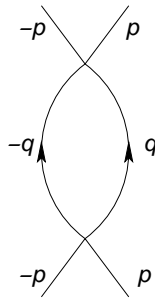


Fig. 2. The basic loop integral.

For S-wave scattering this integral is

$$M \int \frac{q^2 dq}{p^2 - q^2} \sim -M \int dq, \quad \text{for large } q, \quad (1)$$

and so contains a linear divergence. We therefore need to regulate the theory. There are many ways to do this: dimensional regularisation [4], a simple momentum cut-off [3], or adding a term to the kinetic energy to suppress high-energy modes [5]. All of these are equivalent, but each introduces some arbitrary scale,  $\Lambda$ . This is essentially the highest momentum that is included explicitly in the theory. Physical predictions should be independent of  $\Lambda$  and this leads us to the RG.

As we lower  $\Lambda$ , the couplings must run. This is because more and more physics is “integrated out” (see Fig. 1) and so must be included implicitly in the effective couplings. Ultimately we lose all memory of the underlying physics and the only scale we have left is  $\Lambda$ . In units of  $\Lambda$ , everything is then just a number. We have arrived at a fixed point of the RG – a scale-free system. These are the end-points of the RG flow. Two are shown in Fig. 3. The one on the left is stable: any nearby theory will flow towards it as the the cut-off is lowered. In contrast, the one on the right has an unstable direction: the flow can take theories away from the fixed point unless they lie on the “critical surface”.

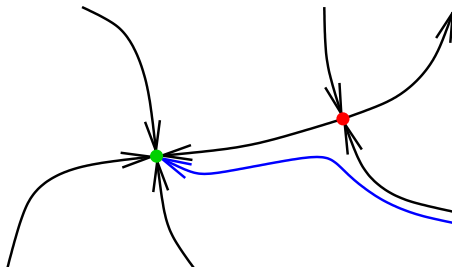


Fig. 3. Fixed points.

Close to a fixed point, we can find perturbations that show a power-law dependence on  $\Lambda$  and we can use this power counting to organise the terms in our effective theory. They can be classified into three types:

- $\Lambda^{-\gamma}$ : relevant/super-renormalisable<sup>1</sup>,  
for example mass terms in quantum field theories like QED;
- $\Lambda^0$ : marginal/renormalisable,  
for example the couplings familiar in gauge theories like the Standard Model (typically these show a  $\log \Lambda$  dependence on the cut-off);
- $\Lambda^{+\gamma}$ : irrelevant/nonrenormalisable,  
for example the interactions in Chiral Perturbation Theory.

## 2 RG equation for two-body scattering

Let us look at scattering of two non-relativistic particles at low enough energies that the range of the forces is not resolved (for example, two nucleons with an energy below about 10 MeV). This can be described by an effective Lagrangian with two-body contact interactions or, equivalently, a Hamiltonian with a  $\delta$ -function potential. In momentum space, the S-wave potential can be written

$$V(k', k, p) = C_{00} + C_{20}(k^2 + k'^2) + C_{02} p^2 \dots, \quad (2)$$

where  $k$  and  $k'$  denote the initial and final relative momenta and the energy-dependence is expressed in terms of the on-shell momentum  $p = \sqrt{ME}$ .

<sup>1</sup> The term “relevant” is commonly used in condensed-matter physics, whereas “super-renormalisable” is more usual in particle physics.

Scattering can be described by the reactance matrix ( $K$ ), defined similarly to the scattering matrix ( $T$ ) but with standing-wave boundary conditions. This has the advantage that it is real below the particle-production threshold. For S-wave scattering, it satisfies the Lippmann-Schwinger equation

$$K(k', k, p) = V(k', k, p) + \frac{M}{2\pi^2} \mathcal{P} \int_0^\Lambda q^2 dq \frac{V(k', q, p)K(q, k, p)}{p^2 - q^2}, \quad (3)$$

where  $\mathcal{P}$  denotes the principal value. This integral equation sums chains of the bubble diagrams in Fig. 2 to all orders. On-shell ( $k' = k = p$ ), the  $K$ -matrix is related to the  $T$ -matrix by

$$\frac{1}{K(p)} = \frac{1}{T(p)} - i \frac{Mp}{4\pi} = -\frac{Mp}{4\pi} \cot \delta(p), \quad (4)$$

where  $\delta(p)$  is the phase shift.

With contact interactions, the integral over the momentum  $q$  of the virtual states is divergent and so we need to regulate it. Here I follow the method developed in [3] and simply cut the integral off at  $q = \Lambda$ . We can write the integral equation in the schematic form

$$K = V + VGK. \quad (5)$$

Demanding that the off-shell  $K$ -matrix be independent of  $\Lambda$ ,

$$\dot{K} \equiv \frac{\partial K}{\partial \Lambda} = 0, \quad (6)$$

ensures that scattering observables will be independent of the arbitrary cut-off. Differentiating the integral equation gives

$$0 = \dot{V} + \dot{V}GK + V\dot{G}K, \quad (7)$$

where  $\dot{G}$  implies differentiation with respect to the cut-off on the integral. Multiplying this by  $(1 + GK)^{-1}$  and using the integral equation for  $K$ , we arrive at

$$\dot{V} = -V\dot{G}V. \quad (8)$$

This equation has a very natural structure: as states at the cut-off, with  $q = \Lambda$ , are removed from the loop integral in Fig. 2, their effects are added into the potential to compensate. Written out explicitly, it is

$$\frac{\partial V}{\partial \Lambda} = \frac{M}{2\pi^2} V(k', \Lambda, p, \Lambda) \frac{\Lambda^2}{\Lambda^2 - p^2} V(\Lambda, k, p, \Lambda). \quad (9)$$

Note that the use of the fully off-shell  $K$ -matrix was essential to obtaining an equation involving only the potential; a similar approach based on the half-off-shell  $T$ -matrix yields an equation that still involves the scattering matrix [6].

This equation for the cut-off dependence of the effective potential is still not quite the RG equation: the final step is to express all dimensioned quantities in

units of  $\Lambda$ . Rescaled momentum variables (denoted with hats) are defined by  $\hat{k} = k/\Lambda$  etc., and a rescaled potential by

$$\hat{V}(\hat{k}', \hat{k}, \hat{p}, \Lambda) = \frac{M\Lambda}{2\pi^2} V(\Lambda\hat{k}', \Lambda\hat{k}, \Lambda\hat{p}, \Lambda). \quad (10)$$

(The factor  $M$  in this corresponds to dividing an overall factor of  $1/M$  out of the Schrödinger equation.) This satisfies the RG equation

$$\begin{aligned} \Lambda \frac{\partial \hat{V}}{\partial \Lambda} = \hat{k}' \frac{\partial \hat{V}}{\partial \hat{k}'} + \hat{k} \frac{\partial \hat{V}}{\partial \hat{k}} + \hat{p} \frac{\partial \hat{V}}{\partial \hat{p}} + \hat{V} \\ + \hat{V}(\hat{k}', 1, \hat{p}, \Lambda) \frac{1}{1 - \hat{p}^2} \hat{V}(1, \hat{k}, \hat{p}, \Lambda). \end{aligned} \quad (11)$$

The sum of logarithmic derivatives is similar to the structure of analogous RG equations in condensed-matter physics; it counts the powers of low-energy scales present in the potential. The boundary conditions on solutions to this equation are that they should be analytic functions of  $\hat{k}^2$ ,  $\hat{k}'^2$  and  $\hat{p}^2$  (since they should arise from an effective Lagrangian constructed out of  $\partial/\partial t$  and  $\nabla^2$ ). For small values of these quantities the potential should thus have an expansion in non-negative integer powers of them.

### 3 Fixed points and perturbations

Having constructed the RG equation, the first thing we should do is to look for fixed points – solutions that are independent of  $\Lambda$ . There is one obvious one: the trivial fixed point

$$\hat{V} = 0. \quad (12)$$

(Since there is no scattering, this obviously describes a scale-free system.)

To describe more interesting physics, we need to expand around the fixed point, looking for perturbations that scale with definite powers of  $\Lambda$ . These are eigenfunctions of the linearised RG equation. They have the form

$$\hat{V}(\hat{k}', \hat{k}, \hat{p}, \Lambda) = \Lambda^\nu \phi(\hat{k}', \hat{k}, \hat{p}), \quad (13)$$

and they satisfy the eigenvalue equation

$$\hat{k}' \frac{\partial \phi}{\partial \hat{k}'} + \hat{k} \frac{\partial \phi}{\partial \hat{k}} + \hat{p} \frac{\partial \phi}{\partial \hat{p}} + \phi = \nu \phi. \quad (14)$$

Its solutions are

$$\phi(\hat{k}', \hat{k}, \hat{p}) = C \hat{k}'^{2l} \hat{k}^{2m} \hat{p}^{2n}, \quad (15)$$

with  $l, m, n \geq 0$  since only non-negative, even powers satisfy the boundary condition. The corresponding eigenvalues are

$$\nu = 2(l + m + n) + 1. \quad (16)$$

These are all positive and so the fixed point is stable. The eigenvalues simply count the powers of low-energy scales. ( $\nu = d + 1$  where  $d$  is the “engineering dimension”, as in Weinberg’s original power counting for ChPT [7].)

There are also many nontrivial fixed points, all of which are unstable. The most interesting one is purely energy-dependent. To study it, I focus on potentials of the form  $V(p, \Lambda)$ . The RG equation for these simplifies to

$$\Lambda \frac{\partial \hat{V}}{\partial \Lambda} = \hat{p} \frac{\partial \hat{V}}{\partial \hat{p}} + \hat{V} + \frac{\hat{V}(\hat{p}, \Lambda)^2}{1 - \hat{p}^2}. \quad (17)$$

Since all terms involve just one function, we can divide by  $\hat{V}^2$  to get

$$\Lambda \frac{\partial}{\partial \Lambda} \left( \frac{1}{\hat{V}} \right) = \hat{p} \frac{\partial}{\partial \hat{p}} \left( \frac{1}{\hat{V}} \right) - \frac{1}{\hat{V}} - \frac{1}{1 - \hat{p}^2}, \quad (18)$$

which is just a linear equation for  $1/\hat{V}(\hat{p}, \Lambda)$ .

To find the fixed point, we set the LHS of this equation to zero. The resulting ODE can then be integrated easily. The general solution is

$$\frac{1}{\hat{V}_0(\hat{p})} = - \int_0^1 \frac{\hat{q}^2 d\hat{q}}{\hat{q}^2 - \hat{p}^2} + C\hat{p}. \quad (19)$$

The final term is not analytic in  $\hat{p}^2$  and so the boundary condition requires  $C = 0$ . The fixed-point potential is thus

$$\frac{1}{\hat{V}_0(\hat{p})} = -1 + \frac{\hat{p}}{2} \ln \frac{1 + \hat{p}}{1 - \hat{p}}. \quad (20)$$

The precise form of this is regulator-dependent (for example, it is just a constant for dimensional regularisation [4]), but the presence of a negative constant of order unity is generic.

Since this potential has no momentum dependence, the integral equation for the K-matrix simplifies to an algebraic equation. In rescaled, dimensionless form, it can be written

$$\frac{1}{\hat{K}(\hat{p})} = \frac{1}{\hat{V}_0(\hat{p})} - \int_0^1 \frac{\hat{q}^2 d\hat{q}}{\hat{p}^2 - \hat{q}^2}. \quad (21)$$

The integral here is just the negative of the one above in  $1/\hat{V}_0$  itself and so we get

$$\frac{1}{\hat{K}(\hat{p})} = 0. \quad (22)$$

The corresponding T-matrix,

$$\frac{1}{\hat{T}(\hat{p})} = \frac{1}{\hat{K}(\hat{p})} + i \frac{\pi}{2} \hat{p}, \quad (23)$$

has a pole at  $\hat{p} = 0$ . The fixed-point therefore describes a system with a bound state at exactly zero energy (another scale-free system).

More general systems can be described by perturbing around the fixed point. In particular, energy-dependent perturbations can be found by substituting

$$\frac{1}{\hat{V}(\hat{p}, \Lambda)} = \frac{1}{\hat{V}_0(\hat{p})} + \Lambda^\nu \phi(\hat{p}) \quad (24)$$

into the RG equation. The functions  $\phi(\hat{p})$  satisfy the eigenvalue equation

$$\hat{p} \frac{\partial \phi}{\partial \hat{p}} - \phi = \nu \phi. \quad (25)$$

The solutions to this are powers of the energy,

$$\phi(\hat{p}) = C \hat{p}^{2n}, \quad (26)$$

with eigenvalues

$$\nu = 2n - 1. \quad (27)$$

The RG eigenvalues for these perturbations have been shifted by  $-2$  compared to the simple “engineering” power counting. There is one negative eigenvalue and so the fixed point is unstable.

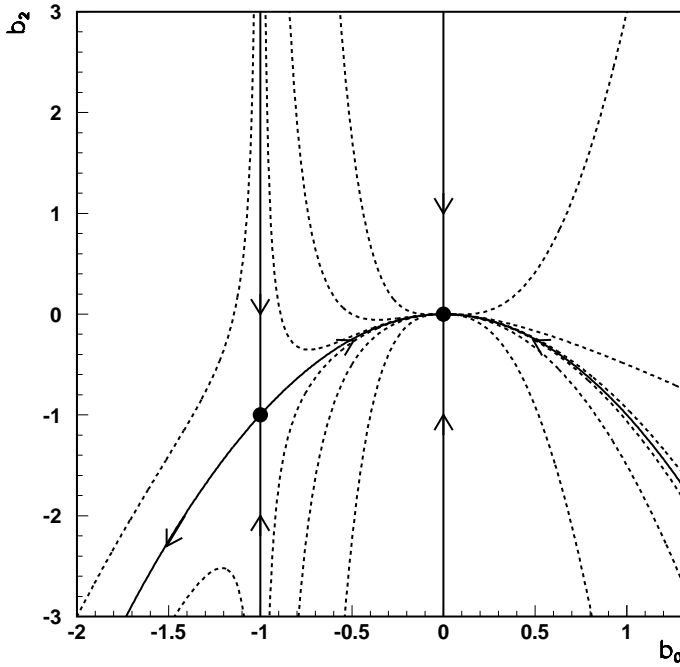


Fig. 4. RG flow of the potential  $\hat{V}(\hat{p}, \Lambda) = b_0(\Lambda) + b_2(\Lambda) \hat{p}^2 + \dots$ .

A slice through the RG flow is shown in Fig. 4. The two fixed points can be seen, as well as the critical line through the nontrivial one. Potentials close to this line initially flow towards the fixed point as we lower the cut-off but are then diverted away from it. A potential to the right of the line is not quite strong enough to produce a bound state. As  $\Lambda$  passes through the scale associated with the virtual state, the flow turns to approach the trivial fixed point from the weakly

attractive side. In contrast, a potential to the left of the critical line generates a finite-energy bound state. This state drops out of our low-energy effective theory when the cut-off reaches the corresponding momentum scale. As this happens, the RG flow takes the potential to infinity and it then reappears from the right, ultimately approaching the trivial fixed point from the weakly repulsive side.

**Exercise:** Repeat this analysis for a general number of space dimensions, in particular for  $D = 1$  and  $2$ , and interpret your results.

Physical observables are given by the on-shell K-matrix. Returning to physical units, this is

$$\frac{1}{\mathbb{K}(p)} = \frac{M}{2\pi^2} \sum_{n=0}^{\infty} C_n p^{2n}, \quad (28)$$

where the  $C_n$  are the coefficients of the RG eigenfunctions in  $1/\hat{V}$ . Comparing this with

$$\frac{1}{\mathbb{K}(p)} = -\frac{Mp}{4\pi} \left( -\frac{1}{a} + \frac{1}{2} r_e p^2 + \dots \right), \quad (29)$$

we see that this expansion is, in fact, just the effective-range expansion (first applied to the nucleon-nucleon interaction by Bethe in 1949 [8]). Note that the terms in the expansion of our effective theory have a direct connection to scattering observables. This is as it should be: effective theories are systematic tools to analyse data, not fundamental theories that aim to predict everything in terms of a small number of parameters.

Finally, I should make a brief comment about momentum-dependent perturbations around the nontrivial fixed point, which I have not discussed above. These terms change the off-shell dependence of the scattering matrix, without affecting physical observables. Their explicit forms can be found in Ref. [3]. In contrast to the expansion around the trivial fixed point, momentum- and energy-dependent terms appear at different orders. Specifically, the momentum-dependent perturbations around the nontrivial point have even RG eigenvalues. Each term is one order higher in the expansion than the corresponding energy-dependent one. This means that using them to eliminate energy dependence will leave an effective potential without an obvious power counting (like the potential obtained in Ref. [6]).

## 4 Extensions

Here I have discussed only the application of the RG to systems where the range of the forces is not resolved and the interactions can all be represented by contact terms. There are many other systems with known long-range forces, for example: Coulomb, pion exchange, dipole-dipole or van der Waals interactions. Similar RG methods can be applied to the unresolved short-range forces accompanying these [9,10]. The resulting expressions are either distorted-wave Born expansions or distorted-wave versions of the effective-range expansion. (In the case of the Coulomb potential, it was again Bethe who first wrote this expansion down [8].)

Another important application is to the  $1/r^2$  potential that arises in three-body systems with attractive short-range forces [11]. If the two-body scattering length is infinite, the Efimov effect leads to a tower of geometrically-spaced bound states [12]. This is the origin of the limit cycle that has been found in the RG flows for these systems [13] (one of the few known examples of such a cycle).

## Acknowledgments

I am grateful to M. Rosina, B. Golli and S. Širca for the invitation to participate in the Bled 2007 Workshop “Hadron structure and lattice QCD”. I should also thank them and L. Glozman for providing the impetus to write up this lecture. Finally, I acknowledge the contributions of my collaborators, J. McGovern, K. Richardson and T. Barford, to the work outlined here.

## References

1. K. G. Wilson, *Rev. Mod. Phys.* **55** (1983) 583.
2. P. F. Bedaque and U. van Kolck, *Ann. Rev. Nucl. Part. Sci.* **52** (2002) 339 [nucl-th/0203055]; E. Epelbaum, *Prog. Part. Nucl. Phys.* **57** (2006) 654 [nucl-th/0509032].
3. M. C. Birse, J. A. McGovern and K. G. Richardson, *Phys. Lett.* **B464**, 169 (1999) [hep-ph/9807302].
4. *Nucl. Phys.* **B534** (1998) 329 [nucl-th/9802075].
5. K. Harada, H. Kubo and A. Ninomiya, nucl-th/0702074.
6. S. K. Bogner, A. Schwenk, T. T. S. Kuo and G. E. Brown, nucl-th/0111042; see also: S. K. Bogner *et al.*, *Phys. Lett.* **B576** (2003) 265 [nucl-th/0108041].
7. S. Weinberg, *Physica* **A96** (1979) 327; *Phys. Lett.* **B251** (1990) 288.
8. H. A. Bethe, *Phys. Rev.* **76** (1949) 38.
9. T. Barford and M. C. Birse, *Phys. Rev.* **C67** (2003) 064006 [hep-ph/0206146].
10. M. C. Birse, *Phys. Rev.* **C74** (2006) 014003 [nucl-th/0507077].
11. T. Barford and M. C. Birse, *J. Phys. A: Math. Gen.* **38** (2005) 697 [nucl-th/0406008].
12. V. N. Efimov, *Sov. J. Nucl. Phys.* **12** (1971) 589; **29** (1979) 546.
13. P. F. Bedaque, H.-W. Hammer and U. van Kolck, *Phys. Rev. Lett.* **82**, 463 (1999) [nucl-th/9809025]; *Nucl. Phys.* **A646**, 444 (1999) [nucl-th/9811046]; *Nucl. Phys.* **A676**, 357 (2000) [nucl-th/9906032].



## Large- $N_c$ Regge models and the $\langle A^2 \rangle$ condensate\*

Wojciech Broniowski<sup>a,b</sup> and Enrique Ruiz Arriola<sup>c</sup>

<sup>a</sup>Institute of Nuclear Physics PAN, PL-31342 Cracow, Poland

<sup>b</sup>Institute of Physics, Świętokrzyska Academy, PL-25406 Kielce, Kielce, Poland

<sup>c</sup>Departamento de Física Atómica, Molecular y Nuclear, Universidad de Granada E-18071 Granada, Spain

**Abstract.** We explore the role of the  $\langle A^2 \rangle$  gluon condensate in matching Regge models to the operator product expansion of meson correlators.

This talk is based on Ref. [1], where the details may be found. The idea of implementing the principle of parton-hadron duality in Regge models has been discussed in Refs. [2–8]. Here we carry out this analysis with the dimension-2 gluon condensate present. The dimension-two gluon condensate,  $\langle A^2 \rangle$ , was originally proposed by Celenza and Shakin [9] more than twenty years ago. Chetyrkin, Narison and Zakharov [10] pointed out its sound phenomenological as well as theoretical [11–15] consequences. Its value can be estimated by matching to results of lattice calculations in the Landau gauge [16,17], and their significance for non-perturbative signatures above the deconfinement phase transition was analyzed in [18]. Chiral quark-model calculations were made in [19] where  $\langle A^2 \rangle$  seems related to constituent quark masses. In spite of all this flagrant need for these unconventional condensates the dynamical origin of  $\langle A^2 \rangle$  remains still somewhat unclear; for recent reviews see, *e.g.*, [20,21].

For large  $Q^2$  and fixed  $N_c$  the modified OPE (with the  $1/Q^2$  term present) for the chiral combinations of the transverse parts of the vector and axial currents is

$$\begin{aligned}\Pi_{V+A}^T(Q^2) &= \frac{1}{4\pi^2} \left\{ -\frac{N_c}{3} \log \frac{Q^2}{\mu^2} - \frac{\alpha_S}{\pi} \frac{\lambda^2}{Q^2} + \frac{\pi \langle \alpha_S G^2 \rangle}{3 Q^4} + \dots \right\} \\ \Pi_{V-A}^T(Q^2) &= -\frac{32\pi \alpha_S \langle \bar{q}q \rangle^2}{9 Q^6} + \dots\end{aligned}\quad (1)$$

On the other hand, at large- $N_c$  and any  $Q^2$  these correlators may be saturated by infinitely many mesonic states,

$$\Pi_V^T(Q^2) = \sum_{n=0}^{\infty} \frac{F_{V,n}^2}{M_{V,n}^2 + Q^2} + \text{c.t.}, \quad \Pi_A^T(Q^2) = \frac{f^2}{Q^2} + \sum_{n=0}^{\infty} \frac{F_{A,n}^2}{M_{A,n}^2 + Q^2} + \text{c.t.} \quad (2)$$

\* Talk delivered by Wojciech Broniowski

The basic idea of parton-hadron duality is to match Eq. (1) and (2) for both large  $Q^2$  and  $N_c$  (assuming that both limits commute). We use the radial Regge spectra, which are well supported experimentally [22]

$$M_{V,n}^2 = M_V^2 + a_V n, \quad M_{A,n}^2 = M_A^2 + a_A n, \quad n = 0, 1, \dots \quad (3)$$

The vector part,  $\Pi_V^\top$ , satisfies the once-subtracted dispersion relation

$$\Pi_V^\top(Q^2) = \sum_{n=0}^{\infty} \left( \frac{F_{V,n}^2}{M_V^2 + a_V n + Q^2} - \frac{F_{V,n}^2}{M_V^2 + a_V n} \right). \quad (4)$$

We need to reproduce the  $\log Q^2$  in OPE, for which only the asymptotic part of the meson spectrum matters. This leads to the condition that at large  $n$  the residues become independent of  $n$ ,  $F_{V,n} \simeq F_V$  and  $F_{A,n} \simeq F_A$ . Thus all the highly-excited radial states are coupled to the current with equal strength! Or: asymptotic dependence of  $F_{V,n}$  or  $F_{A,n}$  on  $n$  would damage OPE. Next, we carry out the sum explicitly (the dilog function is  $\psi(z) = \Gamma'(z)/\Gamma(z)$ )

$$\begin{aligned} \sum_{n=0}^{\infty} \left( \frac{F_i^2}{M_i^2 + a_i n + Q^2} - \frac{F_i^2}{M_i^2 + a_i n} \right) &= \frac{F_i^2}{a_i} \left[ \psi \left( \frac{M_i^2}{a_i} \right) - \psi \left( \frac{M_i^2 + Q^2}{a_i} \right) \right] \\ &= \frac{F_i^2}{a_i} \left[ -\log \left( \frac{Q^2}{a_i} \right) + \psi \left( \frac{M_i^2}{a_i} \right) + \frac{a_i - 2M_i^2}{2Q^2} + \frac{6M_i^4 - 6a_i M_i^2 + a_i^2}{12Q^4} + \dots \right], \end{aligned} \quad (5)$$

where  $i = V, A$ .  $\Pi_{V-A}$  satisfies the unsubtracted dispersion relation (no  $\log Q^2$  term), hence

$$F_V^2/a_V = F_A^2/a_A. \quad (6)$$

This complies to the chiral symmetry restoration in the high-lying spectra [23,24]. Further, we assume  $a_V = a_A = a$ , or  $F_V = F_A = F$ , which is well-founded experimentally, as  $\sqrt{\sigma_A} = 464\text{MeV}$ ,  $\sqrt{\sigma_V} = 470\text{MeV}$  [22].

The simplest model we consider has strictly linear trajectories all the way down,

$$\begin{aligned} \Pi_{V-A}^\top(Q^2) &= \frac{F^2}{a} \left[ -\psi \left( \frac{M_V^2 + Q^2}{a} \right) + \psi \left( \frac{M_A^2 + Q^2}{a} \right) \right] - \frac{f^2}{Q^2} \\ &= \left( \frac{F^2}{a} (M_A^2 - M_V^2) - f^2 \right) \frac{1}{Q^2} + \left( \frac{F^2}{2a} (M_A^2 - M_V^2) (a - M_A^2 - M_V^2) \right) \frac{1}{Q^4} + \dots \end{aligned}$$

Matching to OPE yields the two Weinberg sum rules:

$$f^2 = \frac{F^2}{a} (M_A^2 - M_V^2), \quad (\text{WSR I})$$

$$0 = (M_A^2 - M_V^2) (a - M_A^2 - M_V^2). \quad (\text{WSR II})$$

The  $V + A$  channel needs regularization. We proceed as follows: carry  $d/dQ^2$ , compute the convergent sum, and integrate back over  $Q^2$ . The result is

$$\begin{aligned}\Pi_{V+A}^T(Q^2) &= \frac{F^2}{a} \left[ -\psi\left(\frac{M_V^2 + Q^2}{a}\right) - \psi\left(\frac{M_\Lambda^2 + Q^2}{a}\right) \right] + \frac{f^2}{Q^2} + \text{const.} \\ &= -\frac{2F^2}{a} \log \frac{Q^2}{\mu^2} + \left( f^2 + F^2 - \frac{F^2}{a}(M_\Lambda^2 + M_V^2) \right) \frac{1}{Q^2} \\ &\quad + \frac{F^2}{6a} (a^2 - 3a(M_\Lambda^2 + M_V^2) + 3(M_\Lambda^4 + M_V^4)) \frac{1}{Q^4} + \dots\end{aligned}$$

Matching of the coefficient of  $\log Q^2$  to OPE gives the relation

$$a = 2\pi\sigma = \frac{24\pi^2 F^2}{N_c}, \quad (7)$$

where  $\sigma$  denotes the (long-distance) string tension. From the  $\rho \rightarrow 2\pi$  decay one extracts  $F = 154$  MeV [25] which gives  $\sqrt{\sigma} = 546$  MeV, compatible to the value obtained in lattice simulations:  $\sqrt{\sigma} = 420$  MeV [26]. Moreover, from the Weinberg sum rules

$$M_\Lambda^2 = M_V^2 + \frac{24\pi^2}{N_c} f^2, \quad a = M_\Lambda^2 + M_V^2 = 2M_V^2 + \frac{24\pi^2}{N_c} f^2. \quad (8)$$

Matching higher twists fixes the dimension-2 and 4 gluon condensates:

$$-\frac{\alpha_s \lambda^2}{4\pi^3} = f^2, \quad \frac{\alpha_s \langle G^2 \rangle}{12\pi} = \frac{M_\Lambda^4 - 4M_V^2 M_\Lambda^2 + M_V^4}{48\pi^2}. \quad (9)$$

Numerically, it gives  $-\frac{\alpha_s \lambda^2}{\pi} = 0.3 \text{ GeV}^2$  as compared to  $0.12 \text{ GeV}^2$  from Ref. [10,20]. The short-distance string tension is  $\sigma_0 = -2\alpha_s \lambda^2 / N_c = 782$  MeV, which is twice as much as  $\sigma$ . The major problem of the strictly linear model is that the dimension-4 gluon condensate is negative for  $M_V \geq 0.46$  GeV. Actually, it never reaches the QCD sum-rules value. Thus, the strictly linear radial Regge model is *too restrictive!*

We therefore consider a modified Regge model where for low-lying states both their residues and positions may depart from the linear trajectories. The OPE condensates are expressed in terms of the parameters of the spectra. A very simple modification moves only the position of the lowest vector state, the  $\rho$  meson.

$$\begin{aligned}M_{V,0} &= m_\rho, \quad M_{V,n}^2 = M_V^2 + an, \quad n \geq 1 \\ M_{\Lambda,n}^2 &= M_\Lambda^2 + an, \quad n \geq 0.\end{aligned} \quad (10)$$

For the Weinberg sum rules (we use  $N_c = 3$  from now on)

$$M_\Lambda^2 = M_V^2 + 8\pi^2 f^2, \quad a = 8\pi^2 F^2 = \frac{8\pi^2 f^2 (4\pi^2 f^2 + M_V^2)}{4\pi^2 f^2 - m_\rho^2 + M_V^2}. \quad (11)$$

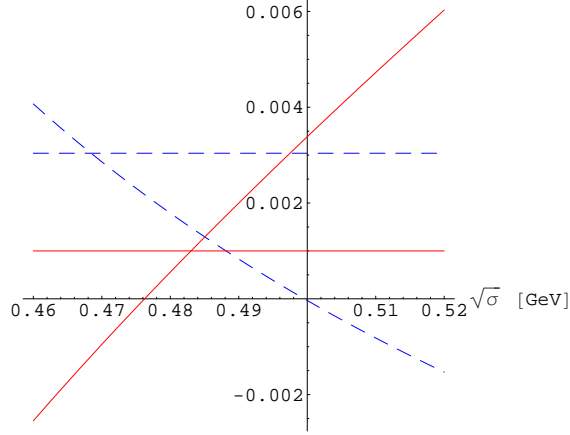


**Fig. 1.** Dimension-2 (solid line, in  $\text{GeV}^2$ ) and -4 (dashed line, in  $\text{GeV}^4$ ) gluon condensates plotted as functions of the square root of the string tension. The straight lines indicate phenomenological estimates. The fiducial region in  $\sqrt{\sigma}$  for which both condensates are positive is in the acceptable range compared to the values of Ref. [22] and other studies.

We fix  $m_\rho = 0.77 \text{ GeV}$ , and  $\sigma$  is the only free parameter of the model. Then

$$M_V^2 = \frac{-16\pi^3 f^4 + 4\pi^2 \sigma f^2 - m_\rho^2 \sigma}{4f^2 \pi - \sigma}, \quad -\frac{\alpha_S \lambda^2}{4\pi^3} = \frac{16\pi^3 f^4 - \pi \sigma^2 + m_\rho^2 \sigma}{16f^2 \pi^3 - 4\pi^2 \sigma},$$

$$\frac{\alpha_S \langle G^2 \rangle}{12\pi} = 2\pi^2 f^4 - \pi \sigma f^2 + \frac{3\sigma \left( \frac{m_\rho^2 \sigma}{(\sigma - 4f^2 \pi)^2} - 2\pi \right) m_\rho^2}{8\pi^2} + \frac{\sigma^2}{12}. \quad (12)$$

The window for which both condensates are positive yields very acceptable values of  $\sigma$ . The consistency check of near equality of the long- and short-distance string tensions,  $\sigma \simeq \sigma_0$ , holds for  $\sqrt{\sigma} \simeq 500 \text{ MeV}$ . The magnitude of the condensates is in the ball park of the “physical” values. The value of  $M_V$  in the “fiducial” range is around 820 MeV. The experimental spectrum in the  $\rho$  channel is has states at 770, 1450, 1700, 1900\*, and 2150\* MeV, while the model gives 770, 1355, 1795, 2147 MeV (for  $\sigma = (0.47 \text{ GeV}^2)$ ). In the  $a_1$  channel the experimental states are at 1260 and 1640 MeV, whereas the model yields 1015 and 1555 MeV.

We note that the  $V - A$  channel well reproduced with radial Regge models. The Das-Mathur-Okubo sum rule gives the Gasser-Leutwyler constant  $L_{10}$ , while the Das-Guralnik-Mathur-Low-Yuong sum rule yields the pion electromagnetic mass splitting. In the strictly linear model with  $M_A^2 = 2M_V^2$  and  $M_V = \sqrt{24\pi^2/N_c} f = 764 \text{ MeV}$  we have  $\sqrt{\sigma} = \sqrt{3/2\pi} M_V = 532 \text{ MeV}$ ,  $F = \sqrt{3} f = 150 \text{ MeV}$ ,  $L_{10} = -N_c/(96\sqrt{3}\pi) = -5.74 \times 10^{-3} (-5.5 \pm 0.7 \times 10^{-3})_{\text{exp}}$ ,  $m_{\pi^\pm}^2 - m_{\pi_0}^2 = (31.4 \text{ MeV})^2 (35.5 \text{ MeV})_{\text{exp}}^2$ . In our second model with  $\sigma = (0.48 \text{ GeV}^2)$  we find  $L_{10} = -5.2 \times 10^{-3}$  and  $m_{\pi^\pm}^2 - m_{\pi_0}^2 = (34.4 \text{ MeV})^2$ .

To conclude, let us summarize our results and list some further related studies.

- Matching OPE to the radial Regge models produces in a natural way the  $1/Q^2$  correction to the  $V$  and  $A$  correlators. Appropriate conditions are satisfied by the asymptotic spectra, while the parameters of the low-lying states are tuned to reproduce the values of the condensates.
- In principle, these parameters of the spectra are measurable, hence the information encoded in the low-lying states is the same as the information in the condensates.
- Yet, sensitivity of the values of the condensates to the parameters of the spectra, as seen by comparing the two explicit models considered in this paper, makes such a study difficult or impossible at a more precise level.
- Regge models work very well in the  $V - A$  channel. In [28] it is shown how the spectral (in fact chiral) asymmetry between vector and axial channel is generated via the use of  $\zeta$ -function regularization for *each* channel separately.
- We comment that effective low-energy chiral models produce  $1/Q^2$  corrections (*i.e.* provide a scale of dimension 2), *e.g.*, the instanton-based chiral quark model gives [19]

$$-\frac{\alpha_S}{\pi}\lambda^2 = -2N_c \int du \frac{u}{u + M(u)^2} M(u) M'(u) \simeq 0.2 \text{ GeV}^2. \quad (13)$$

- In the presented Regge approach the pion distribution amplitude is constant,  $\phi(x) = 1$ , at the low-energy hadronic scale, similarly as in chiral quark models [27].

## References

1. E. Ruiz Arriola, W. Broniowski, Phys. Rev. D73 (2006) 097502.
2. M. Golterman, S. Peris, JHEP 01 (2001) 028.
3. S. R. Beane, Phys. Rev. D64 (2001) 116010.
4. Y. A. Simonov, Phys. Atom. Nucl. 65 (2002) 135–152.
5. M. Golterman, S. Peris, Phys. Rev. D67 (2003) 096001.
6. S. S. Afonin, Phys. Lett. B576 (2003) 122–126.
7. S. S. Afonin, A. A. Andrianov, V. A. Andrianov, D. Espriu, JHEP 04 (2004) 039.
8. S. S. Afonin, Nucl. Phys. B 779 (2007) 13.
9. L. S. Celenza, C. M. Shakin, Phys. Rev. D34 (1986) 1591–1600.
10. K. G. Chetyrkin, S. Narison, V. I. Zakharov, Nucl. Phys. B550 (1999) 353–374.
11. F. V. Gubarev, L. Stodolsky, V. I. Zakharov, Phys. Rev. Lett. 86 (2001) 2220–2222.
12. F. V. Gubarev, V. I. Zakharov, Phys. Lett. B501 (2001) 28–36.
13. K.-I. Kondo, Phys. Lett. B514 (2001) 335–345.
14. H. Vershelde, K. Knecht, K. Van Acoleyen, M. Vanderkelen, Phys. Lett. B516 (2001) 307–313.
15. M. A. L. Capri, D. Dudal, J. A. Gracey, V. E. R. Lemes, R. F. Sobreiro, S. P. Sorella and H. Vershelde, Phys. Rev. D 74 (2006) 045008.
16. P. Boucaud, et al., Phys. Rev. D63 (2001) 114003.
17. E. Ruiz Arriola, P. O. Bowman, W. Broniowski, Phys. Rev. D70 (2004) 097505.

18. E. Megias, E. Ruiz Arriola, L. L. Salcedo, JHEP 01 (2006) 073.
19. A. E. Dorokhov, W. Broniowski, Eur. Phys. J. C32 (2003) 79–96.
20. V. I. Zakharov, Nucl. Phys. Proc. Suppl. 164 (2007) 240–247.
21. S. Narison, Nucl. Phys. Proc. Suppl. 164 (2007) 225–231.
22. A. V. Anisovich, V. V. Anisovich, A. V. Sarantsev, Phys. Rev. D62 (2000) 051502.
23. L. Y. Glozman, Phys. Lett. B539 (2002) 257–265.
24. L. Y. Glozman, Phys. Lett. B587 (2004) 69–77.
25. G. Ecker, J. Gasser, A. Pich, E. de Rafael, Nucl. Phys. B321 (1989) 311.
26. O. Kaczmarek, F. Zantow, Phys. Rev. D71 (2005) 114510.
27. E. Ruiz Arriola, W. Broniowski, Phys. Rev. D74 (2006) 034008.
28. E. Ruiz Arriola, W. Broniowski, Eur. Phys. J. A 31 (2007) 739



## In order to form a more perfect fluid ... Is there a fundamental bound on $\eta/s$ for fluids?

Thomas D. Cohen

Department of Physics, University of Maryland, College Park, MD 20742-4111

The talk presented at Bled 2007, dealt with an issue superficially very far from the main thrust of the workshop—namely the question of whether or not there is a lower bound on the ratio of the shear viscosity ( $\eta$ ) to the entropy density has a fundamental lower bound. However, surprisingly the properties of hadrons in a controlled limit of QCD play an essential role. The context of this problem is a remarkable result based on the famed AdS/CFT correspondence in which all it is shown that all theories which have a supergravity dual when taken in the large  $N_c$  and infinite 't Hooft coupling limits have  $\eta/s = (4\pi)^{-1}$ . It is very plausible within this class of theory that the ratio goes up one moves from the infinite 't Hooft coupling limit. Motivated by this, a conjecture was proposed by Kovtan, Son and Starinets (KSS): namely that  $(4\pi)^{-1}$  was a lower bound for  $\eta/s$  for *all* fluids. However, it is readily apparent that one can construct theoretical systems in nonrelativistic quantum mechanics which violate the conjectured bound. This is done by making a system with *very* many species of particles so that the Gibbs mixing entropy becomes large while the viscosity remains essentially the same as for few species. One might try to evade such a counter example by arguing that bound is not a consequence of quantum mechanics but rather of quantum field theory. However, what was shown in this talk was that a system based a well-defined quantum field theory also violates the bound. The system is a gas of heavy mesons in a very carefully constructed generalization of QCD. In this generalization the number of heavy flavors, the number of colors and the mass of the heavy quark all scale are all taken to be large (in a particular controlled way) while the temperature and density of the system are taken to be small (also in a controlled way). The fluid constructed in this way is metastable but can be made arbitrarily long lived. Thus, one concludes that quantum field theory alone does not imply the KSS bound—at least for metastable fluids. The issue is discussed in detail in two papers (T.D. Cohen Phys. Rev. Lett. **99** 021602 (2007) and A. Cherman, T.D. Cohen, P.M. Hohler, arXiv:0708.4201); the reader is referred there for details.



# Does nucleon parity doubling imply $U_A(1)$ symmetry restoration?\*

V. Dmitrašinović<sup>a</sup>, K. Nagata<sup>b</sup>, A. Hosaka<sup>c</sup>

<sup>a</sup> Vinča Institute of Nuclear Sciences, lab 010, P.O.Box 522, 11001 Beograd, Serbia

<sup>b</sup> Department of Physics, Chung-Yuan Christian University, Chung-Li 320, Taiwan

<sup>c</sup> Research Center for Nuclear Physics, Osaka University, Mihogaoka 10-1, Osaka 567-0047, Japan

**Abstract.** We examine the role of  $U_A(1)$  symmetry and its breaking/restoration in two complete chiral multiplets consisting of the nucleon and the Roper and their two “chiral mirror” odd-parity resonances. We base our work on the recent classification of the chiral  $SU_L(2) \times SU_R(2)$  transformation properties of the two (Ioffe) independent local tri-quark nucleon interpolating fields in QCD [1].

## 1 Introduction

Over the past five years there has been considerable activity on the question if the chiral  $U_A(1)$  symmetry restoration is in any way related to the (purported) parity doubling in the nucleon spectrum [2,3]. In the previous additions to the literature [2], following an old and to a large extent formal example by Ben Lee [4], it was assumed that the nucleons admitted only certain specific linear non-Abelian chiral transformation properties - no assumptions were made about the Abelian ones, however.

Rather than guess at the chiral properties of the nucleon, we use the results of our study [1] of the  $SU_L(2) \times SU_R(2)$  and  $U_A(1)$  (the non-Abelian and the Abelian chiral symmetries, respectively) transformations of the over-complete set of (five) three-quark non-derivative (local) nucleon interpolating fields. We showed that the two independent nucleon fields form two different irreducible  $U_A(1)$  representations: one with the axial baryon number minus one (the Abelian “mirror” field), and another with three (the Abelian triply “naive” nucleon in the parlance of Ref. [5]).

For odd-parity nucleons, on the other hand, the inclusion of at least one space-time derivative is natural. Once we allow for a derivative to exist in the interpolating field, we find two nucleon fields with chiral properties opposite to the non-derivative ones, e.g. the non-Abelian chiral properties of the derivative fields are “mirror” compared to the “naive” non-derivative ones. Thus, altogether we have four independent nucleon fields constructed from three quarks with or

---

\* Talk delivered by V. Dmitrašinović

without one derivative. They can be classified as being non-Abelian “naive” or “mirror” and similarly for the Abelian chiral transformation properties.

As an illustrative example, we identify these four specific nucleon fields with the four lowest-lying nucleon resonances: the nucleon-Roper even-parity pair and the  $N^*(1535)$ ,  $N^*(1650)$  pair of odd-parity resonances, and construct an effective Lagrangian with the  $U_A(1)$  and  $SU_L(2) \times SU_R(2)$  symmetries. We show that, after spontaneous symmetry breakdown to  $SU(2)_V$ , the mass splitting induced by this effective interaction can reproduce all four nucleon’s masses *even without explicit  $U_A(1)$  symmetry breaking*. This is an explicit counter-example to the statement in the literature that the parity doubling in the nucleon spectrum is related to the restoration of the  $U_A(1)$  symmetry.

Our method applies equally well to any, and not just the low-lying,  $U_A(1)$  chiral quartet, i.e., pair of nucleon parity doublets. Of course, this result is subject to the assumption of three-quark nature of the corresponding nucleon states.

## 2 Three-quark nucleon interpolating fields

We start by summarizing the transformation properties of various quark trilinear forms with quantum numbers of the nucleon as shown in Ref. [1]. It turns out that every nucleon, i.e., spin- and isospin 1/2 field, besides having same non-Abelian transformation properties, comes in two varieties: one with “mirror” and another with “triple-naive” Abelian chiral properties. This allows us to address the old (Ioffe) problem of duplication/ambiguity of nucleon fields: For  $J^P = \frac{1}{2}^+$  nucleons there is only one non-Abelian representation allowed, the  $(\frac{1}{2}, 0) \oplus (0, \frac{1}{2})$ , but with the two afore-mentioned Abelian chiral properties, thus lending physical distinction to Ioffe’s two nucleon fields: the nucleon ground state, the two odd-parity resonances and the Roper are the four mutually orthogonal admixtures of the Abelian “mirror”- (so called Ioffe current), the Abelian “triple naive”- and their non-Abelian mirror fields.

**Table 1.** The Abelian axial charges (+ sign indicates “naive”, - sign “mirror” transformation properties) and the non-Abelian chiral multiplets of  $J^P = \frac{1}{2}^+$  nucleon interpolating fields in the Lorentz group representation  $D(\frac{1}{2}, 0)$  without derivatives. In the last column we show the Fierz identical fields, see [1].

	$U_A(1)$	$SU_A(2)$	$SU_V(2) \times SU_A(2)$	Fierz identical
$N_1 - N_2$	-1	+1	$(\frac{1}{2}, 0) \oplus (0, \frac{1}{2})$	$N_3, N_4$
$N_1 + N_2$	+3	+1	$(\frac{1}{2}, 0) \oplus (0, \frac{1}{2})$	$N_5$

We can construct nucleon fields with “opposite” chiral transformations to those shown above by replacing  $\gamma_\mu$  with  $i\partial_\mu$ : for example we may use the following two nucleon interpolating fields involving three quarks and one derivative

$$N_1'^- = \epsilon_{abc} i\partial_\mu (\tilde{q}_a q_b) \gamma^\mu \gamma^5 q_c, \quad (1)$$

$$N_2'^- = \epsilon_{abc} i\partial_\mu (\tilde{q}_a \gamma^5 q_b) \gamma^\mu q_c. \quad (2)$$

They are odd-parity, spin 1/2 and isospin 1/2 fields, i.e. they describe (some) nucleon resonances. A prime in the superscript implies that the fields contain a derivative, and we show below that therefore they have opposite, i.e., “mirror” non-Abelian chiral transformation properties to those of the corresponding non-derivative fields.

Taking the symmetric and antisymmetric linear combinations of two nucleon fields  $N'_{1,2}$  as the new canonical fields

$$N'_m = \frac{1}{\sqrt{2}}(N'_1 + N'_2) \quad (3)$$

$$N'_n = \frac{1}{\sqrt{2}}(N'_1 - N'_2), \quad (4)$$

their Abelian chiral transformation properties read

$$\delta_5 N'_m = -3i\alpha\gamma_5 N'_m \quad (5)$$

$$\delta_5 N'_n = i\alpha\gamma_5 N'_n, \quad (6)$$

whereas the non-Abelian ones remain “mirror”

$$\delta_5 N'_{m,n} = -i\gamma_5 \boldsymbol{\tau} \cdot \boldsymbol{\alpha} N'_{m,n}. \quad (7)$$

In summary, we have explicitly constructed four independent nucleon fields: two fields with “naive” and two fields with “mirror” Abelian and non-Abelian chiral transformation properties. In the present paper, we identify these fields with the nucleon ground state  $N(940)$  and its resonances  $N(1440)$ ,  $N(1535)$  and  $N(1650)$ . We summarize the properties of the four fields in Table.2. With these fields we can construct the “naive-mirror” interactions.

**Table 2.** The axial charges of the nucleon fields.

Interpolating fields	$U_A(1)$	$SU_A(2)$	Assigned states
$N_m$	-1	+1	$N(940)$
$N_n$	+3	+1	$N(1440)$
$N'_n$	+1	-1	$N(1650)$
$N'_m$	-3	-1	$N(1535)$

### 3 The $U_A(1)$ symmetry in baryons

The  $U_A(1)$  symmetry’s explicit breaking due to the triangle anomaly and topologically non-trivial configurations in QCD has only a few firmly established observable consequences, all of which are in the flavor-singlet spin-less meson sector, see Ref. [11] and references therein, with lots of recent speculation about its role in the baryon sector (“parity doubling”), especially with regard to its alleged/purported “restoration high up in the hadron spectrum” Ref. [2]. This scenario has effectively been disproven in the meson case in Refs. [2].

The baryon case is much more difficult to handle, due to, *inter alia*, a fundamental lack of knowledge of the baryon chiral transformation properties. In the baryon sector, the empirically observed parity doubling has been quantitatively analyzed by Jaffe et. al. [3], who proposed that the physics behind that might be the (explicitly broken)  $U_A(1)$  symmetry. In the absence of direct lattice measurements the best one can do is resort to chiral models.

Lee, DeTar, Kunihiro, Jido, Oka and others [4,5] have developed a Lagrangian formalism based on one pair of “naive” and “mirror” opposite-parity nucleon fields. They did not consider the  $U_A(1)$  symmetry, however. Christos [8] has shown that there are two independent cubic interactions for each parity doublet that preserve both  $U_A(1)$  and  $SU(2)_L \times SU(2)_R$  symmetry. However Christos did not include Abelian chiral mirror fields, so he obtained vanishing off-diagonal  $\pi NN^*$  couplings. Our strategy was first to construct the  $SU_L(2) \times SU_R(2)$  chiral invariant interaction(s) for two pairs of nucleon ( $N_{m,n}^+$  and  $N_{m,n}'^-$ ) fields; and then to include the  $U_A(1)$  symmetry [12]. We have classified these terms according to the power of the meson fields. We found that besides the linear (in meson fields) interactions there are also quadratic and cubic ones. The form of these interactions is uniquely dictated by the  $U_A(1)$  symmetry; higher-order terms may appear only as products of these three lower-order ones. That allows altogether six interactions: four diagonal ones in the two doublets and two “inter-doublet” ones. Furthermore, we included all quadratic terms allowed by the non-Abelian “mirror” properties of the baryons. Then we found that one does not need any  $U_A(1)$  symmetry breaking to describe the nucleon mass spectrum, provided one uses a complete set of interactions.

## 4 Results

In the following discussion, it is convenient to group the four nucleon fields as follows;  $\Psi = (N_m^+, N_n'^-)$  for the pair of the single Abelian charge (the single-Abelian doublet), and  $\Phi = (N_n^+, N_m'^-)$  for that of the triple Abelian charge (the triple-Abelian doublet). We emphasize that the two nucleons in each of these pairs are in “mirror” relations to each other, with regard to both the Abelian and non-Abelian chiral symmetries. Manifestly, the identification of fields, or their admixtures, with actual resonances *viz.*  $N(940)$ ,  $R(1440)$ ,  $N^*(1535)$  and  $N^*(1650)$  is not unique. In this brief review we consider only one choice; another scenario is considered in Ref. [12]. A substantial body of QCD sum rule evidence is pointing towards  $N(940)$  being the “Ioffe current”  $N_{1m}^+$ . Together with the lowest negative parity nucleon  $N(1535)$  in the partner of the parity doublet, we have  $\Psi = (N_m^+, N_n'^-)$  =  $(N(940), N(1535))$  and consequently  $\Phi = (N_n^+, N_m'^-)$  =  $(N(1440), N(1650))$ .

The nucleon mass matrix is already in a simple block-diagonal form when the nucleon fields form the following  $1 \times 4$  row/column “vector”:

$$(\Psi, \Phi) = (N_m^+, N_n'^-, N_n^+, N_m'^-) \rightarrow (N_m^+, \gamma_5 N_n'^-, N_n^+, \gamma_5 N_m'^-),$$

$$\lim_{U_A(1)\text{symm.}} M = \begin{pmatrix} g_1 f_\pi & m_{12}\gamma_5 & 0 & g_5 f_\pi \gamma_5 \\ m_{12}\gamma_5 & g_2 f_\pi & g_6 f_\pi \gamma_5 & 0 \\ 0 & g_6 f_\pi \gamma_5 & g_3 f_\pi & m_{34}\gamma_5 \\ g_5 f_\pi \gamma_5 & 0 & m_{34}\gamma_5 & g_4 f_\pi \end{pmatrix}. \quad (8)$$

Note that only the parity-changing interaction  $g_{5,6}$  mixes these two new equal parity doublets. Without inter-doublet interactions ( $g_{5,6} = 0$ ) one can immediately read off the eigenvalues following Ref. [5]. We determine the coupling and mass parameters and show them in Table 3 and Fig. 1.

**Table 3.** Coupling constants obtained from the nucleon masses with doublets (N(940), N\*(1535)), (R(1440), N\*(1650)) and the decay widths  $N^*(1535) \rightarrow \pi N(940)$  and  $N^*(1650) \rightarrow \pi R(1440)$ .

constant	$g_1$	$g_2$	$m_{12}$	$g_3$	$g_4$	$m_{34}$
value	10.4	16.8	270 MeV	14.6	16.8	503 MeV

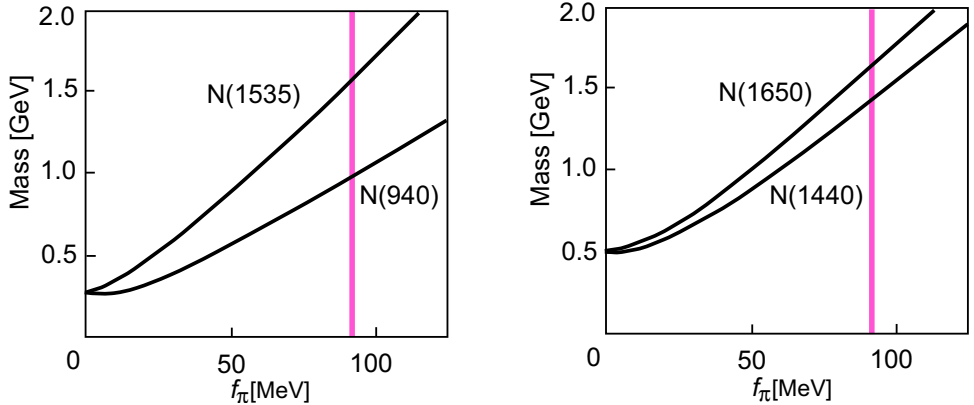


**Fig. 1.** The nucleon masses as functions of  $\langle \sigma \rangle_0$ .

Manifestly, the good  $U_A(1)$  symmetry limit is sufficient to reproduce the nucleon spectrum. Thence our **main conclusion**: *the mass degeneracy of opposite-parity nucleon resonances is not a consequence of the explicit  $U_A(1)$  symmetry (non) breaking.* This conclusion was also reached by Christos [8], albeit for one parity doublet and without mirror fields, which means that his  $N^*(1535)$  can not decay into  $N(940)$  by  $\pi$  emission.

## 5 Summary and Discussion

We have analyzed the  $U_A(1)$  symmetry in the nucleon-Roper-two-odd-parity-nucleon-resonances system, under the assumption that the above four nucleon

states are described by a particular set of independent interpolating fields. The four nucleon fields naturally split into two “parity doublets” due to their  $U_A(1)$  symmetry transformation properties.

Our analysis has been based on the Born approximation: Higher-order (one-, two-, etc. meson loop) corrections belong to the  $\mathcal{O}(1/N_c)$  corrections, that have been studied only intermittently in chiral quark models of the nucleon and then only in certain simple models with one kind of nucleon. In principle, instanton effects are expected to vanish in the large- $N_c$  limit, which justifies our assumption of good  $U_A(1)$  symmetry, *ex post facto*. The extracted value of the “bare mirror” nucleon mass ( $m_{12}=270$  MeV, see also Ref. [6]) is something that can be checked on the lattice, now that the interpolating fields have been specified for the mirror nucleons.

The insight that the nucleon and the Roper fields may form two different representations of the  $U_A(1)$  symmetry, and that their mass difference can be viewed as a consequence of  $U_A(1)$  symmetry conservation and not of the symmetry breaking, are the main results of this work. A corollary of this result is that the parity-doublet mass splittings are not entirely determined by the  $U_A(1)$  symmetry breaking, as was conjectured in the literature [3]. Moreover, the nucleon-Roper mass difference in some calculations, such as the one of Ref. [10] in the NJL model, are not a consequence of the broken  $U_A(1)$  symmetry in that model.

$U_A(1)$  symmetry in nucleon spectra has been discussed before, most notably by Christos [8], who used only one parity doublet ( $N(940)$  and  $N^*(1535)$ ), however. He argued that the parity doublet mass difference is proportional to a particular  $\eta NN^*$  coupling constant, which is in close agreement with our results. He did not try to relate other mass differences, such as the Roper-nucleon one, to this mechanism, as he did not know of an alternative (“mirror”) set of fields, which is a novel feature/contribution of our paper. Consequently his  $N^*(1535)$  can not decay into  $N(940)$  by  $\pi$  emission, in blatant conflict with experiment.

## References

1. K. Nagata, A. Hosaka and V. Dmitrašinović, arXiv:0705.1896 [hep-ph].
2. T. D. Cohen and L. Ya. Glozman, Phys.Rev.D **65**, 016006 (2002); Int.J.Mod.Phys. **A 17**, 1327 (2002).
3. R. L. Jaffe, D. Pirjol and A. Scardicchio, Phys. Rev. Lett. **96** (2006) 121601, and R. L. Jaffe, D. Pirjol and A. Scardicchio, Phys. Rept. **435** (2006) 157.
4. B. W. Lee, *Chiral Dynamics*, (Gordon and Breach, New York, 1972).
5. D. Jido, M. Oka and A. Hosaka, Prog. Theor. Phys. **106**, 873 (2001).
6. C. DeTar and T. Kunihiro, Phys. Rev. D **39**, 2805 (1989).
7. B.L. Ioffe, Nucl. Phys. **B 188**, 317 (1981); *ibid.* **B 191**, 591 (1981) (E); Z. Phys. **C 18**, 67 (1983).
8. G.A. Christos, Z. Phys. **C 21**, 83 (1983); Phys. Rev. **D 35**, 330 (1987).
9. D. Jido, M. Oka and A. Hosaka, Phys. Rev. Lett. **80**, 448 (1998).
10. K. Nagata and A. Hosaka, J. Phys. G **32** (2006) 777 ; K. Nagata, A. Hosaka, Laith J. Abu-Raddad, Phys.Rev. **C72**:035208 (2005), (E)-*ibid.* **C 73**:049903 (2006).
11. V. Dmitrašinović, Phys. Rev. **C 53**, 1383 (1996), Nucl. Phys. **A 686**, 377 (2001); E. Klempt, B. C. Metsch, C. R. Münz, and H. R. Petry, Phys. Lett. **B 361**, 160 (1995); M. Hirata and

- N. Tsutsui, Phys. Rev. **D 56**, 5696 (1997); M. Takizawa, and T. Umekawa, Prog. Theor. Phys. **109**, 969 (2003) and T. Umekawa, K. Naito, M. Oka, and M. Takizawa, Phys.Rev. **C 70**:055205 (2004).
12. K. Nagata, A. Hosaka and V. Dmitrašinović, in preparation (2007).



## **Constituent quarks as quasiparticles of QCD**

Harald Fritzsch

Arnold Sommerfeld Center, University of Munich, Theresienstraße 37, D-8033 München



## Covariant description of the few-nucleon systems from chiral dynamics\*

L. Girlanda<sup>a</sup>, M. Viviani<sup>a</sup> and W.H. Klink<sup>b</sup>

<sup>a</sup>INFN, Sez. di Pisa, Largo Bruno Pontecorvo, 56127 Pisa, Italy

<sup>b</sup>Department of Physics and Astronomy and Department of Mathematics  
University of Iowa, Iowa City, Iowa 52242

**Abstract.** We discuss some aspects of our relativistic framework for the few-nucleon systems (Ref. [1] to which we refer for further details), which were discussed at the Workshop, particularly the issue of renormalization.

The understanding of the few-nucleon systems based on Chiral Perturbation Theory (ChPT, see Ref. [2] for a review), provides the link of nuclear physics with QCD: as a matter of fact the low-energy constants, in terms of which the chiral nuclear forces are expressed, are QCD Green functions, in principle calculable on the lattice. The ChPT setting is perturbative, in the sense that it is a low-energy expansion, the small parameter being the typical momentum  $p$  divided by the hadronic scale. This type of ordering is the only justification, from first principles, of the hierarchy of nuclear forces. Indeed ChPT predicts that 3-nucleon forces are suppressed by a factor  $O(p^2)$  compared to 2-nucleon forces, 4-nucleon forces by a factor  $O(p^4)$ , and so on. In order to maintain the power counting a non relativistic expansion of the ChPT Lagrangian is usually performed, referred to as heavy baryon ChPT (HBChPT). Moreover, in the original Weinberg's definition of a nucleon-nucleon effective potential, a non relativistic setting was used, based on old-fashioned (time ordered) perturbation theory. By these two steps relativistic corrections and chiral corrections get mixed together and are treated on the same footing. However relativity and chiral symmetry are symmetries on a completely different status: chiral symmetry (which is always approximate) can be useful in this context as an ordering criterium, whereas Poincaré invariance is required by Nature. There are several instances where one might want to have relativity exactly. Most importantly, a relativistic scheme would allow to describe particle production, which is out of the scope of non-relativistic quantum mechanics. Our aim is therefore to devise a scheme which satisfies all requirements of relativity and use chiral symmetry merely as a bookkeeping device to order terms, in order to have a systematic expansion. This is why we have considered the point-form formulation of relativistic quantum mechanics proposed in [3]. It relies on a Bakamjian-Thomas construction, which is a way (although not the most

---

\* Talk delivered by L. Girlanda

general one) to solve Dirac's covariance problem in the construction of a dynamical theory of interacting particles. The problem consists of finding expressions for the generators of the Poincaré group,  $H$ ,  $\mathbf{P}$ ,  $\mathbf{J}$  and  $\mathbf{K}$  in terms of the coordinates of the particles. In the usual formulation (instant-form of the dynamics) the interactions are contained in the Hamiltonian  $H$  and in the boost generators  $\mathbf{K}$ , while the other operators are said kinematical, they are the same as in the non-interacting theory. In the point-form the interactions are contained in all components of the four-momentum, whereas Lorentz transformations are kinematical. In the Bakamjian-Thomas construction this is accomplished by introducing auxiliary operators, the mass operator  $M_0 = \sqrt{\mathbf{P}_0^2 \mathbf{P}_{0\mu}}$  and a four-velocity operator  $V^\mu$  such that  $\mathbf{P}_0^\mu = M_0 V^\mu$  (the subscripts 0 refer to the non-interacting theory); one then adds the interactions only to the mass operator  $M = M_0 + M_I$ , and reconstructs the interacting four-momentum as  $P^\mu = M V^\mu$ . Poincaré commutation relations are then satisfied provided the interacting mass operator is a Lorentz scalar which commutes with the four-velocity  $V^\mu$ . It is therefore particularly convenient to consider the "velocity states"  $|v\rangle$  [3]: these are linear combinations of multiparticle momentum states which are eigenstates of the four-velocity operator. However, starting from a quantum-field theoretical Lagrangian the interacting four-momentum is

$$P_I^\mu = \int d^4x \frac{\partial F(x)}{\partial x^\mu} \delta(F(x) - \tau^2) \mathcal{H}_I(x), \quad (1)$$

where in the point-form  $F(x) = x^2$ . This operator is not diagonal in the four-velocity,

$$\langle v | P_I^\mu | v' \rangle = \langle v | \mathcal{H}_I(0) | v' \rangle \int d^4x \delta(x^2 - \tau^2) 2x^\mu \theta(x_0) e^{-i(mv - m'v')x} \quad (2)$$

and therefore it is not of the Bakamjian-Thomas type. In order to enforce that, one has to introduce a velocity-conserving delta-function by hand, such that the interacting four-momentum has matrix elements of the form

$$\langle v | P_I^\mu | v' \rangle = (2\pi)^3 \delta^3(\mathbf{v} - \mathbf{v}') v^\mu \frac{f(m, m')}{\sqrt{m^3 m'^3}} \langle v | \mathcal{H}_I(0) | v' \rangle. \quad (3)$$

The form factor  $f(m, m')$ , depending on the relativistic energies, is meant to compensate somehow for the neglect of the off-diagonal elements in the velocity, and also to regulate the ultraviolet behaviour. The square-root factor in the denominator is included so that one recovers the quantum-field theoretical result when  $v = v'$  and  $m = m'$  with  $f = 1$ . We have taken for  $f$  a real symmetric function of its arguments, further specified as a Gaussian function centered around zero with cutoff  $\Lambda$ ,

$$f(m, m') = \exp \left[ -\frac{(m - m')^2}{2\Lambda^2} \right] \xi. \quad (4)$$

The cutoff  $\Lambda$  is to be understood as the scale at which new physics starts to become relevant. There will be one such form factor for each vertex of the interaction Hamiltonian. For some vertices the gaussian alone is not enough to regulate all

integrals, so one has to include an additional cutoff  $\xi$ , function of the relativistic invariants.

For illustration purposes, we consider the simple case of a scalar nucleon field  $\Psi$  interacting with a pion field  $\phi$ , with the interactions provided by a Hamiltonian density of the form  $\mathcal{H}(x) = g\Psi^\dagger(x)\Psi(x)\phi(x)$ . Creation of nucleon-antinucleon pairs is neglected and a truncation of the Fock space to a given maximum number of pions is considered from the beginning. In the 1-nucleon sector, truncating the states containing two or more pions, the mass operator takes the form

$$M = \begin{pmatrix} m_N + \delta_1^{\text{ren}} & gK \\ gK^\dagger & D_{1+1} \end{pmatrix}, \quad (5)$$

where  $m_N$  is the physical nucleon mass, and  $D_{1+1}$  is the relativistic 1-nucleon + 1-pion free particle energy. The counterterm  $\delta_1^{\text{ren}}$  is needed for the mass renormalization. Due to the form of  $\mathcal{H}(x)$ , the interactions show up as off-diagonal entries in the mass operator. The nucleon mass renormalization and pion-nucleon scattering are described as eigenvalue-eigenvector problems for this mass operator. For instance, for the eigenvalue  $m_N$ , the physical nucleon mass, one finds an equation for the counterterm

$$\delta_1^{\text{ren}} = g^2 K^\dagger (D_{1+1} - m_N)^{-1} K, \quad (6)$$

with  $D_{1+1} = \omega_{\mathbf{k}} + \omega_{\mathbf{k}}^\pi$ , having defined  $\omega_{\mathbf{k}} \equiv \sqrt{m_N^2 + \mathbf{k}^2}$  and  $\omega_{\mathbf{k}}^\pi = \sqrt{M_\pi^2 + \mathbf{k}^2}$ . Taking the expectation value of the above equation between 1-nucleon states and inserting a complete set of velocity states in the subspace of 1-nucleon + 1-pion states one arrives at the nucleon mass renormalization due to the ‘‘pion cloud’’,

$$\delta_1^{\text{ren}} = \frac{g^2}{2m_N} \int \frac{d^3\mathbf{k}}{(2\pi)^3} \frac{1}{4\omega_{\mathbf{k}}\omega_{\mathbf{k}}^\pi} \frac{|f^{(1)}(m_N, \omega_{\mathbf{k}} + \omega_{\mathbf{k}}^\pi)|^2}{\omega_{\mathbf{k}} + \omega_{\mathbf{k}}^\pi - m_N}. \quad (7)$$

The superscript  $(1)$  refers to the sector of the Fock space with baryon number 1: the mass operator commutes with the baryon number, and there is the freedom to choose a different structure function  $f$  for each sector of the Fock space.

In the 2-nucleon sector, an analogous equation describes the deuteron,

$$(D_2 + \delta_2^{\text{ren}}) \phi_2^D + g^2 K^\dagger (m_D - D_{2+1})^{-1} K \phi_2^D = m_D \phi_2^D, \quad (8)$$

where  $\phi_2^D$  is a state vector in the subspace of 2-nucleon states, and the operators  $D_2$  and  $D_{2+1}$  are respectively the relativistic 2-nucleon and 2-nucleon + 1-pion energy. As in the 1-nucleon sector, a counterterm  $\delta_2^{\text{ren}}$  is introduced in the corresponding diagonal element of the mass operator, in order to properly renormalize the 2-particle states. By left-multiplying Eq. (8) with the bra  $\langle v, \mathbf{k}, -\mathbf{k} |$  representing a 2-nucleon state with four velocity  $v$  and relative momentum (in the center-of-mass system)  $2\mathbf{k}$ , one arrives, after insertion of a complete set of states in the subspace of 2-nucleon + 1-pion states, to an eigenvalue wave equation for the center-of-mass wave function  $\phi_2^D(\mathbf{k}) = \langle v = (1, \mathbf{0}), \mathbf{k}, -\mathbf{k} | \phi_2^D \rangle$ ,

$$(2\omega_{\mathbf{k}} + \delta_2^{\text{ren}}(\mathbf{k})) \phi_2^D(\mathbf{k}) + 2\omega_{\mathbf{k}} A(\mathbf{k}) \phi_2^D(\mathbf{k}) + \int \frac{d^3\mathbf{q}}{(2\pi)^3} B(\mathbf{k}, \mathbf{q}) \phi_2^D(\mathbf{q}) = m_D \phi_2^D(\mathbf{k}), \quad (9)$$

The term proportional to  $A(\mathbf{k})$  represents a wave function renormalization of the two-nucleon state: it describes diagrams in which the nucleon lines are disconnected and dressed with pion loops. Its explicit expression reads

$$A(\mathbf{k}) = \int \frac{d^3\mathbf{q}}{(2\pi)^3} \left\{ \frac{g^2}{16\omega_{\mathbf{k}}^2\omega_{\mathbf{q}}\omega_{\mathbf{k}+\mathbf{q}}^\pi} \left| \frac{f^{(2)}(2\omega_{\mathbf{k}}, \omega_{\mathbf{k}} + \omega_{\mathbf{q}} + \omega_{\mathbf{k}+\mathbf{q}}^\pi)}{m_D - \omega_{\mathbf{k}} - \omega_{\mathbf{q}} - \omega_{\mathbf{k}+\mathbf{q}}^\pi} \right|^2 + \mathbf{q} \leftrightarrow -\mathbf{q} \right\}. \quad (10)$$

We can choose the counterterm  $\delta_2^{\text{ren}}$  so as to cancel the disconnected kernel,  $\delta_2^{\text{ren}}(\mathbf{k}) = -2\omega_{\mathbf{k}}A(\mathbf{k})$ . Correspondingly, the NN scattering is described by the Lippmann-Schwinger equation for the scattering amplitude,

$$T(\mathbf{q}, \mathbf{k}) = V(\mathbf{q}, \mathbf{k}) + \int \omega_{\mathbf{p}} \frac{d^3\mathbf{p}}{(2\pi)^3} \frac{V(\mathbf{q}, \mathbf{p})T(\mathbf{p}, \mathbf{k})}{\sqrt{s} - 2\omega_{\mathbf{p}} + i\epsilon}, \quad (11)$$

where the potential consists only of the connected kernel  $B$ ,

$$V(\mathbf{q}, \mathbf{k}) = g^2 \langle v, \mathbf{q}, -\mathbf{q} | K^\dagger [\sqrt{s} - D_{2+1}]^{-1} K |_{\text{conn}} | v, \mathbf{k}, -\mathbf{k} \rangle = B(\mathbf{q}, \mathbf{k}). \quad (12)$$

The renormalization of the 2-nucleon lines describing NN scattering, realized by the choice of the counterterm  $\delta_2^{\text{ren}}(\mathbf{k}) = -2\omega_{\mathbf{k}}A(\mathbf{k})$ , and of the 1-nucleon line, Eq. (7), correspond to the same physical processes, as can be seen diagrammatically. Physical considerations would require that, when the two nucleons are far apart and at rest, their energies should be renormalized as their respective masses. This implies the condition

$$\delta_2^{\text{ren}}(\mathbf{0}) = 2\delta_1^{\text{ren}}, \quad (13)$$

which can be regarded as the manifestation of the cluster decomposition principle in the simple case of two particles. We can see by direct inspection, replacing in Eq. (10)  $m_D$  by  $\sqrt{s} = 2m_N$ , since we are considering the case of two widely separated nucleons at rest, that the equation is fulfilled provided  $f^{(1)} = f^{(2)} = f$ , with  $f$  depending on  $m - m'$  as in Eq. (4), independently of the baryon number sector. Notice that this would not happen had we chosen the original formulation of Ref. [3]: the crucial point was the inclusion of a different normalization for the matrix elements of the interacting mass operator, Eq. (3), which in turn was dictated by a proper matching to the quantum field theory. The cluster decomposition principle, satisfied by local quantum field theories, could in general be violated by a truncation of the full quantum field theory to a relativistic quantum mechanics. In view of the above consideration, we can drop the superscripts and use the same structure function  $f$  for all sectors of the Fock space.

Having identified the general features of the construction of the interacting mass operator from a vertex Lagrangian, one can proceed to make full use of the constraints given by chiral symmetry. Most importantly, the Goldstone theorem requires that the coupling between pion and nucleons be of derivative type (suppressed at low energy). This provides a power-counting justification for the truncation of the Fock space, since the creation of pions brings more and more

powers of momentum. The complete combined analysis of  $\pi N$  and  $NN$  systems at the leading order of the chiral counting can be found in Ref. [1]. By comparison with the non relativistic limit (realized in our framework as  $m_N \rightarrow \infty$ ), the (all order) relativistic effects are found to be smaller than the NLO chiral corrections, in the  $NN$  case, while they are sizeable in the  $\pi N$  case.

I thank Mitja Rosina, Bojan Golli and Simon Sirca for the very nice Workshop.

## References

1. L. Girlanda, M. Viviani and W. H. Klink, *Phys. Rev. C* **76**, 044002 (2007).
2. E. Epelbaum, *Prog. Part. Nucl. Phys.* **57** (2006) 654.
3. W. H. Klink, *Nucl. Phys. A* **716** (2003) 123; *Phys. Rev. C* **58** (1998) 3617.



## Excited baryons and QCD symmetries

L. Ya. Glozman

Institute for Theoretical Physics, University of Graz, Universitätsplatz 5, A-8010 Graz,  
Austria

Recent developments for chiral and  $U(1)_A$  restorations in excited baryons and more generally in hadrons are reviewed. We discuss predictions of the chiral symmetry restoration scenario for axial charges and couplings to Goldstone bosons. Strict chiral restoration in a given baryon predicts that its axial charge must be zero and it must decouple from the pion. It is unclear, however, how to measure these quantities. Using very general chiral symmetry arguments it is shown that strict chiral restoration in a given excited nucleon forbids its decay into the  $N\pi$  channel. We confront this prediction with the  $N^*N\pi$  coupling constants extracted from the decay widths and observe a 100 % correlation of these data with the spectroscopic parity doublet patterns. These results suggest that the lowest approximate chiral parity doublet is the  $N(1440) - N(1535)$  pair. In the meson sector we discuss predictions of the chiral symmetry restoration for still missing states and a signature of the higher symmetry observed in new  $\bar{p}p$  data. The observed large degeneracy might be understood if, on top of chiral restoration, a principal quantum number  $N=n+J$  existed. We conclude with the exactly solvable chirally symmetric and confining model that can be considered as a generalization of the 1+1 dimensional 't Hooft model to 4 dimensions. Complete spectra of  $\bar{q}q$  mesons demonstrate a fast chiral restoration with increasing  $J$  and a slow one with increasing  $n$ .

### References

1. L. Ya. Glozman, Phys. Rep. **444**, 1 (2007).
2. L. Ya. Glozman, arXiv:0706.3288 [hep-ph], Phys. Rev. Lett., in print.
3. L. Ya. Glozman and A. V. Nefediev, arXiv:0704.2673 [hep-ph], Phys. Rev. D., in print
4. R. F. Wagenbrunn and L. Ya. Glozman, Phys. Lett. **B 643**, 98 (2006); Phys. Rev. **D 75**, 036007 (2007).



## Modeling the QCD Vacuum

W. H. Klink

Department of Physics and Astronomy University of Iowa, Iowa City, Iowa

**Abstract.** A central issue in quantum field theory and in particular QCD is to find the physical vacuum state. Point form quantum field theory provides a useful setting in which to model the physical vacuum state. In this note the defining equations and elementary properties of the physical vacuum are discussed in the context of the point form. A simple model is presented which illustrates some of the general ideas.

In point form relativistic quantum mechanics [1] all interactions are in the four-momentum operator  $P^\mu$  and Lorentz transformations are kinematic. The equations that express the relativistic content of a point form theory are

$$[P_\mu, P_\nu] = 0 \quad (1)$$

$$U_\Lambda P_\mu U_\Lambda^{-1} = (\Lambda^{-1})^\nu{}_\mu P_\nu, \quad (2)$$

where  $U_\Lambda$  is the unitary operator representing the Lorentz transformation  $\Lambda$  on some model Hilbert or generalized Fock space.

Given a four-momentum operator, the goal is to solve the eigenvalue problem

$$P^\mu |\Psi_p\rangle = p^\mu |\Psi_p\rangle \quad (3)$$

and from this get the physical vacuum, bound and scattering states.

There are several ways of generating four-momentum operators  $P^\mu$  that satisfy the point form equations. One, called the Bakamjian-Thomas method [2], is relevant for finite degree of freedom systems. The other, integrating free fields over the forward hyperboloid [3], is of primary interest in this paper.

If a four-momentum operator is constructed that satisfies the above point form equations, solving the vacuum problem means finding a vector  $|\Omega\rangle$  in a suitable space such that

$$P^\mu |\Omega\rangle = 0 \quad (4)$$

$$U_\Lambda |\Omega\rangle = |\Omega\rangle. \quad (5)$$

Here it should be noted that, unlike the situation in nonrelativistic quantum mechanics, where eigenvalues of a Hamiltonian are only defined up to a constant, and only energy differences are observable, it is not possible to add constants to the four-momentum operator and still maintain Lorentz covariance; that is, if

$P_\mu \rightarrow P'_\mu = P_\mu + c_\mu I$ , where the  $c$ 's are constants and  $I$  is the identity operator, then  $P'_\mu$  will not satisfy Eq.(2).

Just as a Hamiltonian can be written as the sum of free and interacting Hamiltonians, so also the four-momentum operator can be written as the sum of free and interacting four-momentum operators. If there are no interactions and  $P^\mu = P_{fr}^\mu$ , then the well known solution to the vacuum problem is the Fock vacuum. If an interaction is added, so that  $P^\mu = P_{fr}^\mu + \alpha P_I^\mu$ , then the vacuum solution, Eq.(4) must reduce to the Fock vacuum when the bare coupling constant  $\alpha = 0$ . Conversely, since it is not possible to add constants to the four-momentum operator, the solution to the vacuum problem, Eq.(4) entails the possibility of fine tuning the coupling constant  $\alpha$ . A simple model of such a possibility is given in the following paragraphs.

To investigate the vacuum structure it suffices to analyze only the zero component of Eq.(4), for if  $|\Omega\rangle$  is Lorentz invariant, Eq.(5), it follows that

$$U_\Lambda P^0 |\Omega\rangle = U_\Lambda P^0 U_\Lambda^{-1} U_\Lambda |\Omega\rangle \quad (6)$$

$$= ((\Lambda_0^0)^{-1} P^0 + (\Lambda_i^0)^{-1} P^i) |\Omega\rangle >$$

$$= (\Lambda_i^0)^{-1} P^i |\Omega\rangle >$$

$$= 0, \quad (7)$$

which implies that the momentum operator acting on the physical vacuum also gives zero, as required. Thus, in the following we will look only at the ground state eigenvalue problem for the energy operator  $P^0$ .

The purpose of this contribution to the Bled Workshop is to look at a single mode "approximation" to the energy operator of a full infinite degree of freedom system. Thus, let  $a_i, b_i, c_k$  denote respectively bare fermion, antifermion, and boson annihilation operators where the indices include both space-time (four-velocity  $v = \frac{p}{m}$  and spin projections) and internal variables such as charge or isospin. Then the free four-momentum operator can be written as

$$P^\mu(fr) := m \sum \int dv v^\mu (a_i^\dagger a_i + b_i^\dagger b_i + \kappa c_k^\dagger c_k), \quad (8)$$

where  $dv := \frac{d^3 v}{v_0}$  is the Lorentz invariant measure in four-velocity space,  $\kappa$  is a dimensionless relative bare boson mass parameter and  $m$  is a constant with the dimensions of mass; its value is determined by relating a physical mass such as the nucleon mass to the dimensionless eigenvalue of the corresponding stable particle. Because of the transformation properties of the creation and annihilation operators inherited from the one particle states, the free four-momentum operator, as defined in Eq.(8), satisfies the point form equations (1) and (2).

Interactions are obtained by integrating vertices, products of free fields, over the forward hyperboloid[3][4]. The fundamental vertex is the trilinear vertex, which is bilinear in fermion-antifermion creation and annihilation operators, and linear in boson creation and annihilation operators. That is, such vertices have the general form  $V \sim (a^\dagger + b)(a + b^\dagger)(c + c^\dagger) = (a^\dagger a + b b^\dagger + a^\dagger b^\dagger + b a)(c + c^\dagger)$  so,

as shown in reference [4] the interacting four-momentum operator for trilinear vertices can be written as

$$P^\mu(I) = \alpha \sum \int dv (\mathcal{A}(X_k^\mu) c_k + \mathcal{A}(X_k^\mu)^\dagger c_k^\dagger), \quad (9)$$

where  $\mathcal{A}(X_k^\mu) := (a_{i_1}^\dagger, b_{i_1})(X_k^\mu)_{i_1 i_2} (a_{i_2}, b_{i_2}^\dagger)^\top$ , and the  $X$ 's depend on the type of fermionic-bosonic coupling.

The zeroth component of the eigenvector equation, Eq.(3), is

$$P_F^0(\text{fr}) + \sum \int dv (\kappa v^0 c_k^\dagger c_k + \alpha \mathcal{A}(X_k^0) c_k + \alpha \mathcal{A}(X_k^0)^\dagger c_k^\dagger) |\Psi_\lambda\rangle = \lambda |\Psi_\lambda\rangle \quad (10)$$

To distinguish between the continuum energy operator in Eq.(10) and its finite approximation, the fundamental operator to be diagonalized is ( a Hamiltonian) denoted by  $H$ , made out of creation and annihilation operators with a finite number of modes, whose form mimics Eq.(10):

$$H = \sum e_i (a_i^\dagger a_i + b_i^\dagger b_i + \kappa c_i^\dagger c_i) + \alpha \sum \mathcal{A}(X_k) c_k + \mathcal{A}(X_k^\dagger) c_k^\dagger \quad (11)$$

$$= \sum e_i + \sum e_i (a_i^\dagger a_i - b_i b_i^\dagger + \kappa c_i^\dagger c_i) + \alpha (\mathcal{A}(X_i) c_i + \mathcal{A}(X_i^\dagger) c_i^\dagger) \quad (12)$$

$$= \sum e_i + \mathcal{A}(E) + \kappa \sum e_i c_i^\dagger c_i + \alpha \sum (\mathcal{A}(X_i) c_i + \mathcal{A}(X_i^\dagger) c_i^\dagger), \quad (13)$$

$$E := \text{diag}(e_1, e_2, \dots, e_N, -e_1, -e_2, \dots, -e_N), \quad (14)$$

where the discrete "energy"  $e_i = \sqrt{1 + v_i^2}$

Reference [4] shows that for a large choice of the  $X$ 's, the ground state for the Hamiltonian in Eq.(13) goes as  $-|\text{constant}|\alpha$  for  $\alpha \gg 1$ . Therefore there is no ground state solution equal to zero other than the free field solution.

One possibility is to add boson selfcoupling interactions. Consider a simple one mode Hamiltonian model, in which the selfcoupling is generated by the quartic anharmonic oscillator:

$$\begin{aligned} H &= \frac{1}{2}(x^2 + p^2) + \alpha^2 x^4 \\ &= c^\dagger c + \alpha^2 (c + c^\dagger)^4 \end{aligned} \quad (15)$$

References [4] and [5] show how the boson Lie algebra is given as the contraction limit of a compact Lie algebra (of the group  $U(2)$ ) whose Hamiltonian is

$$H_M = J_1 + \alpha^2 (\tilde{J}_+ + \tilde{J}_-)^4 \quad (16)$$

$$= \frac{M - J_z}{2} + \alpha^2 \rho^4 J_x^4 \quad (17)$$

$$= \frac{M + J_x}{2} + \frac{\alpha^2}{M^2} J_z^4, \quad (18)$$

and in the contraction limit, in which the Lie algebra contraction parameter  $\rho \rightarrow 0$  as  $M \rightarrow \infty$ , such that  $\rho M^2 = 1$ , the eigenvalues of  $H_M$ , Eq.(18) converge to the

eigenvalues of  $H$ , Eq.(15). In Eq.(17) the Lie algebra basis of  $U(2)$  has been written in a  $U(1) \times SU(2)$  basis, and in Eq.(18), the contraction parameter has been eliminated by writing  $\rho = \frac{1}{M^2}$ . The goal is to numerically find the lowest eigenvalues for fixed coupling as  $M$ , the  $U(2)$  irrep label, gets large. Using an  $SU(2)$  Lie algebra automorphism to interchange the  $x$  and  $z$  generators generates a tridiagonal matrix in the basis given in Eq.(18). Reference [4] shows that the true eigenvalue is approached for  $M$  about 100.

Next consider a one mode system coupling fermions and bosons, with no quartic boson selfcoupling. The Hamiltonians are now

$$H = 1 + (a^\dagger a - b b^\dagger) + c^\dagger c + \alpha(\mathcal{A}(X)c + \mathcal{A}(X^\dagger)c^\dagger) \quad (19)$$

$$= 1 + \mathcal{A}(E) + c^\dagger c + \alpha(\mathcal{A}(X)c + \mathcal{A}(X^\dagger)c^\dagger); \quad (20)$$

$$H_M = 1 + \mathcal{A}(E) + J_1 + \alpha(\mathcal{A}(X)J_- + \mathcal{A}(X^\dagger)J_+) \quad (21)$$

$$E = \begin{bmatrix} 1 & 0 \\ 0 & -1 \end{bmatrix}, X = \begin{bmatrix} 1 & 1 \\ 1 & 1 \end{bmatrix}. \quad (22)$$

For one mode the fermion space is two dimensional ( $|0 \rangle$  and  $a^\dagger b^\dagger |0 \rangle$ ) and the boson space is  $M+1$  dimensional. When  $H_M$  is diagonalized, the lowest eigenvalue linearly decreases with respect to the bare coupling constant  $\alpha$ , for  $\alpha \gg 1$ . Reference [4] shows this behavior of the ground state holds even for many mode systems.

Finally, if the boson selfcoupling term, the anharmonic term in Eq.(17) is added to the Hamiltonian, Eq.(21), the result is a model of trilinear coupling with a quartic boson selfcoupling, a simple "QCD" one mode model:

$$H_M^{\text{QCD}} = 1 + \mathcal{A}(E) + J_1 + \alpha(\mathcal{A}(X)J_- + \mathcal{A}(X^\dagger)J_+) + \alpha^2(J_- + J_+)^4; \quad (23)$$

the lowest eigenvalue for small values of  $M$ , as a function of the bare coupling parameter have been numerically calculated. The ground state eigenvalue as a function of the bare coupling parameter starts at zero, becomes negative and then rises, passing through zero; if such behavior persists in the large mode limit, this raises the possibility of fine tuning the bare coupling parameter.

## References

1. See for example, W. H. Klink, Few-Body Systems Supplement 14 (2003) 387.
2. See the article by B. D. Keister and W. N. Polyzou in Adv. in Nucl. Phys., vol 20, Plenum Press, NY, 1991 page 225, for an overview of the Bakamjian-Thomas method; an example of a point form calculation using the Bakamjian-Thomas method is given by R. F. Wagenbrunn, S. Boffi, W. Klink, W. Plessas and M. Radici, Phys. Lett. B 511 (2001) 33.
3. E. P. Biernat, W. H. Klink, W. Schweiger and S. Zelzer, "Point Form Quantum Field Theory", to be published in Ann. Phys., nucl. th./0708.1703.
4. W. H. Klink, "Quantum Field Theory on Velocity Grids I: Boson Contractions", in preparation.
5. W. H. Klink, Proceedings of the Mini-Workshop "Progress in Quark Models", vol. 7, edited by B. Golli, M. Rosina, and S. Sirca, DMFA, Ljubljana, Slovenia, 2006



## Dynamical CI fermions: Some results for Hadron Masses

C.B. Lang

Institut für Physik, FB Theoretische Physik Universität Graz, A-8010 Graz, Austria

In my presentation in Bled I gave an overview on lattice QCD and the challenge of implementing chiral symmetry for the quarks. Emphasis was put on the Bern-Graz-Regensburg (BGR) results with the so-called Chirally Improved (CI) fermions. These are realized as truncated solutions to the GW equations for a general ansatz for the Dirac operator [1,2]. For each site this fermion action includes several hundred neighbors with distances ranging up to three links.

Extensive quenched calculations have demonstrated good chiral as well as good scaling behavior [3]. Within the Bern-Graz-Regensburg (BGR) collaboration we have obtained results for the hadron spectrum and mesonic low energy constants in quenched simulations. These included several lattice spacings and volumes and three valence quarks. Emphasis in these studies has been put on deriving sophisticated techniques to analyze excited hadron states [4–6] and we expect to utilize that experience for full QCD configurations.

Our results for the excited hadrons were obtained with the so-called variational method and I discussed results for baryons and mesons for a quenched simulation with three light (u, d, s) valence quarks. The u- and d- mass were assumed degenerate and the s-mass fixed by the K-meson mass. In the meson sector we find good ground state masses and also excitations extrapolating for smaller quark masses towards the experimental values [4]. The only exception is the isovector scalar  $a_0$  which comes out too high, extrapolating to the  $a_0(1450)$ . The even parity baryons tend to have too high excitation masses, in particular the notorious problematic Roper state. In the odd parity sector we find values close to the experimental ones [5].

We have now implemented the CI fermions dynamically, i.e., full QCD (with a pair of mass degenerate light quarks). First results were presented in the Bled-meeting as well as in [7]. We identify an  $a_0$  compatible with the ground state  $a_0(980)$ .

I want to thank my colleagues (see references) for a fruitful and enjoyable collaboration.

## References

1. C. Gattringer, Phys. Rev. D **63**, (2001) 114501 [hep-lat/0003005].

2. C. Gattringer, I. Hip, and C. B. Lang, Nucl. Phys. B **597** (2001) 451 [hep-lat/0007042].
3. BGR (Bern-Graz-Regensburg) collaboration, C. Gattringer *et al.*, Nucl. Phys. B **677** (2004) 3 [hep-lat/0003005].
4. T. Burch, C. Gattringer, L. Y. Glozman, C. Hagen, and C. Lang, Phys. Rev. D **73** (2006) 017502 [hep-lat/0511054].
5. T. Burch *et al.*, Phys. Rev. D **74** (2006) 014504 [hep-lat/0604019].
6. C. Gattringer, L. Y. Glozman, C. B. Lang, D. Mohler, and S. Prelovsek, PoS(LATTICE2007)123 [arXiv:0709.4456 (hep-lat)].
7. R. Frigori, C. Gattringer, C. B. Lang, M. Limmer, D. Mohler, T. Maurer, and A. Schäfer, PoS(LATTICE2007)114 [arXiv:0709.4416 (hep-lat)].



# Charges in QED and QCD

Martin Lavelle

School of Mathematics and Statistics, University of Plymouth, Plymouth, PL4 8AA, UK

**Abstract.** In this talk we analyse possible descriptions of the gluonic cloud around quarks both analytically and on a lattice. This includes clarifying the role of Gribov copies in confinement and the construction of a class of such copies. In the perturbative sector we review the infra-red problem and difficulties with the Lee Nauenberg theorem.

## 1 Charges in Gauge Theories

Electrons are detected via the electric and magnetic fields around them. Only these composite systems, matter plus electromagnetic field, are physical [1]. *Dressing* a matter field

$$\Psi := h^{-1}[A] \psi. \quad (1)$$

produces a locally gauge invariant system if under a gauge transformation

$$h^{-1}[A^U] = h^{-1}[A]U \quad \text{where } \psi^U = U\psi. \quad (2)$$

This minimal requirement is fulfilled by

$$\Psi = \exp \left[ -ie \frac{\partial_i A_i}{\nabla^2} \right] \psi, \quad (3)$$

which using the equal time commutator with the electric field can be seen to have the Coulomb electric field. It also couples correctly to photons and has much improved infra-red (IR) properties compared to on-shell Green's functions with matter fields [2].

In QCD the colour charge operator is not locally gauge invariant but it can be shown to be invariant on physical states (obeying the non-abelian Gauss law). However, the allowed gauge transformations must at spatial infinity tend to a constant in the centre of the group. From this important restriction, it can be shown that it is impossible to non-perturbatively construct a gauge invariant quark with well defined colour. Essentially this is because the transformation (2) above could be used to produce a gauge fixing (for the dressing in (3) it would be Coulomb gauge) and with the above condition on gauge transformations it is known that there is no good gauge fixing due to the Gribov ambiguity [3].

There are very few explicit constructions of Gribov copies in the literature (see [3] and references therein). Starting in Coulomb gauge we have shown how a

wide class of spherically symmetric solutions may be constructed. Configurations of the form

$$A_i^c(x) = \frac{a(r) - 1}{r} \epsilon_{icb} \frac{x^b}{r} \quad (4)$$

are in Coulomb gauge and gauge transforming with

$$U(x) = \cos gu(r) - i \sin gu(r) \frac{\sigma^c x^c}{r} \quad (5)$$

one has two degrees of freedom:  $u(r)$  and  $a(r)$ . Demanding that the transformed field is in Coulomb gauge generates a differential equation for  $u(r)$  given  $a(r)$ . The trick is to reverse the procedure and having chosen  $u(r)$  which satisfies conditions like finite energy and any desired boundary conditions solve the equation for  $a(r)$ . There are very many choices of  $u$  and they generate  $a(r)$  for us! For example,

$$u(r) = \frac{r}{1+r^3}, \quad \Rightarrow \quad a(r) = \frac{2r(-7r^3 + r^6 + 1)}{(1+r^3)^3 \sin\left(\frac{2gr}{1+r^3}\right)} + 1 - \frac{1}{g}. \quad (6)$$

The factors of  $1/g$  betray the non-perturbative nature of the Gribov problem.

Having seen the non-perturbative obstruction to the construction of constituent quarks with well defined colour charge, we would like to see how far it is possible to describe quarks. The perturbative extension in QCD of the static dressing in (3) can be shown to generate the anti-screening glue around quarks while a separately gauge invariant structure is responsible for the screening by glue [4]. This has been studied in part up to NNLO. These perturbative studies of the interquark potential have more recently been complemented by simulations on the lattice [5].

Wilson loops correspond to the time evolution of a gauge invariant state formed by two fermions linked by a string. In the large (Euclidean) time limit, this yields the interquark potential due to the state's non-zero overlap with the true ground state. It is known that smearing the Wilson loop improves this overlap and we interpret this as due to the unsmearred string being narrower than the true flux tube.

Instead of the string-like state it is possible, by rotating the links into Coulomb gauge, to construct a state made of two gauge invariant fermions. This construction is of course only possible up to the Gribov copies.

Fitting to the potential

$$V(r) = V_0 - \frac{\alpha}{r} + \sigma r, \quad (7)$$

the Coulombic state yields a good fit to the potential for shorter separations,  $r$ , as might be expected. However, we find a lower string tension using the Coulombic description which implies it has a better overlap with the ground state even for larger separations. Below are some fits [5] for SU(2) on a  $16^4$  lattice with  $\beta = 2.4$ :

	$V_0$	$\alpha$	$\sigma\alpha^2$	$\chi_V^2/\text{dof}$
Coulomb	0.510(2)	0.217(1)	0.0807(4)	6.5
String	0.501(3)	0.212(2)	0.0847(8)	4.7

It is interesting to note that in the Coulomb gauge simulations the interquark potential is non-zero at large separations despite the impact of Gribov copies. We have shown that summing over such copies does not change the slope of the potential although they do alter the intercept [5].

## 2 The Infra-Red is Still a Problem

We now review the IR problem and will see that there are many unsolved difficulties [7]. To be explicit we consider Coulomb scattering in QED. For electrons with *small* masses,  $m$ , there are two kinds of divergences: soft divergences (manifest as  $1/\epsilon$  poles in dimensional regularisation) and collinear divergences (factors of  $\ln(m)$ ). The main practical response is to only calculate quantities free of IR divergences (e.g.,  $F_2(q^2)$  rather than  $F_1(q^2)$ ), however, the Lee Nauenberg (LN) theorem [6] is supposed to tell us how to deal with them. This quantum mechanical argument indicates that one should sum over all possible initial and final state degeneracies (indistinguishable processes). Such inclusive cross-sections, it is argued, will be finite.

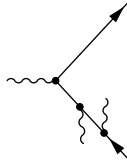
The *standard approach* to Coulomb scattering would be to use the Bloch Nordsieck (BN) trick to deal with the soft divergences: i.e., sum over emission of soft (unobservable) photons with energy less than some scale  $\Delta$ . Then one uses the LN approach to collinear divergences: i.e., sum over outgoing photons which are collinear to the outgoing matter field and have energy greater than  $\Delta$  and *additionally* sum over incoming collinear photons which have energy greater than  $\Delta$ . It is crucial to note that outgoing soft photons are included (via the BN trick) but incoming soft photons, whether collinear or not, are not included at all. Two *natural questions* are: why are incoming collinear photons only included if they are not soft and why are all outgoing soft photons included but no incoming ones?

In fact these artificial divides are not safe. One finds that terms like  $\Delta \ln(m)$  arise when one integrates over collinear photons with a minimum energy  $\Delta$ . These collinear divergences have no counterpart in virtual loops where energy resolutions play no role. For the outgoing photons these terms can be cancelled (one integrates over outgoing soft photons too), but for the incoming photons the only way<sup>1</sup> to cancel them is to include incoming soft photons. This removes the above  $\Delta \ln(m)$  type divergences, but at the price of also reintroducing soft divergences.

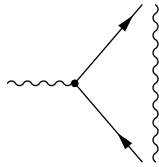
To kill the soft divergences left from combining virtual loop diagrams, photon emission and photon absorption, it is natural to include emission and absorption processes such as:

---

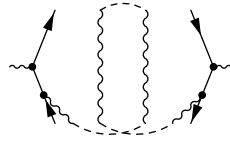
<sup>1</sup> It would be wrong to say that  $\Delta$  can be set to zero. Firstly, experiments have non-vanishing resolutions and secondly it is known that the BN prediction for the cross-section vanishes as  $\Delta \rightarrow 0$ .



For this to contribute to the cross-section at lowest order ( $e^4$ ) one needs, see Appendix D of [6], interference with a disconnected photon as in (a) below. This can then produce a connected contribution at the level of the cross-section, see (b).

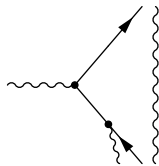


(a)

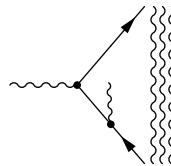


(b)

Adding together such diagrams plus the connected interference contribution to the cross section from diagrams like (c) below



(c)



(d)

produces a finite answer (see [7] and references therein). However, at order  $e^4$  there are infinitely many such diagrams! One can include arbitrarily many disconnected photons, see e.g., (d), and still have a connected contribution to the cross-section.

In fact it turns out [7] that the combinatorics are such that this infinite series (at a fixed order of perturbation theory) does not converge. The connected contribution to the cross-section is exactly the same from the diagrams with three hundred disconnected photons as it is for those with one disconnected photon. This infinite oscillating series is mathematically ill-defined and there is no physical reason to truncate the series of diagrams. Thus there is no meaningful prediction for the overall result.

### 3 Conclusions

We have seen that describing a gauge invariant quark is impossible outside of perturbation theory due to the Gribov ambiguity. It was possible to construct a wide class of explicit Gribov copies which clarify why colour cannot be observed and the non-perturbative nature of the Gribov problem.

The interquark potential offers a way to probe the glue around quarks. Perturbative calculations reveal the different gluonic structures underlying screening and anti-screening while lattice results show the importance of including the width of the flux tube linking heavy quarks in any model of a meson.

Finally, it was shown that nobody knows how to deal with the IR divergences in any problem with initial and final state charged particles. This is a very serious problem which urgently deserves further study.

**Acknowledgments:** I thank the organisers for making this such an interesting and enjoyable workshop and my collaborators on the work reported here, Emili Bagan, Tom Heinzl, Anton Ilderton, Kurt Langfeld and David McMullan.

## References

1. M. Lavelle and D. McMullan, Phys. Rep. C279 (1997) 1; hep-ph/9509344.
2. E. Bagan, M. Lavelle and D. McMullan, Ann. Phys. 282 (2000) 503; hep-ph/9909262.
3. A. Ilderton, M. Lavelle and D. McMullan, JHEP 03 (2007) 044; hep-th/0701168.
4. E. Bagan, M. Lavelle and D. McMullan, Phys. Lett. B632 (2006) 652; hep-th/0510077.
5. T. Heinzl, K. Langfeld, M. Lavelle and D. McMullan, "Coulomb gauge Gribov copies and the confining potential", arXiv:0709.3486v1 [hep-lat].
6. T.D. Lee and M. Nauenberg, Phys. Rev. 133 (1964) B1549.
7. M. Lavelle and D. McMullan, JHEP 03 (2006) 026; hep-ph/0511314.



## Pattern of scalar mesons

Keh-Fei Liu

University of Kentucky, Department of Physics and Astronomy,  
Lexington, KY 40506-0055, USA

Combining the recent lattice calculation of  $a_0(1450)$  and  $\sigma(600)$  mesons with the overlap fermion in the chiral regime with the pion mass less than 300 MeV, the quenched lattice calculation of the scalar glueball, and the phenomenological study of the mixing of isoscalar scalar mesons  $f_0(1710)$ ,  $f_0(1500)$ ,  $f_0(1370)$ , through their decays, a simple pattern for the light scalar mesons begins to emerge. Below 1 GeV, the scalar mesons form a nonet of tetraquark mesoniums. Above 1 GeV, the nonet  $q\bar{q}$  mesons are made of an octet with largely unbroken SU(3) symmetry and a fairly good singlet which is  $f_0(1370)$ .  $f_0(1710)$  is identified as an almost pure scalar glueball with a  $\sim 10\%$  mixture of  $q\bar{q}$ .



# Topology of non-commutative U(1) gauge theory on the lattice<sup>\*</sup>

R. Achleitner<sup>a</sup>, W. Frisch<sup>a</sup>, H. Grosse<sup>b</sup>, H. Markum<sup>\*\*a</sup>, F. Teutschinger<sup>a</sup>

<sup>a</sup>Atominstitut, Vienna University of Technology, Austria

<sup>b</sup>Department for Theoretical Physics, University of Vienna, Austria

**Abstract.** Theories with non-commutative space-time coordinates represent alternative candidates of grand unified theories. We discuss U(1) gauge theory in 2 dimensions on a lattice with N sites. The mapping to a U(N) one-plaquette model in the sense of Eguchi and Kawai can be used for computer simulations. We are discussing the formulation and evaluation of topological objects. We performed quantum Monte Carlo simulations and calculated the topological charge for different matrix sizes and several values of the coupling constant. We constructed classical gauge field configurations with large topological charge and used them to initialize quantum simulations. It turned out that the value of the topological charge is decreasing during a Monte Carlo history. Our results show that the topological charge is in general suppressed. The situation is similar to lattice QCD where quantum gauge field configurations are topologically trivial and one needs to apply some cooling procedure on the gauge fields to unhide the integer number of the instantons. A few recent analyses are added to this paper.

## 1 Motivation

In non-commutative geometry, where the coordinate operators  $\hat{x}_\mu$  satisfy the commutation relation  $[\hat{x}_\mu, \hat{x}_\nu] = i\theta_{\mu\nu}$ , a mixing between ultraviolet and infrared degrees of freedom takes place [1]. Lattice simulations are a promising tool to get deeper insight into non-commutative quantum field theories. In this work we have studied non-commutative U(1) gauge theory on a two-dimensional torus. The advantage of this theory is that there exists an equivalent matrix model which makes numerical calculations feasible [2].

The main topic of the underlying contribution is to study the topological charge in two-dimensional non-commutative U(1) gauge theory. The instanton configurations carry a topological charge  $q$  which can be non-integer in this case [3]. We performed Monte Carlo simulations with different values of the coupling constant  $\beta$  and looked at the topological charge  $q$  in the equilibrium [4].

---

<sup>\*</sup> Talk delivered by H. Markum

<sup>\*\*</sup> Thanks to the organizers of the Mini-Workshop 2007 on Hadron Structure and Lattice QCD in Bled.

## 2 Topology and instantons in QCD

The Lagrangian of pure gluodynamics (the Yang-Mills theory with no matter fields) in Euclidean spacetime can be written as

$$\mathcal{L} = \frac{1}{4g^2} G_{\mu\nu}^a G_{\mu\nu}^a \quad (1)$$

where  $G_{\mu\nu}^a$  is the gluon field strength tensor

$$G_{\mu\nu}^a = \partial_\mu A_\nu^a - \partial_\nu A_\mu^a + f^{abs} A_\mu^b A_\nu^c \quad (2)$$

and  $f^{abs}$  are structure constants of the gauge group considered. The classical action of the Yang-Mills fields can be identically rewritten as

$$S = \frac{1}{8g^2} \int dx^4 (G_{\mu\nu}^a \pm \tilde{G}_{\mu\nu}^a)^2 \mp \frac{8\pi^2}{g^2} Q \quad (3)$$

where  $Q$  denotes the topological charge

$$Q = \frac{1}{32\pi^2} \int dx^4 G_{\mu\nu}^a \tilde{G}_{\mu\nu}^a \quad (4)$$

with

$$\tilde{G}_{\mu\nu}^a = \frac{1}{2} \epsilon_{\mu\nu\alpha\beta} G_{\alpha\beta}^a. \quad (5)$$

## 3 Topological charge in two dimensions

### 3.1 Lattice regularization of non-commutative gauge theory

The lattice regularized version of the theory can be defined by an analog of Wilson's plaquette action

$$S = -\beta \sum_x \sum_{\mu < \nu} U_\mu(x) \star U_\nu(x + a\hat{\mu}) \star U_\mu(x + a\hat{\nu})^\dagger \star U_\nu(x)^\dagger + \text{c.c.} \quad (6)$$

where the symbol  $\hat{\mu}$  represents a unit vector in the  $\mu$ -direction and we have introduced the lattice spacing  $a$ . The link variables  $U_\mu(x)$  ( $\mu = 1, 2$ ) are complex fields on the lattice satisfying the star-unitarity condition. The star-product [1] on the lattice can be obtained by rewriting its definition within non-commutative derivatives in terms of Fourier modes and restricting the momenta to the Brillouin zone.

Let us define the topological charge for a gauge field configuration on the discretized two-dimensional torus. In the language of fields, we define the topological charge as

$$q = \frac{1}{4\pi i} \sum_x \sum_{\mu\nu} \epsilon_{\mu\nu} U_\mu(x) \star U_\nu(x + a\hat{\mu}) \star U_\mu(x + a\hat{\nu})^\dagger \star U_\nu(x)^\dagger \quad (7)$$

which reduces to the usual definition of the topological charge in 2d gauge theory

$$q = \frac{1}{4\pi} \int d^2x \epsilon_{\mu\nu} G_{\mu\nu} \quad (8)$$

in the continuum limit.

### 3.2 Matrix-model formulation

It is much more convenient for computer simulations to use an equivalent formulation, in which one maps functions on a non-commutative space to operators so that the star-product becomes nothing but the usual operator product, which is non-commutative. The action (6) can then be written as

$$S = -N\beta \sum_{\mu \neq \nu} \text{tr} \left\{ \hat{U}_\mu (\Gamma_\mu \hat{U}_\nu \Gamma_\mu^\dagger) (\Gamma_\nu \hat{U}_\mu^\dagger \Gamma_\nu^\dagger) \hat{U}_\nu^\dagger \right\} + 2\beta N^2 \quad (9)$$

$$= -N\beta \sum_{\mu \neq \nu} \mathcal{Z}_{\nu\mu} \text{tr} \left( V_\mu V_\nu V_\mu^\dagger V_\nu^\dagger \right) + 2\beta N^2 \quad (10)$$

where  $V_\mu \equiv \hat{U}_\mu \Gamma_\mu$  is a  $U(N)$  matrix with  $N$  the linear extent of the original lattice. An explicit representation of  $\Gamma_\mu$  in the  $d = 2$  case shall be given in Sec. 5. This is the twisted Eguchi-Kawai (TEK) model [5], which appeared in history as a matrix model equivalent to the large  $N$  gauge theory [6]. We have added the constant term  $2\beta N^2$  to what we would obtain from (6) in order to make the absolute minimum of the action zero.

By using the map between fields and matrices, the topological charge (7) can be represented in terms of matrices as

$$q = \frac{1}{4\pi i} N \sum_{\mu\nu} \epsilon_{\mu\nu} \text{tr} \left\{ \hat{U}_\mu (\Gamma_\mu \hat{U}_\nu \Gamma_\mu^\dagger) (\Gamma_\nu \hat{U}_\mu^\dagger \Gamma_\nu^\dagger) \hat{U}_\nu^\dagger \right\} \quad (11)$$

$$= \frac{1}{4\pi i} N \sum_{\mu\nu} \epsilon_{\mu\nu} \mathcal{Z}_{\nu\mu} \text{tr} \left( V_\mu V_\nu V_\mu^\dagger V_\nu^\dagger \right). \quad (12)$$

## 4 Numerical results for the TEK model

We have computed the topological content of gauge field configurations produced by quantum Monte Carlo simulations. In Fig. 1 we display scatter plots of the action  $S$  without a factor of  $\beta$  in its definition Eq. (10) and the topological charge  $q$  performing a cold start. The size of the matrix is  $N = 25$  and the values of the coupling  $\beta$  are chosen to yield a non-commutativity parameter  $\theta = 2.55, 1.27, 0.63$ , respectively. One observes a decrease of the action with increasing  $\beta$  due to stronger coupling of the matrices in analogy to lower temperature in an Ising model. The importance sampling of the system with smaller action generates smaller values of its topological content. This can also be seen from the distributions of the topological charge in Fig. 2 where the peaks become narrower with increasing  $\beta$ . Similar plots have been obtained for a larger matrix size  $N = 35$ , for more results see Ref. [4]. To compare the topology-action diagrams on the same scale, we display in Fig. 3 our simulation for  $N = 25$  with all  $\beta$ -values considered in a single plot.

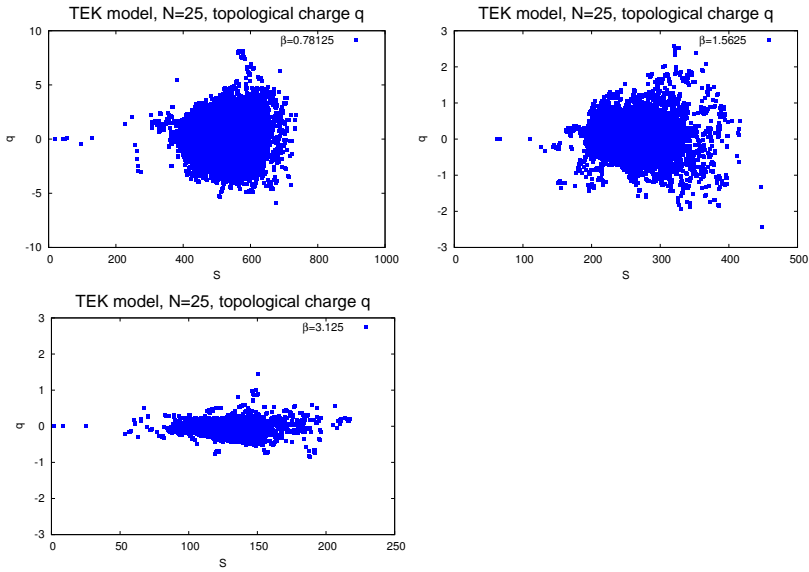


**Fig. 1.** Scatter plots of the action  $S$  divided by  $\beta$  (x-axis) and the topological charge  $q$  (y-axis) for a Monte Carlo simulation (cold start) at  $N = 25$  and  $\beta = 0.78125, 1.5625$  and  $3.125$ .

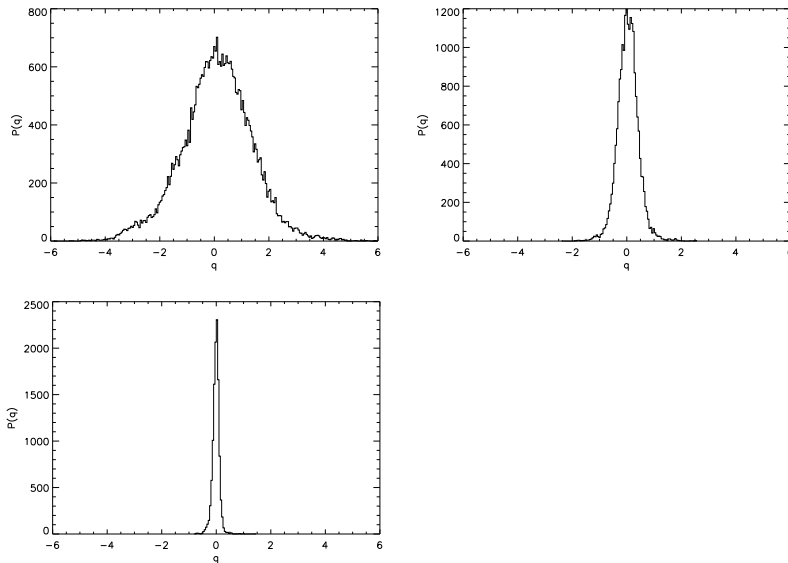


**Fig. 2.** Distribution  $P$  of the topological charge  $q$  in the Twisted Eguchi-Kawai model for  $N = 25$  and  $\beta = 0.78125, 1.5625$  and  $3.125$ .

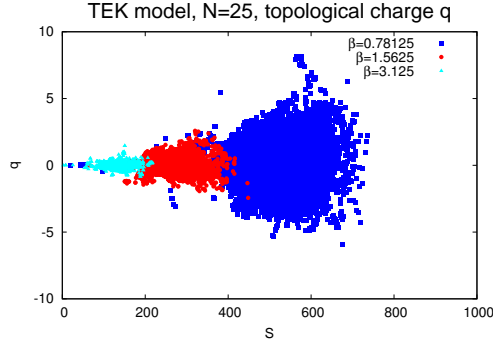


**Fig. 3.** Scatter plots of the action  $S$  divided by  $\beta$  (x-axis) and the topological charge  $q$  (y-axis) for the Monte Carlo simulations at  $N = 25$  and  $\beta = 0.78125, 1.5625$  and  $3.125$ , combining different couplings.

## 5 Classical solutions

The classical equation of motion can be obtained from the action (10) as [7,3]

$$V_{\mu}^{\dagger}(W - W^{\dagger})V_{\mu} = W - W^{\dagger} \quad (13)$$

where the unitary matrix  $W$  is defined by

$$W = Z_{\nu\mu} V_{\mu} V_{\nu} V_{\mu}^{\dagger} V_{\nu}^{\dagger} \quad (14)$$

The general solutions to this equation can be brought into a block-diagonal form [7]

$$V_{\mu} = \begin{pmatrix} \Gamma_{\mu}^{(1)} & & & \\ & \Gamma_{\mu}^{(2)} & & \\ & & \ddots & \\ & & & \Gamma_{\mu}^{(k)} \end{pmatrix} \quad (15)$$

by an appropriate  $SU(N)$  transformation, where  $\Gamma_{\mu}^{(k)}$  are  $n_k \times n_k$  unitary matrices satisfying the 't Hooft-Weyl algebra

$$\Gamma_{\mu}^{(j)} \Gamma_{\nu}^{(j)} = Z_{\mu\nu}^{(j)} \Gamma_{\nu}^{(j)} \Gamma_{\mu}^{(j)} \quad (16)$$

$$Z_{12}^{(j)} = Z_{21}^{(j)*} = \exp\left(2\pi i \frac{m_j}{n_j}\right) \quad (17)$$

$$m_j = \frac{n_j + 1}{2} \quad (18)$$

An explicit representation is given, for instance, by the clock and shift operators,  $Q$  and  $P$

$$\Gamma_1^{(j)} = P_{n_j}, \quad \Gamma_2^{(j)} = (Q_{n_j})^{m_j} \quad (19)$$

For each solution, the action and the topological charge can be evaluated as

$$S = 4N\beta \sum_j n_j \sin^2 \left\{ \pi \left( \frac{m_j}{n_j} - \frac{M}{N} \right) \right\} \quad (20)$$

$$q = \frac{N}{2\pi} \sum_j n_j \sin \left\{ 2\pi \left( \frac{m_j}{n_j} - \frac{M}{N} \right) \right\} \quad (21)$$

Note that the topological charge  $q$  is not an integer in general. If we require the action to be less than of order  $N$ , however, the argument of the sine has to vanish for all  $j$ . In that case the topological charge approaches an integer

$$q \simeq N \left( \sum_j m_j - M \right) \quad (22)$$

which is actually a multiple of  $N$ .

## 6 Quantum Monte Carlo versus classical solutions

In the following analysis we compare the classical topological charges taken from Ref. [3] with our quantum Monte Carlo simulation at  $N = 25$ . In Fig. 4 we plot our data for a cold start from Fig. 3 together with the classical solutions. One sees from the scatter plots that the quantum simulation reaches only small topological numbers. This brings the situation of QCD into mind where one has to apply some cooling or smoothing procedure to damp the quantum fluctuations and get in touch with the integer-valued topological charges. Since a configuration from a cold start is topologically trivial, we constructed classical solutions and started with them. In Fig. 5 we overlay the Monte Carlo histories at  $\beta = 1.5625$  starting with  $q = -25$  and  $q = -50$ , respectively, to the scatter plots of the classical topological charges from Ref. [3]. One observes that the equilibrium configurations tend to smaller values of  $q$ . Remarkably, the equilibration seems to proceed along a “classical branch”.

## 7 Analyses for large topological charge

The question was how to produce start configurations with different large values of  $q$ . One idea was to apply some “cooling procedure” to the topological charge in contrast to the action, being the imaginary part instead of the real part of the plaquette, respectively. The topological charge  $q$  is now forced to become larger or smaller every step without posing a condition on the action. In Fig. 6 we start with an equilibrium configuration of  $q = -15.7034$ . It turns out that the negative value of  $q$  is decreasing and configurations of higher action are preferred. In principle, one could use those configurations with different values of  $q$  to start a Metropolis Monte Carlo simulation [8].

Another idea was to look at random gauge field configurations. This leads to an ensemble with a large spread in  $q$  and large action. In Fig. 7 we present

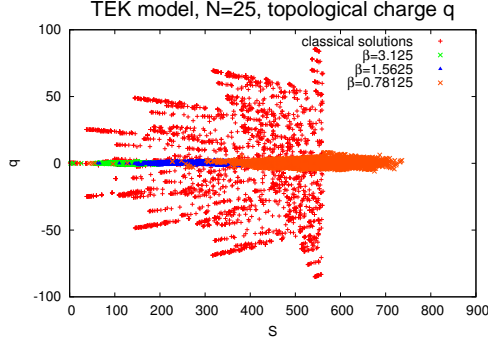


**Fig. 4.** Scatter plots of the action  $S$  divided by  $\beta$  (x-axis) and the topological charge  $q$  (y-axis) for Monte Carlo histories at  $N = 25$  with cold starts being topologically trivial,  $q = 0$ . The numbers of the classical topological charges are superimposed.

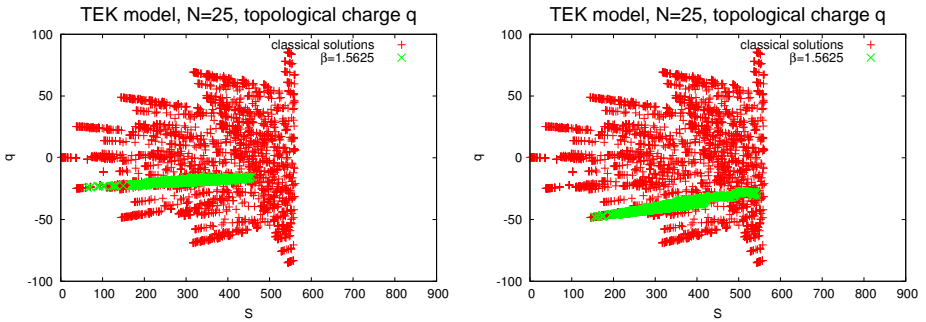


**Fig. 5.** Scatter plots of the action  $S$  divided by  $\beta$  (x-axis) and the topological charge  $q$  (y-axis) for Monte Carlo histories at  $N = 25$  and  $\beta = 1.5625$  with starts at  $q = -25$  and  $-50$ . The numbers of the classical topological charges are superimposed.

several Metropolis Monte Carlo simulations which were initialized with topological charges in the range  $-60 < q < 60$ . This preliminary plot is taken from our ongoing research [9].

## 8 Conclusion and outlook

The diagram of the classical topological charges and the corresponding action from Ref. [3] allows for large values of  $q$ . The equilibrium configurations visit only a small part of this charge-action diagram. Thus we constructed classical gauge field configurations with large topological charge and used them as start configuration for quantum simulations. It turned out that the value of the topological charge is decreasing during a Monte Carlo history, preferably along the classical minima. To summarize, our results show that the topological charge is in general suppressed.

The situation is reminiscent of lattice QCD where quantum gauge field configurations are topologically trivial and one needs to apply some smoothing pro-

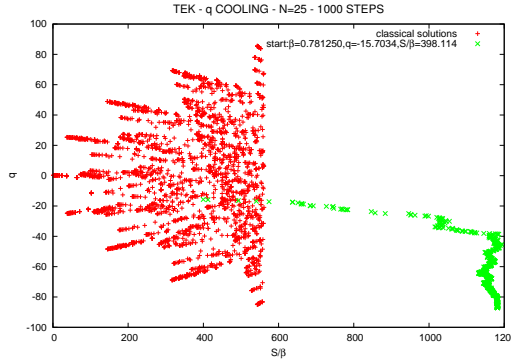


**Fig. 6.** Scatter plots of the action  $S$  divided by  $\beta$  (x-axis) and the topological charge  $q$  (y-axis) for “cooling” of the topological charge, starting with an equilibrium configuration at  $N = 25$ ,  $\beta = 0.78125$  and  $q = -15.7034$ . The numbers of the classical topological charges are superimposed.

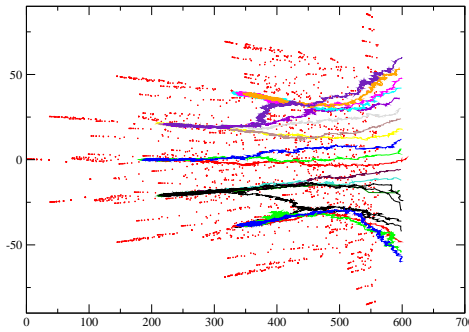


**Fig. 7.** Scatter plots of the action  $S$  divided by  $\beta$  (x-axis) and the topological charge  $q$  (y-axis) for Monte Carlo histories at  $N = 25$  and  $\beta = 1.5625$ , starting with several values  $-60 < q < 60$ . The numbers of the classical topological charges are superimposed.

cedure on the gauge fields to unhide instantons. We adapted cooling techniques known from QCD to the two-dimensional non-commutative  $U(1)$  theory. We further performed quantum Monte Carlo simulations for large topological charges. It is desirable to tackle the four-dimensional non-commutative gauge theory in order to obtain a realistic comparison of its topological content with the well-studied topological objects like instantons and monopoles in QCD.

## References

1. R.J. Szabo, *Quantum Field Theory on Non-Commutative Spaces*, Phys. Rept. **378** (2003) 207 [hep-th/0109162];  
R.J. Szabo, *Discrete Non-Commutative Gauge Theory*, Mod. Phys. Lett. **A16** (2001) 367 [hep-th/0101216].

2. W. Bietenholz, F. Hofheinz, J. Nishimura, *Non-Commutative Field Theories beyond Perturbation Theory*, Fortsch. Phys. **51** (2003) 745 [hep-th/0212258];  
W. Bietenholz, F. Hofheinz, J. Nishimura, Y. Susaki, J. Volkholz, *First Simulation Results for the Photon in a Non-Commutative Space*, Nucl. Phys. Proc. Suppl. **140** (2005) 772 [hep-lat/0409059];  
W. Bietenholz, A. Bigarini, F. Hofheinz, J. Nishimura, Y. Susaki, J. Volkholz, *Numerical Results for U(1) Gauge Theory on 2d and 4d Non-Commutative Spaces*, Fortsch. Phys. **53** (2005) 418 [hep-th/0501147].
3. H. Aoki, J. Nishimura, Y. Susaki, *The Index of the Overlap Dirac Operator on a Discretized 2d Non-Commutative Torus*, J. High Energy Phys. **02** (2007) 033 [hep-th/0602078];  
H. Aoki, J. Nishimura, Y. Susaki, *Suppression of Topologically Nontrivial Sectors in Gauge Theory on 2d Non-Commutative Geometry* [hep-th/0604093].
4. W. Frisch, *Simulation and Topology of Two-Dimensional Non-Commutative U(1) Gauge Theory*, Diploma Thesis, Vienna University of Technology (Vienna 2007); W. Frisch, H. Grosse, H. Markum, *Instantons in Two-Dimensional Non-Commutative U(1) Gauge Theory*, PoS(LAT2007)317.
5. A. González-Arroyo, M. Okawa, *A Twisted Model for Large-N Lattice Gauge Theory*, Phys. Rev. **D27** (1983) 2397.
6. T. Eguchi, H. Kawai, *Reduction of Dynamical Degrees of Freedom in the Large-N Gauge Theory*, Phys. Rev. Lett. **48** (1982) 1063.
7. L. Griguolo, D. Seminara, *Classical Solutions of the TEK Model and Non-Commutative Instantons in Two Dimensions*, J. High Energy Phys. **03** (2004) 068 [hep-th/0311041].
8. F. Teischinger, *Construction of Configurations in Two-Dimensional Non-Commutative U(1) Gauge Theory with Large Topological Charges*, Pre-Diploma Project, Vienna University of Technology (Vienna 2007).
9. R. Achleitner, *Simulation of Two-Dimensional Non-Commutative U(1) Gauge Theory with Large Topological Charges*, Pre-Diploma Project, Vienna University of Technology (Vienna 2007).



## Chiral extrapolation of the nucleon mass<sup>\*</sup>

Judith A. McGovern, Michael C. Birse

Theoretical Physics Group, School of Physics and Astronomy  
The University of Manchester, Manchester, M13 9PL, U.K.

**Abstract.** A number of papers recently have used fourth-order chiral perturbation theory to extrapolate lattice data for the nucleon mass; the process seems surprisingly successful even for large pion masses. In this talk I explored the effect of including the fifth-order term in the expansion.

Over the last few years there has been an explosion of activity in the field of chiral extrapolations of lattice QCD data. However for many quantities of interest unquenched calculations have typically only been performed at relatively high quark masses, the pion mass is 500 MeV or more. There are real questions about the convergence of chiral expansions in this region.

One quantity for which the chiral expansion has seemed to work surprisingly well is the nucleon mass. Various groups have looked at the  $O(p^4)$  (technically  $N^3\text{LO}$ ) expansion of the nucleon mass in heavy baryon chiral perturbation theory (HB $\chi$ PT) and found good agreement with unquenched lattice data up to pion masses of 800 MeV or more. Of course the results are quite sensitive to the input parameters which include some rather poorly known low-energy constants, but when these are used as fit parameters the results agree well with other determinations. The most thorough investigation of this type was done by Procura *et al* [1] (see also Musch [2]).

However there is no reason to do the fit at  $O(p^4)$ , as the  $O(p^5)$  corrections to the nucleon mass were calculated almost ten years ago [3]. There, it was found that genuine two-loop contributions vanish, and almost all other contributions could be absorbed in the renormalised pion-nucleon coupling constant, pion mass and decay constant etc calculated at the physical pion mass. Only an extremely small relativistic correction to the basic one-loop self-energy is left (and in fact this piece was included by Procura *et al*). However this is not relevant to a lattice extrapolation where the running of the nucleon mass with the varying pion mass is being explored; instead the original form expressed in terms of chiral limit quantities is the relevant one. This was not given explicitly in Ref. [3] although enough information was given to reconstruct it; for that reason we recently published a paper in which the relevant expression was given in full, and its effects on the chiral extrapolation were explored [4].

---

<sup>\*</sup> Talk delivered by Judith A. McGovern

Unsurprisingly, the fifth-order terms are far from small for pion masses of 500 MeV and above. They depend on the value of the third-order LEC  $d_{16}$ , which is not well known but has been constrained by  $\pi N \rightarrow \pi\pi N$  scattering; however no value, natural or unnatural, allows the fifth-order terms to be a small perturbation on the fourth-order ones. (As there is both an  $m_\pi^5$  and an  $m_\pi^5 \log m_\pi$  term, and the latter is independent of LECs beyond those from the leading-order Lagrangian, the total cannot be arranged to vanish over a significant range of  $m_\pi$ .)

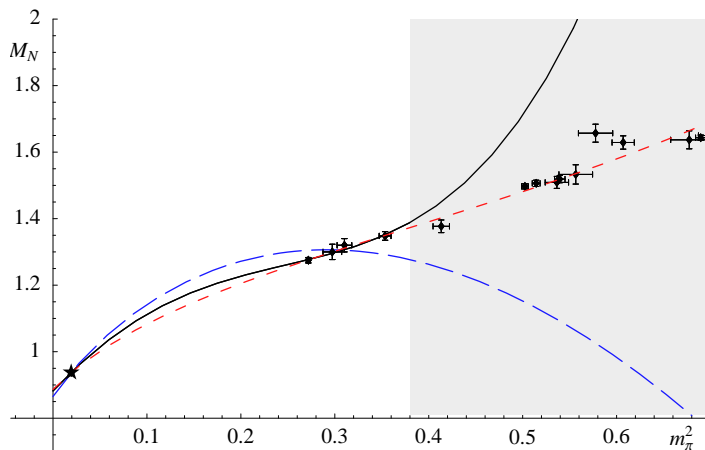


**Fig. 1.** Best fits to the lattice data (constraint to pass through the physical point) for  $M_N$  (in GeV) versus  $m_\pi^2$  (in  $\text{GeV}^2$ ) below  $m_\pi = 600$  MeV (unshaded region) at third- (blue, long dashes), fourth- (red, short dashes) and fifth order (black, solid). (Note that the apparent agreement of the fourth- and fifth-order curves at low  $m_\pi^2$  masks very different fitted values of the LEC  $e'$ .)

As is shown in Fig. 1, it is possible to fit the fifth-order formula to the same four lowest lattice points (plus the physical nucleon mass) as Procura *et al* did, with as good a  $\chi^2$ . However the resulting third and fourth order LECs are grossly unnatural and out of line with other determinations. Furthermore, whereas the fourth-order curve is also a surprising good fit to the points at higher masses, the fifth-order curve fails immediately beyond the points to which it was fit. (See Ref. [2] for the selection of large-volume,  $SU(2)$ , unquenched lattice data.)

The radius of convergence can be estimated by looking at the contributions to various orders with fixed coefficients, as is done in Fig. 2. Since the fifth-order fit is clearly not meaningful, while the LECs in the fourth-order fit are natural and in line with other determinations, we use the latter and add in a band for the fifth-order term using the spread of possible values of  $d_{16}$  quoted by Beane [5]. One can deduce from Fig. 2 that the radius of convergence of the chiral extrapolation might be about  $m_\pi = 300$  MeV, a point made previously made by Bernard *et al* [6]. Fortunately such masses no longer look as unobtainable with dynamical quarks as they did until quite recently.

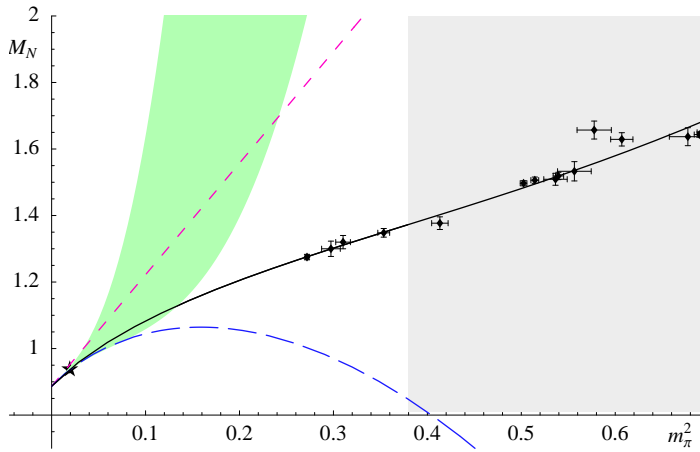


**Fig. 2.** Curves up to second- (magenta, short dashes), third- (blue, long dashes), fourth- (black, solid) and fifth- (green band) order with parameters taken from the fourth-order fit each time, and the fifth-order band showing the spread with  $-2.6 \leq d_{16} \leq 2.4$  and  $l_4 = 4.4 \pm 0.3$  See Ref. [4] for more details.

## References

1. M. Procura, B. U. Musch, T. Wollenweber, T. R. Hemmert and W. Weise, Phys. Rev. D **73** (2006) 114510 (hep-lat/0603001).
2. B. U. Musch, Diploma thesis, TU München, (hep-lat/0602029).
3. J. A. McGovern and M. C. Birse, Phys. Lett. **B446** (1999) 300 (hep-ph/9807384).
4. J. A. McGovern and M. C. Birse, Phys. Rev. **D74** (2006) 097501.
5. S. R. Beane, Nucl. Phys. **B695** 192 (2004) (hep-lat/0403030).
6. V. Bernard, T. Hemmert, U. Meißner, Nucl. Phys. **A732** (2004) 149.



## New Baryon Results from Relativistic Constituent Quark Models

W. Plessas

Theoretical Physics, Institute for Physics, University of Graz, Universitätsplatz 5, A-8010 Graz, Austria

We provide a review of the performance of relativistic constituent quark models (RCQMs) in the low- and intermediate-energy physics of baryons. Three types of models are considered, namely, the ones whose hyperfine interactions are based on one-gluon-exchange (OGE) [1], on Goldstone-boson-exchange (GBE) [2], and on instanton-induced (II) dynamics [3].

First, the invariant mass spectra of the RCQMs are recalled. The ground states and resonances of all light and strange baryons below  $\approx 2$  GeV are fairly well reproduced. The level orderings are correct only for the GBE RCQM. The known problem with the  $\Lambda(1405)$  persists for all RCQMs. The extension of the RCQMs to the charm sector works all right in view of the rather scarce data hitherto available [4].

Next, the covariant predictions for the electroweak nucleon structure are summarized. The GBE RCQM, when treated within the point-form approach of relativistic quantum mechanics employing a spectator-model current operator, is able to reproduce all elastic electromagnetic and axial form factors of the nucleons in surprisingly good agreement with experiment [5–7]. Similarly the electric radii and magnetic moments are well described [8]. This holds true also with regard to all other measured baryon ground states [8,9]. The predictions of the OGE RCQM are rather similar, and the point-form results are basically consistent with the findings by the Bonn group with their II RCQM treated along the Bethe-Salpeter approach [10]. The analogous calculations in instant form cannot produce predictions close to experiment, however. The instant-form spectator model in addition is not frame independent and consequently remains with a considerable arbitrariness in the predictions [11]. Regarding the point-form spectator model the magnitudes of the uncertainties in the results due to different possible choices of a normalization factor needed in the spectator current operator are discussed [11,12].

Finally we report the results of a comprehensive study of all types of mesonic decays of light and strange baryon resonances from a covariant point-form calculation [13–16]. The predictions for partial widths of  $\pi$ ,  $\eta$ , and  $K$  decays calculated with the OGE and GBE RCQMs produce a completely different pattern than has been known hitherto from nonrelativistic or relativized approaches. In general, the experimental decay widths are underestimated by the present theory. This

hints to deficiencies in the decay mechanism and/or the description of resonance states. Obviously a spectator model for the decay operator as used in refs. [13–16] is not enough; in its nonrelativistic reduction it conforms to the simple elementary emission model. Presumably more elaborate vertices, many-body contributions as well as channel couplings are needed. In addition, the resonance states may notably lack explicit contributions from configurations beyond  $\{QQQ\}$ . Nevertheless, the covariant results definitely demonstrate the importance of relativistic effects. Furthermore, they can already provide useful insights for the assignments of excited baryon states to  $SU(3)$  flavor multiplets [17].

## References

1. L. Theussl, R. F. Wagenbrunn, B. Desplanques, and W. Plessas, *Eur. Phys. J. A* **12**, 91 (2001).
2. L. Y. Glozman, W. Plessas, K. Varga, and R. F. Wagenbrunn, *Phys. Rev. D* **58**, 094030 (1998); L. Y. Glozman, Z. Papp, W. Plessas, K. Varga, and R. F. Wagenbrunn, *Phys. Rev. C* **57**, 3406 (1998).
3. U. Loering, B. C. Metsch, and H. R. Petry, *Eur. Phys. J. A* **10**, 395 (2001); *ibid.* **10**, 447 (2001).
4. D. Prieling, Diploma Thesis, University of Graz (2006).
5. R. F. Wagenbrunn, S. Boffi, W. Klink, W. Plessas, and M. Radici, *Phys. Lett. B* **511**, 33 (2001).
6. L. Y. Glozman, M. Radici, R. F. Wagenbrunn, S. Boffi, W. Klink, and W. Plessas, *Phys. Lett. B* **516**, 183 (2001).
7. S. Boffi, L. Y. Glozman, W. Klink, W. Plessas, M. Radici, and R. F. Wagenbrunn, *Eur. Phys. J. A* **14**, 17 (2002).
8. K. Berger, R. F. Wagenbrunn and W. Plessas, *Phys. Rev. D* **70**, 094027 (2004).
9. K. Berger, PhD Thesis, University of Graz (2005).
10. D. Merten, U. Loering, K. Kretzschmar, B. Metsch, and H. R. Petry, *Eur. Phys. J. A* **14**, 477 (2002).
11. T. Melde, K. Berger, L. Canton, W. Plessas, and R. F. Wagenbrunn, *Phys. Rev. D* **76**, 074020 (2007).
12. T. Melde, L. Canton, W. Plessas, and R. F. Wagenbrunn, *Eur. Phys. J. A* **25**, 97 (2005).
13. T. Melde, W. Plessas, and R. F. Wagenbrunn, *Phys. Rev. C* **72**, 015207 (2005); Erratum, *Phys. Rev. C* **74**, 069901 (2006).
14. T. Melde, W. Plessas, and B. Sengl, *Phys. Rev. C* **76**, 025204 (2007).
15. B. Sengl, T. Melde, and W. Plessas, *Phys. Rev. D* **76**, 054008 (2007).
16. B. Sengl, PhD Thesis, University of Graz (2006).
17. T. Melde, W. Plessas, and B. Sengl, in preparation.



## Parity violating electron scattering on ${}^4\text{He}$

M. Viviani

INFN, Sezione di Pisa, Pisa, Italy

**Abstract.** In order to isolate the contribution of the nucleon strange electric form factor to the parity-violating asymmetry measured in  ${}^4\text{He}(e, e'){}^4\text{He}$  experiments, it is crucial to have a reliable estimate of the magnitude of isospin-symmetry-breaking (ISB) corrections in both the nucleon and  ${}^4\text{He}$ . Isospin admixtures in the nucleon are determined in chiral perturbation theory, while those in  ${}^4\text{He}$  are derived from nuclear interactions, including explicit ISB terms. At the low momentum transfers of interest in recent measurements reported by the HAPPEX collaboration at Jefferson Lab, it results that both contributions are of comparable magnitude to those associated with strangeness components in the nucleon electric form factor.

One of the challenges of modern hadronic physics is to determine, at a quantitative level, the role that quark-antiquark pairs, and in particular  $s\bar{s}$  pairs, play in the structure of the nucleon. Parity-violating (PV) electron scattering from nucleons and nuclei offers the opportunity to investigate this issue experimentally. The PV asymmetry ( $A_{PV}$ ) arises from interference between the amplitudes due to exchange of photons and Z-bosons, which couple respectively to the electromagnetic (EM) and weak neutral (NC) currents. These currents involve different combinations of quark flavors, and therefore measurements of  $A_{PV}$ , in combination with electromagnetic form factor data for the nucleon, allow one to isolate, in principle, the electric and magnetic form factors  $G_E^s$  and  $G_M^s$ , associated with the strange-quark content of the nucleon.

Experimental determinations of these form factors have been reported recently by the Jefferson Lab HAPPEX [1] and G0 [2] Collaborations, Mainz A4 Collaboration [3], and MIT-Bates SAMPLE Collaboration [4]. These experiments have scattered polarized electrons from either unpolarized protons at forward angles [1–3] or unpolarized protons and deuterons at backward angles [4]. The resulting PV asymmetries are sensitive to different linear combinations of  $G_E^s$  and  $G_M^s$  as well as the nucleon axial-vector form factor  $G_A^Z$ . However, no robust evidence has emerged so far for the presence of strange-quark effects in the nucleon.

Last year, the HAPPEX Collaboration [5,6] at Jefferson Lab reported on measurements of the PV asymmetry in elastic electron scattering from  ${}^4\text{He}$  at four-momentum transfers of  $0.091 (\text{GeV}/c)^2$  and  $0.077 (\text{GeV}/c)^2$ . Because of the  $J^\pi=0^+$  spin-parity assignments of this nucleus, transitions induced by magnetic and axial-vector currents are forbidden, and therefore these measurements can lead to a direct determination of the strangeness electric form factor  $G_E^s$  [7,8], provided that isospin symmetry breaking (ISB) effects in both the nucleon and  ${}^4\text{He}$ , and

relativistic and meson-exchange (collectively denoted with MEC) contributions to the nuclear EM and weak vector charge operators, are negligible. A realistic calculation of these latter contributions [8] found that they are in fact tiny at low momentum transfers.

Recently, we have completed the first realistic calculations of the ISB and here we will discuss their effect on the PV asymmetry (see Ref. [9] for details). The PV asymmetry measured in  $(e, e')$  elastic scattering from  ${}^4\text{He}$  is given by

$$A_{\text{PV}} = \frac{G_\mu Q^2}{4\pi\alpha\sqrt{2}} \left[ 4 \sin^2 \theta_W - 2 \frac{F^{(1)}(q)}{F^{(0)}(q)} - \frac{2 G_E^I - G_E^S}{(G_E^p + G_E^n)/2} \right], \quad (1)$$

where  $G_\mu$  is the Fermi constant as determined from muon decays, and  $\theta_W$  is the Weinberg mixing angle. The term  $G_E^S(Q^2)$  is the strange electric form factor of the nucleon, while the terms  $G_E^I$  and  $F^{(1)}(q)/F^{(0)}(q)$  are the contributions to  $A_{\text{PV}}$ , associated with the violation of isospin symmetry at the nucleon and nuclear level, respectively.

The most accurate measurement of  $A_{\text{PV}}$  has been recently reported at four-momentum transfer of  $Q^2=0.077$   $(\text{GeV}/c)^2$  [6]:

$$A_{\text{PV}} = [+6.40 \pm 0.23 \text{ (stat)} \pm 0.12 \text{ (syst)}] \text{ ppm}, \quad (2)$$

from which one obtains

$$\Gamma \equiv -2 \frac{F^{(1)}(q)}{F^{(0)}(q)} - \frac{2 G_E^I - G_E^S}{(G_E^p + G_E^n)/2} = 0.010 \pm 0.038 \quad (3)$$

at  $Q^2 = 0.077$   $(\text{GeV}/c)^2$ . This result is consistent with zero. In the following, we discuss the estimates for the ISB corrections first in the nucleon and then in  ${}^4\text{He}$ , respectively  $G_E^I(Q^2)$  and  $F^{(1)}(q)$ , at  $Q^2=0.077$   $(\text{GeV}/c)^2$  (corresponding to  $q=1.4$   $\text{fm}^{-1}$ ).

For  $G_E^I(Q^2)$  we use the estimate obtained in Ref. [10], combining a leading-order calculation in chiral perturbation theory with estimates for low-energy constants using resonance saturation. At the specific kinematical point of interest  $Q^2 = 0.077$   $(\text{GeV}/c)^2$ , it results that  $G_E^I(Q^2) = -0.0017 \pm 0.0006$ , and with

$$G_E^p(Q^2) = 0.799 \text{ and } G_E^n(Q^2) = 0.027$$

[11], we obtain

$$-\frac{2 G_E^I}{(G_E^p + G_E^n)/2} = 0.008 \pm 0.003 \quad (4)$$

at  $Q^2 = 0.077$   $(\text{GeV}/c)^2$ .

We now turn to  $F^{(0)}(q)$  and  $F^{(1)}(q)$ , the isoscalar and isovector form factors of  ${}^4\text{He}$ , respectively. The form factor  $F^{(1)}(q)$  is very small because  ${}^4\text{He}$  is predominantly an isospin  $T = 0$  state, but it contains also tiny  $T = 1$  and  $2$  components. We have computed such components using a variety of Hamiltonian models, in order to have an estimate of the model dependence. We have considered: i) the AV18 NN potential [12]; ii) the AV18 plus Urbana-IX 3N potential [13] (AV18/UIX); iii)

the CD Bonn [14] NN plus Urbana-IXb 3N potentials (CDBonn/UIXb); and iv) the chiral N3LO [15] NN potential (N3LO). The Urbana UIXb 3N potential is a slightly modified version of the Urbana UIX (in the UIXb, the parameter  $U_0$  of the central repulsive term has been reduced by the factor 0.812), designed to reproduce, when used in combination with the CD Bonn potential, the experimental binding energy of  ${}^3\text{H}$ .

The form factors  $F^{(0)}(q)$  and  $F^{(1)}(q)$  calculated with the AV18/UIX Hamiltonian model, are displayed in Fig. 1, where the effect of inclusion of meson-exchange contributions (MEC) is also shown. The dashed curves are the calculations including only the one-body operators, while the solid curves have been obtained including the relativistic one-body and MEC [8] in the electromagnetic charge operators. The experimental data are from Refs. [16]. From the figure it is evident that for  $q \leq 1.5 \text{ fm}^{-1}$ , the effect of MEC in both  $F^{(0)}(q)$  and  $F^{(1)}(q)$  is negligible.

In the inset of Fig. 1, we also show the the model dependence of the ratio  $|F^{(1)}(q)/F^{(0)}(q)|$  (all calculations include MEC). The various Hamiltonian models give predictions quite close to each other; the remaining differences reflect the different percentages of the T=1 component in the  ${}^4\text{He}$  wave function.

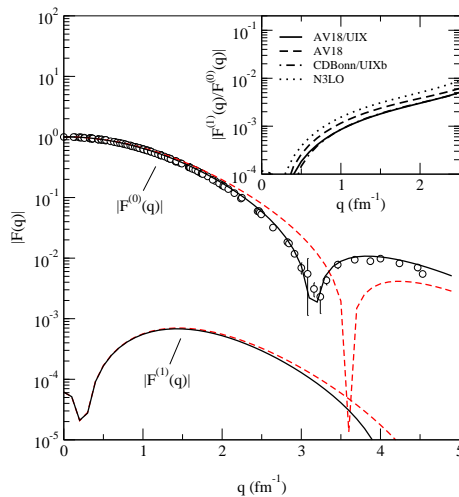


**Fig. 1.** The  $F^{(0)}(q)$  and  $F^{(1)}(q)$  form factors for the AV18/UIX Hamiltonian model. The  $F^{(0)}(q)$  is compared with the experimental  ${}^4\text{He}$  charge form factor [16]. The dashed curves are the calculations including only one-body operators. The solid curves include also MEC. The ratio  $|F^{(1)}(q)/F^{(0)}(q)|$  (all calculations include MEC) is shown in the inset for the four Hamiltonian models considered in this paper.

The calculated ratios  $F^{(1)}(q)/F^{(0)}(q)$  at  $Q^2=0.077 \text{ (GeV}/c)^2$  are of the order of  $-0.002$ . The value corresponding to the N3LO is somewhat larger than for the other models, as can be seen in Fig. 1, reflecting the larger percentage of T=1 admixtures predicted by the N3LO potential. The inclusion of 3N potentials tends

to decrease the magnitude of  $F^{(1)}/F^{(0)}$ , and relativistic and MEC are, at this value of  $Q^2$ , negligible.

Therefore, at  $Q^2=0.077$  (GeV/c)<sup>2</sup>, both contributions  $F^{(1)}/F^{(0)}$  and  $G_E^I$  are found of the same order of magnitude as the central value of  $\Gamma$  in Eq. (3). Using in this equation the value  $F^{(1)}/F^{(0)} \approx -0.00157$  obtained with the Hamiltonian models including 3N potentials, and the chiral result for  $G_E^I = -0.0017 \pm 0.0006$ , one would obtain  $G_E^s [Q^2 = 0.077 \text{ (GeV/c)}^2] = -0.001 \pm 0.016$  thus suggesting that the value of  $\Gamma$  is almost entirely due to isospin admixtures. Of course, the experimental error on  $\Gamma$  is still too large to allow us to draw a more definite conclusion. A recent estimate of  $G_E^s$  using lattice QCD input obtains [17]  $G_E^s(0.1 \text{ (GeV/c)}^2) = +0.001 \pm 0.004 \pm 0.003$ . An increase of the experimental accuracy of one order of magnitude would be necessary in order to be sensitive to  $G_E^s$  at low values of  $Q^2$ . Indeed, if the lattice QCD prediction above is confirmed, the present data would suggest that the leading correction to the PV asymmetry is from isospin admixtures in the nucleon and/or <sup>4</sup>He.

## References

1. K.A. Aniol *et al.*, Phys. Rev. Lett. **82**, 1096 (1999); Phys. Lett. B **509**, 211 (2001); Phys. Rev. C **69**, 065501 (2004); Phys. Lett. B **635**, 275 (2006).
2. D.S. Armstrong *et al.*, Phys. Rev. Lett. **95**, 092001 (2005).
3. F.E. Maas *et al.*, Phys. Rev. Lett. **93**, 022002 (2004); Phys. Rev. Lett. **94**, 152001 (2005).
4. D.T. Spayde *et al.*, Phys. Lett. B **583**, 79 (2004); T.M. Ito *et al.*, Phys. Rev. Lett. **92**, 102003 (2004).
5. K.A. Aniol *et al.*, Phys. Rev. Lett. **96**, 022003 (2006).
6. A. Acha *et al.*, Phys. Rev. Lett. **98**, 032301 (2007).
7. M.J. Musolf *et al.*, Phys. Rep. **239**, 1 (1994).
8. M.J. Musolf, R. Schiavilla, and T.W. Donnelly, Phys. Rev. C **50**, 2173 (1994).
9. M. Viviani *et al.*, Phys. Rev. Lett. **99**, 112002 (2007).
10. B. Kubis and R. Lewis, Phys. Rev. C **74**, 015204 (2006).
11. M. A. Belushkin, H. W. Hammer and U.-G. Meißner, hep-ph/0608337; M. A. Belushkin, private communication.
12. R.B. Wiringa, V.G.J. Stoks, and R. Schiavilla, Phys. Rev. C **51**, 38 (1995).
13. B.S. Pudliner *et al.*, Phys. Rev. C **56**, 1720 (1997).
14. R. Machleidt, Phys. Rev. C **63**, 024001 (2001).
15. D.R. Entem and R. Machleidt, Phys. Rev. C **68**, 041001 (2003).
16. R.F. Froesch *et al.*, Phys. Rev. **160**, 874 (1968); R.G. Arnold *et al.*, Phys. Rev. Lett. **40**, 1429 (1978).
17. D.B. Leinweber *et al.*, Phys. Rev. Lett. **97**, 022001 (2006).



# Dynamics of P11 and P33 resonances in quark models with chiral mesons\*

B. Golli<sup>a,b</sup> and S. Širca<sup>b,c</sup>

<sup>a</sup>Faculty of Education, University of Ljubljana, 1000 Ljubljana, Slovenia

<sup>b</sup>Jožef Stefan Institute, 1000 Ljubljana, Slovenia

<sup>c</sup>Faculty of Mathematics and Physics, University of Ljubljana, 1000 Ljubljana, Slovenia

**Abstract.** We apply the coupled channel formalism for the K-matrix to the calculation of the P11 and P33 scattering amplitudes in the region the N(1440) and  $\Delta(1600)$  resonances.

## 1 Introduction

In this work [1] we extend the coupled channel formalism for the K matrix derived in [2] using the static approximation to take into account the correct relativistic kinematics of the meson-baryon system. We apply this method that has been used in [2] to explain the peculiar behaviour of the scattering amplitudes in the energy range of the Roper resonance to the calculation of the  $\Delta(1600)$  resonance, the Roper's counterpart in the P33 partial wave.

In quark models these two resonances are assumed to have a similar spatial structure, this similarity is however not reflected in the scattering amplitudes. While in the P11 partial wave the phase shift reaches 90 degrees around  $W \sim 1500$  MeV the phase shift in the P33 case shows no sign of resonant behaviour in the energy range of  $W \sim 1600$  and above, which is a strong signal of the important role of inelastic channels. This is further supported by the unusual behaviour of the inelasticity which in the P11 case rapidly rises from zero to unity and remains close to this value in a broad energy region, while in the P33 case it rises rather slowly and reaches the unitarity limit only at much higher energies.

We show that these features can be explained by assuming that in this energy range the inelastic channels are dominated by the two and three-pion decays proceeding mainly through two channels: (i) in the  $\pi\Delta$  channel the resonance first decays into the pion and the  $\Delta$  isobar of invariant mass  $M$ ,  $M_N + m_\pi < M < W - m_\pi$ , and (ii) the  $\sigma$  channel in which the resonance first decays into the  $\sigma$ -meson mimicking two pions in the relative s-state and either the nucleon (in the P11 case) or the  $\Delta$  isobar (in the P33 case).

---

\* Talk delivered by B. Golli

## 2 Coupled-channel K-matrix formalism

We consider a class of chiral quark models in which mesons (the pion and the sigma meson in our case) couple linearly to the quark core:

$$H_{\text{meson}} = \int dk \sum_{lmt} \left\{ \omega_k a_{lmt}^\dagger(k) a_{lmt}(k) + \left[ V_{lmt}(k) a_{lmt}(k) + V_{lmt}^\dagger(k) a_{lmt}^\dagger(k) \right] \right\},$$

where  $a_{lmt}^\dagger(k)$  is the creation operator for a meson with angular momentum  $l$  and the third components of spin  $m$  and isospin  $t$ . In the case of the pion, we include only  $l = 1$  pions, and

$$V_{mt}(k) = -v(k) \sum_{i=1}^3 \sigma_m^i \tau_t^i \quad (1)$$

is the general form of the pion source, with the quark operator,  $v(k)$ , depending on the model. It includes also the possibility that the quarks change their radial function which is specified by the reduced matrix elements  $V_{BB'} = \langle B || V(k) || B' \rangle$ , where  $B$  are the bare baryon states (e.g. the bare nucleon,  $\Delta$ , Roper, ...) In the case of the  $\sigma$  mesons we assume only  $l = 0$  mesons, coupled to the quark core with

$$\tilde{V}^\mu(k) = G_\sigma \frac{k}{\sqrt{2\omega_{\mu k}}} w_\sigma(\mu), \quad w_\sigma(\mu)^2 \approx \frac{1}{\pi} \frac{\frac{1}{2}\Gamma_\sigma}{(\mu - m_\sigma)^2 + \frac{1}{4}\Gamma_\sigma^2}. \quad (2)$$

Here  $\omega_{\mu k}^2 = k^2 + \mu^2$  and  $w_\sigma(\mu)$  is the mass distribution function modeling the resonant decay into two pions. In this work we take the values consistent with the recent analysis of Leutwyler [5],  $m_\sigma = 450$  MeV and  $\Gamma_\sigma = 550$  MeV. The strength parameter  $G_\sigma$  in (2) is a free parameter of the model.

Chew and Low [4] have shown that in such models it is possible to find the exact expression for the T matrix (and consequently for the K matrix) without explicitly specifying the form of asymptotic states. In the basis with good total angular momentum  $J$  and isospin  $T$ , in which the K and T matrices are diagonal, it is possible to express the K matrix for the elastic channel in the form:

$$K_{\pi N \pi N}^{JT}(k, W) = -\pi \mathcal{N}_N \langle \Psi_{JT}^N(W) || V(k) || \Psi_N \rangle,$$

where  $W$  is the invariant mass of the meson-baryon system. In the inelastic channels we find

$$\begin{aligned} K_{\pi \Delta \pi N}^{JT}(k, W, M) &= -\pi \mathcal{N}_\Delta \langle \Psi_{JT}^N(W) || V(k) || \tilde{\Psi}_\Delta(M) \rangle, \\ K_{\pi \Delta \pi \Delta}^{JT}(k, W, M', M) &= -\pi \mathcal{N}_\Delta \langle \Psi_{JT}^\Delta(W, M) || V(k) || \tilde{\Psi}_\Delta(M') \rangle, \end{aligned}$$

where  $\tilde{\Psi}_\Delta(M)$  is the intermediate  $\Delta$  state with invariant mass  $M$  normalized as  $\langle \tilde{\Psi}_\Delta(M') | \tilde{\Psi}_\Delta(M) \rangle = \delta(M - M')$ . The matrix elements of the K matrix involving the  $\sigma N$  channel in the P11 case read

$$\begin{aligned} K_{\sigma N}^{\frac{1}{2}\frac{1}{2}}(k, W, \mu) &= -\pi \mathcal{N}_{\sigma N} \langle \Psi_{\frac{1}{2}\frac{1}{2}}^N(W) | \tilde{V}^\mu(k) | \Psi_N \rangle, \\ K_{\sigma \Delta}^{\frac{1}{2}\frac{1}{2}}(k, W, \mu, M) &= -\pi \mathcal{N}_{\sigma N} \langle \Psi_{\frac{1}{2}\frac{1}{2}}^\Delta(W, M) | \tilde{V}^\mu(k) | \Psi_N \rangle, \\ K_{\sigma \sigma}^{\frac{1}{2}\frac{1}{2}}(k, W, \mu, \mu') &= -\pi \mathcal{N}_{\sigma N} \langle \Psi_{\frac{1}{2}\frac{1}{2}}^\sigma(W, \mu') | \tilde{V}^\mu(k) | \Psi_N \rangle, \end{aligned}$$

and those involving the  $\sigma\Delta$  channel in the P33 case:

$$\begin{aligned} K_{N\sigma}^{\frac{3}{2}\frac{3}{2}}(k, W, M, \mu) &= -\pi\mathcal{N}_{\sigma\Delta} \langle \Psi_{\frac{3}{2}\frac{3}{2}}^N(W) | \tilde{V}^\mu(k) | \tilde{\Psi}_\Delta(M) \rangle, \\ K_{\Delta\sigma}^{\frac{3}{2}\frac{3}{2}}(k, W, \mu, M, M') &= -\pi\mathcal{N}_{\sigma\Delta} \langle \Psi_{\frac{3}{2}\frac{3}{2}}^\Delta(W, M') | \tilde{V}^\mu(k) | \tilde{\Psi}_\Delta(M) \rangle, \\ K_{\sigma\sigma}^{\frac{3}{2}\frac{3}{2}}(k, W, \mu, M, \mu', M') &= -\pi\mathcal{N}_{\sigma\Delta} \langle \Psi_{\frac{3}{2}\frac{3}{2}}^\sigma(W, \mu', M') | \tilde{V}^\mu(k) | \tilde{\Psi}_\Delta(M) \rangle, \end{aligned}$$

where  $\mathcal{N}_B = \sqrt{\omega E_B/kW}$ ,  $\mathcal{N}_{\sigma B} = \sqrt{\omega_\mu E_B/k_\mu W}$ ,  $\omega$  is the energy of the scattering pion,  $k = \sqrt{\omega^2 - m_\pi^2}$ , and  $\omega_\mu$  is the energy of the scattering  $\sigma$ -meson of invariant mass  $\mu$ ,  $k_\mu = \sqrt{\omega_\mu^2 - \mu^2}$ . Here  $\Psi_{JT}^H$  is the principal value state for which we use the following ansatz that takes into account the proper relativistic kinematics and replaces the similar expression in [2] derived in the static (no-recoil) approximation:

$$\begin{aligned} |\Psi_{JT}^H(W, m_H)\rangle &= \mathcal{N}_H \left\{ \sum_B c_B^H(W, m_H) |\Phi_B\rangle + [a^\dagger(k_H) | \tilde{\Psi}_H]^{JT} \right. \\ &\quad + \int dk \frac{\chi_{JT}^{NH}(k, W, m_H)}{\omega_k + E_N(k) - W} [a^\dagger(k) | \Psi_N(k)]^{JT} \\ &\quad + \int dM \int dk \frac{\chi_{JT}^{\Delta H}(k, W, M, m_H)}{\omega_k + E(k) - W} [a^\dagger(k) | \tilde{\Psi}_\Delta(M)]^{JT} \\ &\quad \left. + \int d\mu \int dk \frac{\chi_{JT}^{\sigma H}(k, W, \mu, m_H)}{\omega_{\mu k} + E(k) - W} b^\dagger(k) | \tilde{\Psi}_{JT} \right\}. \end{aligned} \quad (3)$$

Here H stands for either the  $\pi N$ ,  $\pi\Delta$ ,  $\sigma N$  or the  $\sigma\Delta$  channel,  $m_H$  is the invariant mass of the corresponding intermediate hadron in the inelastic channels,  $E(k)$  is the energy of the recoiled baryon (nucleon or  $\Delta$ ). The first term consists of the sum over *bare* tree-quark states  $\Phi_B$ , involving different excitations of the quark core, the next term corresponds to the free meson (pion or  $\sigma$ -meson) and the baryon (N or  $\Delta$ ) and defines the channel, the next two terms represent the pion cloud around the nucleon and the  $\Delta$  isobar, respectively, and the last term the  $\sigma$ -meson cloud around the nucleon (for  $JT = \frac{1}{2}\frac{1}{2}$ ) or the  $\Delta$  (for  $JT = \frac{3}{2}\frac{3}{2}$ ), here  $b^\dagger$  is the creation operator for the  $\sigma$ -meson.

The on-shell meson amplitudes  $\chi_{JT}^{H'H}$ , describing the corresponding meson clouds around the nucleon and the  $\Delta$  are proportional to corresponding matrix elements of the on-shell K matrix

$$K_{H'H} = \pi\mathcal{N}_{H'}\mathcal{N}_H \chi_{JT}^{H'H}(k_{H'}, k_H).$$

From the variational principle for the K matrix it is possible to derive the integral equation for the amplitudes which is equivalent to the Lippmann-Schwinger equation for the K matrix.

Using a simplified ansatz for the principal value states in which the terms involving the integrals are neglected amounts to taking only the non-homogeneous part of the corresponding Lippmann-Schwinger equation. Such an approximation is widely used in phenomenological analysis of scattering amplitudes and is known as the Born approximation for the K matrix.

The T matrix is calculated from the K matrix through the Heitler equation:  $T = -K + iT T$ .

### 3 Results for the scattering amplitudes in the Cloudy Bag Model

We illustrate the method by calculating scattering amplitudes for the P11 and the P33 partial waves. Though the expressions derived in the previous sections are general and can be applied to any model in which mesons linearly couple to the quark core, we choose here the Cloudy Bag Model, primarily because of its simplicity. In this model, the matrix element of the pion source (1) between the model 3-quark states can be written as

$$\langle \Phi_{B'} || V(\mathbf{k}) || \Phi_B \rangle = r_q v(\mathbf{k}) \langle J_{B'}, T_{B'} = J_{B'} || \sum_{i=1}^3 \sigma_m^i \tau_t^i || J_B, T_B = J_B \rangle,$$

where

$$v(\mathbf{k}) = \frac{1}{2f} \frac{k^2}{\sqrt{12\pi^2 \omega_k}} \frac{\omega_{\text{MIT}}}{\omega_{\text{MIT}} - 1} \frac{j_1(kR_{\text{bag}})}{kR_{\text{bag}}}$$

and

$$r_q = \begin{cases} 1 & \text{for } B = B' = (1s)^3 \text{ configuration} \\ r_\omega = \left[ \frac{\omega_{\text{MIT}}^1 (\omega_{\text{MIT}}^0 - 1)}{\omega_{\text{MIT}}^0 (\omega_{\text{MIT}}^1 - 1)} \right]^{1/2} = 0.457 & \text{for } B = (1s)^3, B' = (1s)^2(2s)^1 \\ \frac{2}{3} + r_\omega^2 & \text{for } B = B' = (1s)^2(2s)^1 \end{cases}.$$

In this work we use  $R_{\text{bag}} = 0.9$  fm,  $f = 76$  MeV yielding the correct value for the  $\pi\text{NN}$  coupling constant. Similar results are obtained for  $0.85$  fm  $< R_{\text{bag}} < 1.0$  fm. In addition, the energies of the 3-quark states in different excited states are also taken as free parameters.

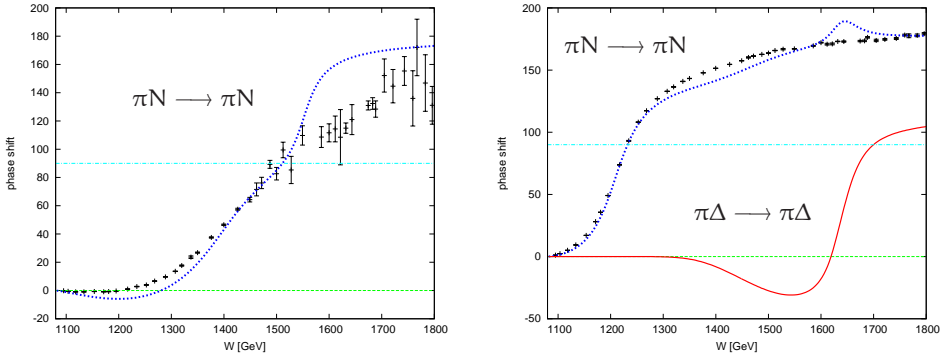


**Fig. 1.** The P11 (left panel) and P33 (right panel) phase shifts. The corresponding thin line in the P33 case represent the phase shift for the pion scattering on the  $\Delta$ . The data points in this and subsequent figures are from the SAID  $\pi\text{N} \rightarrow \pi\text{N}$  partial-wave analysis [6] The model parameters are  $M_R = 1510$  MeV,  $M_\Delta = 1232$  MeV,  $M_{\Delta^*} = 1700$  MeV

The results in the simplest approximation, the Born approximation for the K matrix without background, are displayed in Figure 1. This approximation is

equivalent to keeping only the the first term in the ansatz (3). By increasing the  $\pi N\Delta$  interaction strength by 60 % and the  $\pi NRoper$  by 80 % with respect to the above model values, the widths of the  $N(1440)$  and  $\Delta(1232)$  are reproduced. This simplified approach explains why the resonant behaviour of the phase shift is not observed for the  $\Delta(1600) (\equiv \Delta^*)$  in the elastic channel: in this energy region, the matrix element  $\pi\Delta\Delta^*$  becomes stronger than  $\pi N\Delta^*$  in which case the resonance disappears in the  $\pi N \rightarrow \pi N$  but appears is the non-observable  $\pi\Delta \rightarrow \pi\Delta$  channel.

Including the background in the the Born approximation for the K matrix through the term  $[a^\dagger(k_H)|\tilde{\Psi}_H(M)]]^{JT}$  in (3) we obtain almost perfect agreement of the calculated scattering amplitudes compared to the amplitudes extracted in the partial-wave analysis but still at the expense of considerably larger  $\pi N\Delta$  and  $\pi NRoper$  interaction strength compared to those predicted by the quark model. This inconsistency is resolved when solving the Lippmann-Schwinger equation for the pion amplitudes; it turns out that for our particular choice of the bag radius we are able to reproduce the experimental scattering amplitudes starting from the bare values as predicted by the Cloudy Bag Model (see Fig. 2).

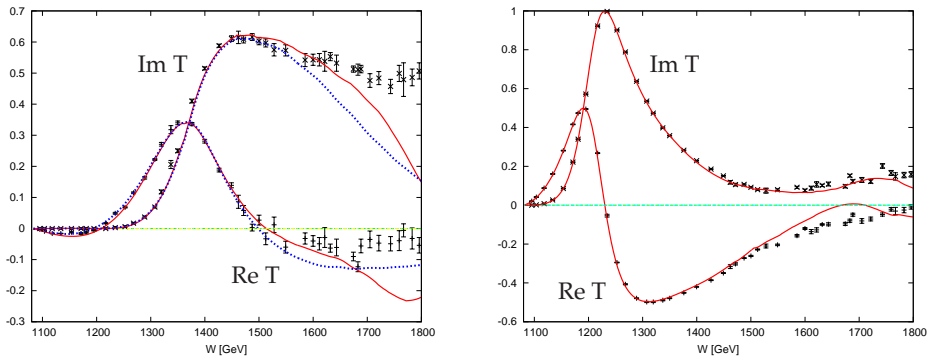


**Fig. 2.** The real and the imaginary parts of the T matrix for the P11 (left panel) and P33 (right panel) partial waves. The dashed/full curves in the left panel show the effect of omitting/including the  $N(1710)$  state in the sum over B in (3)

## References

1. B. Golli and S. Širca, arXiv:0708.3759v1 [hep-ph]
2. B. Golli and S. Širca in: B. Golli, M. Rosina, S. Širca (eds.), *Proceedings of the Mini-Workshop “Progress in Quark Models”*, July 10–17, 2006, Bled, Slovenia, p. 82.
3. P. Alberto, L. Amoreira, M. Fiolhais, B. Golli, and S. Širca, *Eur. Phys. J. A* **26** (2005) 99.
4. G. F. Chew and F. E. Low, *Phys. Rev.* **101**, 1570 (1956).
5. H. Leutwyler, *Int. J. Mod. Phys. A* **22** (2007) 257.
6. R. A. Arndt, W. J. Briscoe, R. L. Workman, I. I. Strakovsky, SAID Partial-Wave Analysis, <http://gwdac.phys.gwu.edu/>.
7. P. Alberto, M. Fiolhais, B. Golli, and J. Marques, *Phys. Lett. B* **523** (2001) 273.



# Sigma meson in a two-level Nambu – Jona-Lasinio model <sup>\*</sup>

Mitja Rosina<sup>a,b</sup> and Borut Tone Oblak<sup>c</sup>

<sup>a</sup>Faculty of Mathematics and Physics, University of Ljubljana, Jadranska 19, P.O. Box 2964, 1001 Ljubljana, Slovenia

<sup>b</sup>J. Stefan Institute, 1000 Ljubljana, Slovenia

<sup>c</sup>National Institute of Chemistry, Hajdrihova 19, 1000 Ljubljana, Slovenia

**Abstract.** We continue the study of a schematic quasispin model similar to the Nambu – Jona-Lasinio model. The model is characterized by a finite number of quarks occupying a finite number of states in the Dirac sea as well as in the valence space (due to a sharp momentum cutoff and a periodic boundary condition). This allows the use of first quantization and an explicit wavefunction. Most low-lying states in the excitation spectrum can be interpreted as multi-pion states and one can deduce the effective pion-pion interaction and scattering length. However, the intruder states can be recognized as sigma-meson excitations or their admixtures to multi-pion states.

## 1 Introduction

In the Mini-Workshop Bled 2006 [1] we presented a soluble two-level quasispin model of spontaneous chiral symmetry breaking, inspired by the Nambu – Jona Lasinio model. It is the hadronic analogue of the Lipkin model in nuclear physics [2].

In our schematic model we enclose  $N = \mathcal{N}$  quarks in a periodic box  $\mathcal{V}$  and use a sharp momentum cutoff  $\Lambda$ , leading to a finite number  $\mathcal{N} = N_c N_f \mathcal{V} \Lambda^3 / 3\pi^2$  of states in the Dirac sea and the same number of states in the valence “shell”. We further simplify the one-flavour Nambu – Jona-Lasinio Hamiltonian by taking all quark kinetic energies equal to  $\frac{3}{4} \Lambda$  and by neglecting the interaction terms which change the individual quark momenta:

$$H = \sum_{k=1}^N \left( \gamma_5(k) h(k) \frac{3}{4} \Lambda + m_0 \beta(k) \right) - \frac{2G}{\mathcal{V}} \left( \sum_{k=1}^N \beta(k) \sum_{l=1}^N \beta(l) + \sum_{k=1}^N i\beta(k) \gamma_5(k) \sum_{l=1}^N i\beta(l) \gamma_5(l) \right)$$

Here  $h = \boldsymbol{\sigma} \cdot \mathbf{p} / p$  is helicity and  $\gamma_5$  and  $\beta$  are Dirac matrices. We use the popular model parameters close to [3,4],  $\Lambda = 648$  MeV,  $G = 40.6$  MeV fm,  $m_0 = 4.58$

<sup>\*</sup> Talk delivered by M. Rosina

MeV, which yield the phenomenological values of quark constituent mass, quark condensate and pion mass both in full Nambu – Jona-Lasinio model as well as in our quasispin model (using in both cases the Hartree-Fock + RPA approximations). It has been shown in [1] that in the large  $N$  limit the exact results of our quasispin model tend in fact to the Hartree-Fock + RPA values.

## 2 What can we learn from the excitation spectrum?

It is very convenient to introduce the quasispin formalism using the fact that the following operators obey (quasi)spin commutation relations

$$j_x = \frac{1}{2} \beta, \quad j_y = \frac{1}{2} i\beta\gamma_5, \quad j_z = \frac{1}{2} \gamma_5,$$

The (quasi)spin commutation relations are also obeyed by separate sums over quarks with right and left helicity as well as by the total sum ( $\alpha = x, y, z$ )

$$R_\alpha = \sum_{k=1}^N \frac{1+h(k)}{2} j_\alpha(k), \quad L_\alpha = \sum_{k=1}^N \frac{1-h(k)}{2} j_\alpha(k), \quad J_\alpha = R_\alpha + L_\alpha = \sum_{k=1}^N j_\alpha(k).$$

The model Hamiltonian can then be written as

$$H = 2P(R_z - L_z) + 2m_0 J_x - 2g(J_x^2 + J_y^2). \quad (1)$$

It commutes with  $R^2$  and  $L^2$  but not with  $R_z$  and  $L_z$ . Nevertheless, it is convenient to work in the basis  $|R, L, R_z, L_z\rangle$ . The Hamiltonian matrix elements can be easily calculated using the angular momentum algebra. By diagonalisation we then obtain the energy spectrum of the system.

**Table 1.** The spectrum of the quasispin model with  $N = 144$ , quantum numbers  $R+L = 36$  and model parameters listed in the Introduction

Parity	$(E - E_0)[\text{MeV}]$	$n$	$\bar{V}[\text{MeV}]$	A	B	C
+	932	10	-9.5	-0.9	-0.0	0.3
-	803	9	-11.7			
+	771	8	-11.3	-0.0	-0.0	-0.0
-	767	7	-8.8			
+	646	6	-11.4	4.8	0.9	-2.2
+	634	6	-12.2	0.3	0.1	-0.1
-	580	5	-10.0			
+	482	4	-10.5	-0.3	-0.2	-0.0
-	378	3	-10.1			
+	261	2	-10.3	3.5	2.3	-0.2
-	136	1				
+	0	0		-18.4	-18.4	-30.0

The ground state is the vacuum. Most excited states can be interpreted as multi-pion states while the intruder state is suggestive of the sigma mesons. Here  $n$  is the guessed number of pions while other columns will be explained in the following subsections where we discuss the harvest of the excitation spectrum.

## 2.1 Pion-pion scattering

Since we are working in a finite volume  $\mathcal{V}$  with periodic boundary conditions we cannot impose scattering boundary conditions. Instead of a continuous spectrum of scattering states we obtain a discrete spectrum. Energy levels of  $n$ -pion states can be interpreted to contain the average effective pion-pion potential  $\bar{V}$  given in Table 1:

$$E_{n\pi} = n m_\pi + \frac{n(n-1)}{2} \bar{V}.$$

Let us repeat our results presented last year [1]. We calculate the s-state scattering length in the first-order Born approximation

$$a = \frac{m_\pi/2}{2\pi} \int V(\mathbf{r}) d^3r = \frac{m_\pi}{4\pi} \bar{V} \mathcal{V}. \quad (2)$$

This formula was first quoted by M.Lüscher [5] in 1986 and 1991 and later by many authors. It was derived in a much more sophisticated way, but in our context it is just the first-order Born approximation.

In our example for  $N = 144$  we have  $\bar{V} = -10.3 \text{ MeV}$  and  $\mathcal{V} = \pi^2 N / \Lambda^3 = 40 \text{ fm}^3$ . This gives

$$a m_\pi = \frac{m_\pi^2}{4\pi} \bar{V} \mathcal{V} = -0.0836. \quad (3)$$

Since there are no experiments with one-flavour pions we compare with the two-flavour value ( $I = 2$ ). The chiral perturbation theory (soft pions) suggests in leading order  $a_0^{I=2} m_\pi = -m_\pi^2 / 16\pi f_\pi^2 = -0.0445$ . The old analysis of Gasser and Leutwyler gave  $-0.019$  and the more recent analysis by Lesniak gave  $-0.034$  (“non-uniform fit”) or  $-0.044$  (“uniform fit”). We get about twice larger value in our one-flavour model due to the artifact that we made up for the second flavour by replacing  $G \rightarrow 2G$ .

## 2.2 The sigma meson

In the spectrum in Table 1 one can clearly distinguish the presence of the sigma meson by noticing the doubling of the positive parity states at 634 and 646 MeV. Moreover, the state at 646 MeV has strong transition matrix elements from the ground state for positive parity one-body operators (see Table 2):

$$\begin{aligned} 2\hat{A} &= R_+ + L_- = J_x + i(R_y - L_y) \\ 2\hat{B} &= R_- + L_+ = J_x - i(R_y - L_y) \\ 2\hat{C} &= R_z - L_z \end{aligned}$$

On the other hand, the state at 634 MeV has much smaller transition matrix elements. This is a good argument that the state at 646 MeV is a rather pure sigma meson. To conclude, we are still devising a method how to extract from the spectrum the width of the sigma meson for the  $\sigma \rightarrow \pi\pi$  decay

### 2.3 Comparison with different particle-hole methods

In *particle-hole methods* (=approximations) sigma meson is introduced as

$$|\sigma\rangle = (a \hat{A} + b \hat{B} + c \hat{C})|g\rangle.$$

In Table 2. we present excitation energies as well as transition matrix elements  $A = \langle \sigma | \hat{A} | g \rangle$  and similar for B and C.

**Table 2.** Excitation energies and transition matrix elements for various approximations

	$(E - E_0)[\text{MeV}]$	A	B	C
Exact	646	4.8	0.9	-2.2
TD	555	5.8	1.8	-2.4
HOM	530	5.8	1.8	-2.4
RPA	668	5.6	1.0	-2.2

In the Tamm-Dancoff approximation (TD) the coefficients  $a, b, c$  are determined by diagonalizing the  $3 \times 3$  Hamiltonian matrix in the corresponding particle-hole space. Similarly, in the Hermitian Operator Method (HOM) [6]  $a = b$  and one diagonalizes a  $2 \times 2$  Hamiltonian matrix. IN The Random Phase Approximation (RPA) one solves the RPA equations assuming for  $\mathcal{O}^\dagger = (a \hat{A} + b \hat{B} + c \hat{C})$ :

$$|\sigma\rangle = \mathcal{O}^\dagger |\Phi_0\rangle, \text{ with } \mathcal{O} |\Phi_0\rangle = 0, \text{ and } |\Phi_0\rangle = |\text{HF}\rangle.$$

### References

1. M. Rosina and B. T. Oblak, Bled Workshops in Physics 7, No.1, 92 (2006); also available at <http://www-f1.ijs.si/BledPub>.
2. H. J. Lipkin, N. Meshkov, A. J. Glick, Nucl. Phys. **62**, 188 (1965).  
N. Meshkov, A. J. Glick, H. J. Lipkin, Nucl. Phys. **62**, 199 (1965).  
A. J. Glick, H. J. Lipkin, N. Meshkov, Nucl. Phys. **62**, 211 (1965).  
D. Agassi, H. J. Lipkin, N. Meshkov, Nucl. Phys. **86**, 321 (1966).
3. M. Fiolhais, J. da Providência, M. Rosina and C. A. de Sousa, Phys. Rev. C **56**, 3311 (1997).
4. M. Buballa, Phys. Reports **407**, 205 (2005).
5. M. Lüscher, Commun. Math. Phys. **104**, 177 (1986); **105**, 153 (1986); Nucl. Phys. **B354**, 531 (1991).
6. M. Bouten, P. van Leuven, M. V. Mihailović and M. Rosina, Nucl. Phys. **A202**, 127 (1973).



# Exclusive processes on the nucleon at MAMI and Jefferson Lab

S. Širca<sup>a, b</sup>

<sup>a</sup>Faculty of Mathematics and Physics, University of Ljubljana, 1000 Ljubljana, Slovenia

<sup>b</sup>Jožef Stefan Institute, 1000 Ljubljana, Slovenia

**Abstract.** The MAMI accelerator (Mainz, Germany) and the CEBAF at Jefferson Laboratory (Newport News, USA) are the world leading electron-scattering facilities in the several 100 MeV to several 1 GeV energy range. A large fraction of the experimental program in these laboratories has recently been focused on the electroweak properties of the nucleon, its spin structure, and on nucleon resonance excitation. Latest results from MAMI (A1 Collaboration) and Jefferson Lab (mostly Hall A) are described.

## 1 Electroweak properties of nucleons

The elastic form factors of the nucleon remain of prime interest. New measurements of the proton electric-to-magnetic form-factor ratio have been performed or are being planned in order to resolve the persistent discrepancy between the double-polarization measurement [1] versus a precise Rosenbluth-separation determination [2], which exhibit different  $Q^2$ -dependencies. Presently the main reason for the disagreement is believed to be the two-photon correction to the elastic scattering process, which contributes differently in both cases. One should also mention the recent precise results at the other end of the spectrum, at very low  $Q^2$  where pion-cloud effects play the dominant role. These were obtained by the BLAST Collaboration at MIT-Bates [3].

An extension of the double-polarized measurement to about  $9 (\text{GeV}/c)^2$  is in progress at Jefferson Lab (Hall C), while a high-precision unpolarized (Rosenbluth) measurement of  $G_E^p$  and  $G_M^p$  at low  $Q^2$  is being pursued at MAMI. Measurements of  $G_E^p$  to as high as  $15 (\text{GeV}/c)^2$  and  $G_M^p$  to  $18 (\text{GeV}/c)^2$  are planned with the 12 GeV-upgrade of CEBAF. There are also efforts in JLab Hall B which are concentrated around the measurement of cross-section differences for electrons versus positrons, which are an independent means of distinguishing the role of the two-photon contributions.

An exciting development in the form-factor arena is the recent high- $Q^2$  measurement of the neutron charge form-factor  $G_E^n$  in Hall A. These measurements are relevant both to explore the transition to pQCD (two-gluon exchanges) and to test the importance of the handbag diagrams (from the perspective of generalized parton distributions (GPDs)), as well as for nucleon spin (sum rules) and lattice QCD. Preliminary results at intermediate  $Q^2$  have been reported at various

conferences this Fall and indicate values of  $G_E^n$  which lie above the conventional (Platchkov) parameterization.

The HAPPEX Collaboration at Jefferson Lab is dedicated to the determination of the strange-quark contributions to the distributions of charge ( $G_E^s$ ) and magnetization ( $G_M^s$ ) within the proton. The parity-violating asymmetry on hydrogen is proportional to a linear combination of  $G_E^s$  and  $G_M^s$ , while it is proportional to  $G_E^s$  only in the case of the spin-less  $^4\text{He}$  nucleus. Both targets have been used at HAPPEX in different kinematical conditions. Most recent results have now been published [5], and the results of this experiment *only* (i.e. without averaging over other experiments) are

$$\begin{aligned} G_E^s &= 0.002 \pm 0.014 \pm 0.007, \\ G_E^s + 0.09 G_M^s &= 0.007 \pm 0.011 \pm 0.006. \end{aligned}$$

Real-photon Compton scattering (RCS) and its virtual counterpart (VCS) are being utilized to access further information on the electromagnetic structure of the proton. The E99-114 experiment at Hall A has measured polarization transfer in RCS off the proton at high momentum transfer [6]. Polarization transfer parameters  $K_{LL}$  and  $K_{LS}$  were extracted and were shown to be in disagreement with the prediction of perturbative QCD based on a two-gluon exchange mechanism. Specifically, the nonzero value of the ratio

$$\frac{K_{LS}}{K_{LL}} \propto \frac{R_T}{R_V} = 0.21 \pm 0.11 \pm 0.03$$

implies that the proton helicity is flipped in the RCS process (which is forbidden in leading-twist pQCD). The RCS studies have been forwarded another step by examining the scaling

$$\frac{d\sigma}{dt} \propto \frac{f(\theta)}{s^n}$$

of the RCS cross-section (at a fixed angle), where pQCD predicts  $n = 6$  based on constituent scaling rules. In contrast to this expectation, a relatively precise value of  $n = 8.0 \pm 0.2$  has been found [7]. The scaling result also disagrees with the predictions based on the handbag reaction mechanism.

The OOPS Collaboration at MIT-Bates has finished analyzing the data from experiments in virtual Compton scattering (VCS) off the proton at low  $Q^2$  [8]. The mean-square electric polarizability of the proton

$$\langle r_\alpha^2 \rangle = 2.16 \pm 0.31 \text{ fm}^2$$

(basically the slope of the  $Q^2$ -dependent electric polarizability  $\alpha(Q^2)$  at low  $Q^2$ ) has been determined for the first time in a VCS process. The magnetic polarizability  $\beta(Q^2)$ , on the other hand, could not be determined well due to poor statistics, although the data is consistent with  $\beta$  having a positive slope at origin, corresponding to a negative magnetic polarizability mean-square radius and characteristic of a diamagnetic contribution from the pion cloud. Unfortunately, the statistics and systematics of the data gathered over the years at MIT-Bates,

MAMI and JLab, are still insufficient to allow for a reliable determination of the  $Q^2$ -dependence of the polarizabilities.

The VCS program on nucleon targets has recently evolved into a much broader effort by including polarization degrees of freedom. Single-spin (beam) asymmetries at low energies have been measured at MAMI/A1 on the proton [9], as well as in the deep-inelastic regime (so-called deeply virtual Compton scattering, DVCS) at JLab Hall A on both the proton and the neutron. The analysis of the Mainz experiment, the goal of which is to determine three different linear combinations of generalized polarizabilities contained in the  $\Psi_0$ ,  $\Delta\Psi_{x0}$ , and  $\Delta\Psi_{z0}$  structure functions is underway while the proton DVCS results from Hall A appeared recently [10]. This is a first DVCS experiment in the valence-quark region (large Bjorken  $x$ ). Real and imaginary parts of twist-2 and twist-3 coefficients of the angular expansion of the cross-section have been measured with great accuracy. One of the conclusions was that perturbative scaling applies in DVCS, indicating that the GPDs are in principle accessible already at modest values of  $Q^2$  in this process.

## 2 Nucleon spin structure

The neutron DVCS experiment E03-106 utilizes the same (single-spin) technique as the proton DVCS to constrain  $\mathcal{E}$ , the least-known GPD, and as such complements nicely the proton case which predominantly depends on  $\mathcal{H}$  and  $\tilde{\mathcal{H}}$ . In addition, the neutron channel is particularly important because of the nucleon total angular momentum sum rule  $J = J_q + J_g = \frac{1}{2}$  (quarks plus gluons), where

$$J_q = \frac{1}{2}\Delta\Sigma + L_q = \frac{1}{2} \int dx x \left[ H(x, \xi, 0) - E(x, \xi, 0) \right].$$

While the spin part  $\Delta\Sigma$  can be determined in DIS experiments (and  $L_g$  in experiments like COMPASS), the nDVCS at high values of Bjorken  $x$  has a unique opportunity to help determine the orbital contribution  $L_q$ . The analysis of the neutron DVCS experiment is underway.

## 3 Nucleon resonances

The multipole character of the  $N \rightarrow \Delta(1232)$  transition is being probed with ever increasing accuracy and at varying kinematical conditions (in particular, at several values of  $Q^2$  accessible at different laboratories). In fact, the experimental methods have been improved to a degree that allows for a rather clear determination of the individual transition amplitudes, such that the model dependence usually dominates the final uncertainties.

Sadly, professor Jim Kelly, the spokesperson and the spiritus agens of the landmark  $N \rightarrow \Delta(1232)$  experiment in Hall A at Jefferson Lab, has passed away this year. It is in respect and admiration that we look at the extensive paper on that experiment [11] which he managed to bring to completion in the very last weeks of his illness.

The A1 Collaboration at MAMI has reported on new precise  $p(e, e'p)\pi^0$  measurements at the peak of the  $\Delta(1232)$  resonance at  $Q^2 = 0.20 \text{ (GeV/c)}^2$  [12]. The new data are sensitive to both the electric (E2) and the Coulomb (C2) quadrupole amplitudes of the  $N \rightarrow \Delta$  transition. New precise values for the quadrupole to dipole amplitude ratios

$$\begin{aligned} \text{CMR} &= (-5.09 \pm 0.28 \text{ (stat + sys)} \pm 0.30 \text{ (model)})\% , \\ \text{EMR} &= (-1.96 \pm 0.68 \text{ (stat + sys)} \pm 0.41 \text{ (model)})\% \end{aligned}$$

have been obtained, with a value for the dominant magnetic dipole amplitude

$$M_{1+} = (39.57 \pm 0.75 \text{ (stat + sys)} \pm 0.40 \text{ (model)}) \cdot 10^{-3} / m_{\pi}^{+} .$$

The results are in disagreement with the predictions of the Constituent Quark Model and in qualitative agreement with models that account for mesonic contributions, including recent Lattice QCD calculations. They thus support the conjecture of deformation in hadronic systems with its origin in the dominance of mesonic effects.

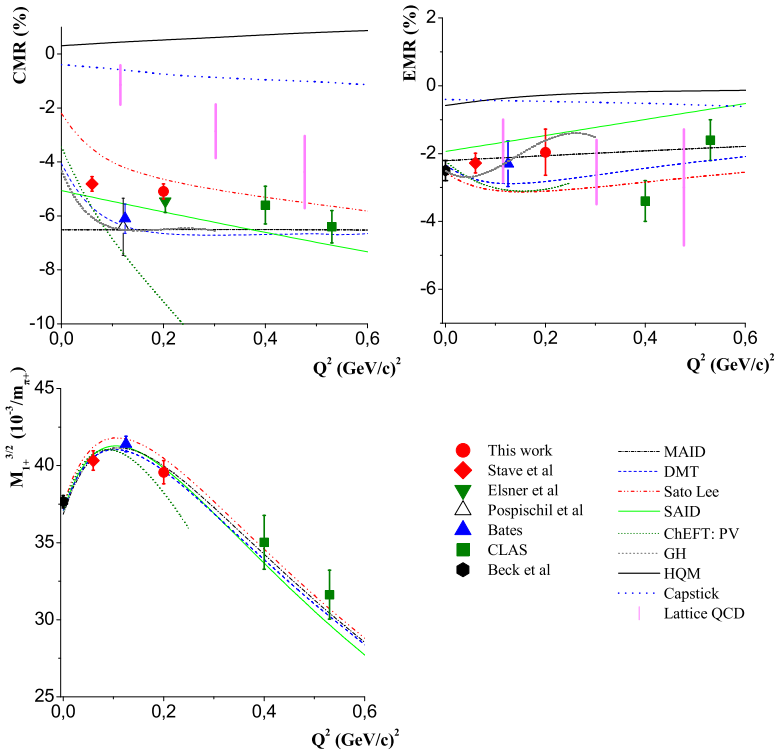


**Fig. 1.** The extracted values for CMR, EMR and  $M_{1+}$  as a function of  $Q^2$  from recent low- $Q^2$  experiments. The theoretical predictions of models MAID, DMT, SAID, Sato-Lee, Capstick, HQM, the linearly extrapolated Lattice-QCD calculation, ChEFT of Pascalutsa-Vanderhaegen and Gail-Hemmert are also shown.

Similar goals have been set by another experiment at MAMI [13], but at a lower value of  $Q^2 = 0.060 \text{ (GeV/c)}^2$ . Here, the reported ratios are even more precise,

$$\text{CMR} = (-4.81 \pm 0.27 \text{ (stat + sys)} \pm 0.26 \text{ (model)})\% ,$$

$$\text{EMR} = (-2.28 \pm 0.29 \text{ (stat + sys)} \pm 0.20 \text{ (model)})\%$$

while the magnetic dipole amplitude is

$$M_{1+} = (40.33 \pm 0.63 \text{ (stat + sys)} \pm 0.61 \text{ (model)}) \cdot 10^{-3} / m_{\pi}^+ ,$$

with similar conclusions. A summary of the results from recent experiments at low  $Q^2$ , where pion cloud physics (long-range effects) is believed to play a most prominent role, is given in Figure 1.

Polarization degrees of freedom have also been exploited in the measurement of  $p(e, e'p)\pi^0$  at  $Q^2 = 0.35 \text{ (GeV/c)}^2$  in the resonance region [14]. The results (unpolarized and polarized structure functions) have been compared to calculations based on dispersion relations for VCS and to the phenomenological pion electroproduction model MAID. There is an overall good agreement between experiment and theoretical calculations. The remaining discrepancies have been mostly attributed to imperfect parameterizations of non-resonant (background) multipoles, to which the measured beam-helicity asymmetry is particularly sensitive.

In another polarized experiment, both beam polarization and proton polarimetry have been utilized in an experiment inaugurating the MAMI-C accelerator with its new, 1.5 GeV CW beam [15]. The beam-recoil polarization transfer coefficients  $P'_x$  and  $P'_z$  as well as the (induced) recoil polarization  $P_y$  were measured for the first time in the  $p(e, e'p)\eta$  reaction at  $Q^2 = 0.1 \text{ (GeV/c)}^2$ , with a center of mass production angle of  $120^\circ$  and spanning a center of mass energy range of  $1500 \text{ MeV} < W < 1550 \text{ MeV}$ , thus covering the region of the S11(1535) and D13(1520) resonances. The values obtained are

$$P'_x = (-67.6 \pm 3.2 \text{ (stat)} \pm 2.6 \text{ (sys)})\% ,$$

$$P_y = (16.1 \pm 3.2 \text{ (stat)} \pm 2.3 \text{ (sys)})\% ,$$

$$P'_z = (-29.3 \pm 2.6 \text{ (stat)} \pm 2.6 \text{ (sys)})\% .$$

The  $P'_x$  and  $P'_z$  are in good agreement with the phenomenological isobar model (Eta-MAID), while  $P_y$  shows a significant deviation, consistent with existing photoproduction data on the polarized-target asymmetry from Bonn. However, if a strong phase change between  $E_{0+}$  and  $(E_{2-} + M_{2-})$  multipoles is applied, which gives a good description of the Bonn polarized target data, the electroproduction data point is also in good agreement with the model. Such a strong phase change is incompatible with a standard Breit-Wigner behavior of the S11(1535) resonance. Indeed this appears to be yet another of the peculiarities of this resonance, the most notable one being the remarkably slow  $Q^2$ -falloff of the helicity amplitude corresponding to  $\eta$  electroproduction seen in Hall B.

## References

1. O. Gayou et al. (Hall A Collaboration), *Phys. Rev. Lett.* **88** (2002) 092301.
2. I. A. Qattan et al. (Hall A Collaboration), *Phys. Rev. Lett.* **94** (2005) 142301.
3. C. B. Crawford et al. (BLAST Collaboration), *Phys. Rev. Lett.* **98** (2007) 052301.
4. G. Cates, K. McCormick, B. Reitz, B. Wojtsekhowski (co-spokespersons), Jefferson Lab Experiment E02-013.
5. A. Acha et al. (HAPPEX Collaboration), *Phys. Rev. Lett.* **98** (2007) 032301.
6. D. Hamilton et al. (Hall A Collaboration), *Phys. Rev. Lett.* **94** (2005) 242001.
7. A. Danagoulian et al. (Hall A Collaboration), *Phys. Rev. Lett.* **98** (2007) 152001.
8. P. Bourgeois et al. (OOPS Collaboration), *Phys. Rev. Lett.* **97** (2006) 212001.
9. N. d'Hose (contact person), MAMI Experiment A1/01-00.
10. C. Munoz Camacho et al. (Hall A Collaboration), *Phys. Rev. Lett.* **97** (2006) 262002.
11. J. J. Kelly et al. (Hall A Collaboration), *Phys. Rev. C* **75** (2007) 025201.
12. N. F. Sparveris et al. (A1 Collaboration), *Phys. Lett. B* **651** (2007) 102.
13. S. Stave et al. (A1 Collaboration), *Eur. Phys. J. A* **30** (2006) 471.
14. I. K. Bensafa et al. (A1 Collaboration), *Eur. Phys. J. A* **32** (2007) 69.
15. H. Merkel et al. (A1 Collaboration), *Phys. Rev. Lett.* **99** (2007) 132301.

---

BLEJSKE DELAVNICE IZ FIZIKE, LETNIK 8, ŠT. 1, ISSN 1580-4992

BLED WORKSHOPS IN PHYSICS, VOL. 8, NO. 1

Zbornik delavnice 'Hadron Structure and Lattice QCD', Bled, 9. – 16. julij 2007

Proceedings of the Mini-Workshop 'Hadron Structure and Lattice QCD', Bled,  
July 9–16, 2007

Uredili in oblikovali Bojan Golli, Mitja Rosina, Simon Širca

Publikacijo sofinancira Javna agencija za raziskovalno dejavnost Republike  
Slovenije

Tehnični urednik Vladimir Bensa

Založilo: DMFA – založništvo, Jadranska 19, 1000 Ljubljana, Slovenija

Natisnila BIROGRAFIKA BORI v nakladi 100 izvodov

Publikacija DMFA številka 1685

Brezplačni izvod za udeležence delavnice

---